

# Chemical resistance of cement paste to the action of deionized water

---

Đuroković, Marija

Doctoral thesis / Disertacija

2019

*Degree Grantor / Ustanova koja je dodijelila akademski / stručni stupanj:* **University of Zagreb, Faculty of Science / Sveučilište u Zagrebu, Prirodoslovno-matematički fakultet**

*Permanent link / Trajna poveznica:* <https://um.nsk.hr/um:nbn:hr:217:449477>

*Rights / Prava:* [In copyright](#)/[Zaštićeno autorskim pravom.](#)

*Download date / Datum preuzimanja:* **2025-03-31**



*Repository / Repozitorij:*

[Repository of the Faculty of Science - University of Zagreb](#)





University of Zagreb  
FACULTY OF SCIENCE

Marija Đuroković

**CHEMICAL RESISTANCE OF CEMENT PASTE TO  
THE ACTION OF DEIONIZED WATER**

DOCTORAL THESIS

Zagreb, 2019





Sveučilište u Zagrebu  
PRIRODOSLOVNO-MATEMATIČKI FAKULTET

Marija Đuroković

# **KEMIJSKA OTPORNOST CEMENTNE PASTE PREMA DJELOVANJU DEIONIZIRANE VODE**

DOKTORSKI RAD

Mentori: Prof. dr. sc. Dubravka Matković-Čalogović  
Dr. sc. Ivan Janotka

Zagreb, 2019.





University of Zagreb  
FACULTY OF SCIENCE

Marija Đuroković

# **CHEMICAL RESISTANCE OF CEMENT PASTE TO THE ACTION OF DEIONIZED WATER**

DOCTORAL THESIS

Supervisors: Prof.dr.sc. Dubravka Matković-Čalogović  
Dr.sc. Ivan Janotka

Zagreb, 2019



## Acknowledgments

This work is a result of my twenty-two years long work within Croatian Portland cement industry. On this long-lasting trip, I have met many people who have encouraged my development by sharing their knowledge, experience and passion for simple grey powder which enables people to create and moderate our surroundings. It is really hard to find appropriate words to describe my gratitude to all of them.

My special acknowledgments go to my supervisors prof. dr. sc. Dubravka Matković-Čalogović and dr. sc. Ivan Janotka for their guidance, help, support and humanity on my way towards scientific approach to Portland cement needs and problems. It has been my honour to be their student.

My acknowledgments go also to the evaluation committee for their suggestions and comments.

I am especially grateful to my colleagues from Institute IGH who has supported my efforts on daily basis.

Finally, I thank members of my family: my husband Tomislav and my children Lucija, Katarina and David, for their unconditional love and support throughout my whole professional life. I am also especially grateful to my parents: Terezija and Josip and my aunt Ivanka who have always believed in me.

Marija





# Contents

<b>ABSTRACT</b> .....	<b>XI</b>
<b>SAŽETAK</b> .....	<b>XIII</b>
<b>PROŠIRENI SAŽETAK</b> .....	<b>XV</b>
<b>§ 1. INTRODUCTION</b> .....	<b>1</b>
<b>1.1. Problem statement</b> .....	<b>1</b>
<b>1.2. Objectives, hypothesis and methods of research</b> .....	<b>3</b>
<b>§ 2. LITERATURE REVIEW</b> .....	<b>4</b>
<b>2.1. Portland cement</b> .....	<b>4</b>
<b>2.2. Portland cement composition</b> .....	<b>5</b>
2.2.1. <i>Bulk composition of Portland cement</i> .....	<b>5</b>
2.2.2. <i>Portland cement phase composition</i> .....	<b>6</b>
2.2.3. <i>Calculation of phase composition</i> .....	<b>9</b>
<b>2.3. X-ray diffraction</b> .....	<b>9</b>
<b>2.4. Minor elements in Portland cement</b> .....	<b>13</b>
<b>2.5. Portland cement hydration</b> .....	<b>14</b>
2.5.1. <i>Hydration of alite</i> .....	<b>14</b>
2.5.2. <i>Hydration of belite</i> .....	<b>18</b>
2.5.3. <i>Experimental considerations</i> .....	<b>18</b>
2.5.4. <i>Hydration of aluminate and ferrite phase</i> .....	<b>18</b>
2.5.5. <i>Portland cement hydration</i> .....	<b>20</b>
2.5.6. <i>Hydration kinetics and mechanism of hydration</i> .....	<b>20</b>
<b>2.6. Microstructure of hardened Portland cement paste</b> .....	<b>21</b>
2.6.1. <i>Scanning electron microscopy</i> .....	<b>22</b>
2.6.2. <i>Distribution of the trace elements in hydrated Portland cement paste</i> .....	<b>24</b>
2.6.3. <i>Pore solution chemistry</i> .....	<b>25</b>
<b>2.7. Portland cement production</b> .....	<b>29</b>
2.7.1. <i>Production process</i> .....	<b>29</b>
2.7.2. <i>CO<sub>2</sub> emission in Portland cement production</i> .....	<b>31</b>
<b>2.8. Calcium sulfoaluminate cement</b> .....	<b>33</b>
<b>2.9. Leaching</b> .....	<b>35</b>
<b>§ 3. MATERIALS AND METHODS</b> .....	<b>37</b>
<b>3.1. Introduction</b> .....	<b>37</b>
<b>3.2. Materials and methods</b> .....	<b>37</b>

3.2.1. Cement .....	39
3.2.2. Deionised water .....	45
<b>3.3. Sample preparation.....</b>	<b>49</b>
3.3.1. Cement paste preparation.....	49
3.3.2. Prismatic samples compaction and curing .....	50
3.3.3. Cylindric samples compaction and curing.....	51
3.3.4. Obtaining pore solution and prime characterisation.....	53
<b>3.4. Testing methods.....</b>	<b>55</b>
3.4.1. Determination of strength and preparation of samples for chemical analysis .....	55
3.4.2. Determination of secant modulus of elasticity.....	55
3.4.3. Powder X-ray diffraction .....	56
3.4.5. Determination of chemical composition of pore solution .....	57
3.4.6. Determination of dimensional stability.....	58
3.4.7. Determination of the mass loss .....	59
3.4.8. Determination of water absorption coefficient due to capillary action.....	59
3.4.9. Determination of permeability to gasses.....	60
3.4.10. SEM determination.....	61
3.4.11. Air voids content.....	61
3.4.12. Used chemicals and reagents .....	63
<b>§ 4. RESULTS AND DISCUSSION .....</b>	<b>66</b>
<b>4.1. Characterization of starting materials .....</b>	<b>66</b>
<b>4.2. Hydration of cement pastes .....</b>	<b>74</b>
<b>4.3. Mechanical and physical properties of hydrated cement pastes.....</b>	<b>77</b>
<b>4.4. Microstructural properties.....</b>	<b>81</b>
<b>4.5. Cement paste and pore solution composition .....</b>	<b>84</b>
<b>§ 5. CONCLUSION .....</b>	<b>91</b>
<b>§ 6. LIST OF ABBREVIATIONS .....</b>	<b>93</b>
<b>§ 7. BIBLIOGRAPHY .....</b>	<b>95</b>
<b>§ 8. APPENDIX.....</b>	<b>XLVII</b>
<b>§ 9. CURRICULUM VITAE.....</b>	<b>LIII</b>



University of Zagreb  
Faculty of Science  
**Department of Chemistry**

Doctoral Thesis

## ABSTRACT

### CHEMICAL RESISTANCE OF CEMENT PASTE TO THE ACTION OF DEIONIZED WATER

Marija Đuroković

Institute IGH d.d., Department for materials and structures, Laboratory for binders and ecology,  
Janka Rakuše 1, 10000 Zagreb, Hrvatska

Introduction of new, sustainable materials into the existing civil engineering standards requires durability data for different degradation processes. Unfortunately, durability tests are not standardized. In this work degradation process of decalcification, also called leaching, of cement pastes was studied. The research was conducted on three different immature cement pastes. Two Portland cements based on calcium silicate or aluminate compounds and a cement based on calcium sulfoaluminate compounds were used for preparation of cement pastes. The change in chemical composition of cement pastes and pore solutions, phase compositions, microstructures of cement pastes and their mechanical properties (strength, modulus of elasticity, dimensional and mass stability) were observed during a 365 days leaching period. The results indicate no significant impact of leaching on microstructure, modulus of elasticity, dimensional and mass stability. The observed strength decrease correlates with the observed changes in phase and chemical composition of the cement pastes and pore solutions.

(106 + LIV pages, 56 figures, 31 tables, 236 references, original in English)

Thesis deposited in Central Chemical Library, Horvatovac 102A, Zagreb, Croatia and National and University Library, Hrvatske bratske zajednice 4, Zagreb, Croatia.

Key words: Calcium sulfoaluminate cement / cement paste/ leaching / Portland cement

Supervisors: Prof. dr. sc. Dubravka Matković –Čalogović, Dr. sc. Ivan Janotka

Thesis accepted: 9<sup>th</sup> October 2019.

Reviewers: izv. prof. dr. sc. Sanda Rončević, MPF, Zagreb  
prof. dr. sc. Dubravka Matković–Čalogović, PMF, Zagreb  
doc. dr. sc. Jelena Bleiziffer, Građevinski fakultet, Zagreb  
zamjena: dr.sc. Goran Štefanić, zn. savj., IRB Zagreb





Sveučilište u Zagrebu  
Prirodoslovno-matematički fakultet  
**Kemijski odsjek**

Doktorska disertacija

## SAŽETAK

### KEMIJSKA OTPORNOST CEMENTNE PASTE PREMA DJELOVANJU DEIONIZIRANE VODE

Marija Đuroković

Institut IGH d.d. , Zavod za materijale i konstrukcije, Laboratorij za veziva i ekologiju,  
Janka Rakuše 1, 10 000 Zagreb, Croatia

Uvođenje novih materijala u postojeće građevinske norme zahtijeva podatke o trajnosnim svojstvima novih materijala. Nažalost, ispitivanja trajnosnih svojstava materijala nisu standardizirana. U ovom radu je opisano istraživanje procesa degradacije dekalifikacijom ili izluživanjem. Istraživanje je provedeno na tri različite nezrele cementne paste. Dva tipa portlandskog cementa izgrađenih od kalcijevih silikata ili aluminata i cement izgrađenog od kalcijevih sulfoaluminata korišteni su za izradu uzoraka cementnih pasti u ovom istraživanju. Praćene su promjene kemijskog sastava cementnih pasta i pornih otopina, faznog sastava, mikrostrukture cementne paste kao i mehaničkih svojstava (čvrstoće, modula elastičnosti, promjene dimenzija i mase) u periodu izluživanja od 365 dana. Rezultati ispitivanja ne pokazuju značajan utjecaj izluživanja na mikrostrukturu, modul elastičnosti, dimenzionalnu i masenu stabilnosti. Uočeni pad čvrstoće povezan je s učenim promjenama faznog i kemijskog sastava cementnih pasti i pornih otopina.

(106 + LIV stranica, 56 slika, 31 tablica, 236 literaturnih navoda, jezik izvornika: engleski)

Rad je pohranjen u Središnjoj kemijskoj knjižnici, Horvatovac 102a, Zagreb i Nacionalnoj i sveučilišnoj knjižnici, Hrvatske bratske zajednice 4, Zagreb.

Ključne riječi: cementna pasta / kalcijev sulfoaluminatni cement / izluživanje / portlandski cement

Mentori: Prof. dr. sc. Dubravka Matković–Čalogović, Dr. sc. Ivan Janotka

Rad prihvaćen: 09. listopada 2019.

Ocjenitelji: izv. prof. dr. sc. Sanda Rončević, MPF, Zagreb  
prof. dr. sc. Dubravka Matković–Čalogović, PMF, Zagreb  
doc. dr. sc. Jelena Bleiziffer, Građevinski fakultet, Zagreb  
zamjena: dr.sc. Goran Štefanić, zn. savj., IRB Zagreb





Sveučilište u Zagrebu  
Prirodoslovno-matematički fakultet  
**Kemijski odsjek**

Doktorska disertacija

## PROŠIRENI SAŽETAK

### UVOD

Doprinos proizvodnje portlandskog cementa ukupnoj emisiji ugljikovog dioksida koji nastaje ljudskim djelovanjem iznosi od 5 % do 8 %. Zbog toga je traženje održivijih rješenja postalo jedan od ključnih pokretača istraživanja i inovacija u području portlandskog cementa [K. L. Scrivener i R. J. Kirkpatrick, *Cem. Concr. Res.* **38** (2008) 128 – 136]. Razvijeni su različiti načini značajnijeg smanjenja emisije CO<sub>2</sub> [K. L. Scrivener i R. J. Kirkpatrick, *Cem. Concr. Res.* **38** (2008) 128 – 136; C. D. Lawrence, *Proizvodnja nisko – energetskih cementa*, u: P. C. Hewlett (ur.) *Lea – Kemija Cementa i Betona četvrto izdanje*, Oxford, Elsevier, 2005, str. 421 - 470 (engleski izvornik); C. Shi, A. F. Jiménez i A. Palomo, *Cem. Concr. Res.* **41** (2011) 750 - 763]. Tradicionalna rješenja utemeljena su na poboljšanju portlandskog cementa opće namjene koji su utemeljeni na spojevima kalcijevih silikata ili aluminata. Inovativnija rješenja uključuju nove cemente utemeljene na sulfoaluminatnim, sulfoferitnim ili fluor-aluminatnim spojevima [C. Shi, A. F. Jiménez i A. Palomo, *Cem. Concr. Res.* **41** (2011) 750 - 763]. Moderno građevinarstvo utemeljeno je na normama koje su vrlo konzervativne jer im je osnovna svrha zaštita od katastrofalnih pogrešaka i gubitka života [K. L. Scrivener i R. J. Kirkpatrick, *Cem. Concr. Res.* **38** (2008) 128 – 136]. Ključan nedostatak cjelovitog pristupa u razvoju novih tipova cementa predstavlja nedostatak standardiziranih metoda ispitivanja trajnosti cementne paste.

U normalnim uvjetima cementni kompoziti imaju dobru trajnost u normalnom vijeku uporabe do 70 godina i više [J. Radić i J. Bleiziffer, *Trajnost betonskih konstrukcija*, u: J. Radić (ur.) *Betonske konstrukcije 4: Sanacije*, Hrvatska sveučilišna naklada, Građevinski fakultet Sveučilišta u Zagrebu, Secon HDGK, 2008, str. 83 – 164]. Tijekom uporabe cementa pasta može biti izložena djelovanju okoliša i degradaciji što može skratiti vijek uporabe. Deionizirana voda koja sadrži male koncentracije otopljenih iona u dodiru s portlandskom



cementnom pastom izaziva dekalifikaciju [F. Adenot i M. Buil, *Cem. Concr. Res.* **22** (1992) 489 - 496; M. Mainguy, C. Tognazzi, J. M. Torrenti i F. Adenot, *Cem. Concr. Res.* **30** (2000) 83 - 90]. Proces se naziva izluživanje. Ključne posljedice izluživanja su povećanje poroznosti i propusnosti i gubitak čvrstoće u konstrukcijama koje su mu izložene [F. P. Glasser, J. Marchand i E. Samson, *Cem. Concr. Res.* **38** (2008) 226 – 246; C. Carde, R. Francois i J. M. Torrenti, *Cem. Concr. Res.* **26** (1996) 1257 – 1268; F. H. Heukamp, F. J. Ulm i J. T. Germaine, *Cem. Concr. Res.* **31** (2001) 767 – 774; G. J. Verbeck i R. H. Helmuth, *Struktura i fizička svojstva cementne paste*, Zbornik radova s Petog međunarodnog simpozija o kemiji cementa, knjiga I, Tokyo, Japan, 1968, str. 1 - 32]. Opći pristup ispitivanju otpornosti portlandske cementne paste prema izluživanju nije još razvijen. Osobito nedostaju ispitivanja u kojima su kemijski i mineraloški sastavi povezani s mehaničkim svojstvima kao što su čvrstoća, modul elastičnosti, dimenzije i slično. Nedostatak pouzdane procedure provjere otpornosti portlandske cementne paste prema izluživanju, sprječava uvođenje novih vrsta cementa u postojeće norme.

Ciljevi ovog rada su:

- odrediti promjene u kemijskom i faznom sastavu i mikrostrukturi nezrelih cementnih pasta različitog početnog kemijskog i mineraloškog sastava izloženih izluživanju deioniziranom vodom, bez zaustavljanja hidratacije;
- odrediti promjenu mehaničkih i fizičkih svojstava: čvrstoće, modula elastičnosti, dimenzionalne i masene stabilnosti izazvanih izluživanjem;
- odrediti utjecaj početnog sastava cementa na proces izluživanja i utjecaj izluživanja na proces hidratacije;
- odrediti mogućnost upotrebe elemenata u tragovima u ispitivanjima izluživanja;
- određivanje mogućnosti provođenja ispitivanja izluživanja na nezrelim cementnim pastama u djelomično otvorenom sustavu.

Osnovna hipoteza rada je da otpornost cementne paste djelovanju deionizarne vode ovisi o svojstvima svih sastavnica cementne paste: hidratacijskim produktima, pornoj otopini i sustavu pora. Ta su svojstva određena faznim sastavom nehidratiziranog cementa i uvjetima njegovanja u kojima se odvijaju kemijske reakcije.

U istraživanju za određivanje faznog sastava nehidratiziranog cementa i za praćenje promjena faznog sastava cementne paste s protekom vremena upotrebljena je rendgenska difrakcija. Kemijski sastav (glavni, sporedni i elementi u tragovima) određeni su metodama

---

---

mokre kemije ili spektrometrijom masa s induktivno spregnutom plazmom. Promjene u mikrostrukturi određene su pretražnim elektronskim mikroskopom, određivanjem sadržaja zraka u mikroporama, određivanjem kapilarnog upijanja vode i određivanjem plinopropusnosti. Kemijska otpornost cementne paste prema djelovanju deionizirane vode praćena je promjenama u čvrstoći, modulu elastičnosti, dimenzionalnoj i masenoj stabilnosti. Znanje o međuovisnosti sastava cementa, cementne paste, porne otopine, mikrostrukture cementne paste, uvjeta njegovanja i otpornosti djelovanju deionizirane vode može pomoći u oblikovanju novih tipova cementa s manjim utjecajem na okoliš.

---

## LITERATURNI PREGLED

### Portlandski cement

Cementom se općenito nazivaju povezujući dijelovi kompozitnog materijala, obično betona, morta ili cementne paste [A. Đureković, *Cement i cementni kompoziti i dodaci za beton*, Školska knjiga, Zagreb, 1996, str. 1-20]. Cement je praškasti materijal koji u dodiru s vodom kemijskim i fizikalnim procesima, prelazi u očvrslu cementnu pastu. Portlandski cement se proizvodi mljevenjem portlandskog cementnog klinkera uz dodatak nekoliko postotaka gipsa [V. Ukrainczyk, *Beton*, Alcor, Zagreb, 1994, str. 11 – 39].

Portlandski cement je izumljen početkom 19. stoljeća. Izum je djelomično utemeljen na graditeljskom znanju iz doba Grčke i Rima [R. G. Blezard, *Povijest kalcijskog cementa*, u: P. C. Hewlett (ur.) *Lea – Kemija Cementa i Betona četvrto izdanje*, Oxford, Elsevier, 2005, str. 1 - 23 (engleski izvornik)]. Danas je portlandski cement u obliku konačnog proizvoda, betona, najviše korišten materijal u graditeljstvu [P. K. Mehta i P. J. M. Monteiro, *Beton: Mikrostruktura, Svojstva i Materijali*, New York, McGraw-Hill, 2006, str. 203 – 251 (engleski izvornik)]. Procijenjena svjetska proizvodnja portlandskog cementa u 2016. godini je 4,6 milijardi tona, od čega se više od 52 % proizvodi u Kini [<https://cembureau.eu/media/1716/activity-report-2017.pdf> (pristup 28. veljače 2019.)]. Proizvodnja cementa ima značajnu ulogu u ekonomskom, društvenom razvoju i razvoju okoliša.

### Sastav portlandskog cementa

Različiti spojevi kalcija nalaze se u sastavu portlandskog cementa. Kemijski sastav portlandskog cementa izražava se u obliku oksida. Oksidi kalcija (CaO), aluminijski (Al<sub>2</sub>O<sub>3</sub>) i željezni (Fe<sub>2</sub>O<sub>3</sub>) određuju kemijski sastav cementa. Kemičari se u svakodnevnom radu koriste skraćenicama za pojedine okside koje su navedene u tablici I.I. Titrimetrijske metode upotrebom etilendiamintetraoctene kiseline najčešće se koriste za određivanje sadržaja CaO, MgO, Al<sub>2</sub>O<sub>3</sub> i Fe<sub>2</sub>O<sub>3</sub> u portlandskom cementu. Selektivnost je kontrolirana s pH i maskiranjem pogodnim reagensima. Silicij se određuje tradicionalnim metodama, obradom uzorka klorovodičnom kiselinom i amonijevim kloridom kako bi se otopili drugi spojevi.

Nakon otapanja slijedi titracija i spaljivanje. Poznata metoda taloženja barijevim kloridom koristi se za određivanje sulfata.

Tablica I.I. Skraćenice oksida u portlandskom cementu

Oksid	Skraćenica
CaO	C
SiO <sub>2</sub>	S
Al <sub>2</sub> O <sub>3</sub>	A
Fe <sub>2</sub> O <sub>3</sub>	F
MgO	M
SO <sub>3</sub>	$\bar{S}$
Na <sub>2</sub> O	N
K <sub>2</sub> O	K
H <sub>2</sub> O	H

Plamena fotometrija primjenjuje se za određivanje alkalijskih elemenata, a spektrofotometrija za određivanje mangana. Kloridi se određuju taloženjem s otopinom srebrvog nitrata i povratnom titracijom s amonijevim tiocijanatom [C. D. Lawrence, *Sastav i specifikacije portlandskog cementa*, u: P. C. Hewlett (ur.) *Lea – Kemija Cementa i Betona četvrto izdanje*, Oxford, Oxford, Elsevier, 2005, str. 131 – 193 (engleski izvornik)].

Kemijski sastav portlandskog cementa nije povezan s mehaničkim svojstvima kao što je čvrstoća i konačan zaključak o portlandskom cementu ne može se izvesti iz kemijske analize. Faze koje nastaju kemijskim reakcijama na visokim temperaturama tijekom proizvodnje cementa određuju ključna svojstva portlandskog cementa [H. F. W. Taylor, *Kemija cementa drugo izdanje*, London, Thomas Telford, 1997, str. 1 – 28; P. K. Mehta i P. J. M. Monteiro, *Beton: Mikrostruktura, Svojstva i Materijali*, New York, McGraw-Hill, 2006, str. 203 – 251 (engleski izvornik); C. D. Lawrence, *Sastav i specifikacije portlandskog cementa*, u: P. C. Hewlett (ur.) *Lea – Kemija Cementa i Betona četvrto izdanje*, Oxford, Elsevier, 2005, str. 131 – 193 (engleski izvornik)].

Složena mineralogija portlandskog cementa posljedica je termodinamičkih odnosa između različitih spojeva tijekom proizvodnje portlandskog cementnog klinkera. Četiri glavne faze prisutne u portlandskom cementu su: alit, belit, aluminat i ferit. Skraćenice koje se koriste za

jednostavnije zapisivanje faza navedene su u tablici I.II. [H. F. W. Taylor, *Kemija cementa drugo izdanje*, London, Thomas Telford, 1997, str. 1 - 28].

Tablica I.II. Skraćenice portlandskih cementnih faza

Faza	Skraćenica	Ime
$3\text{CaO}\cdot\text{SiO}_2$	$\text{C}_3\text{S}$	Trikalcijev silikat, alit
$2\text{CaO}\cdot\text{SiO}_2$	$\text{C}_2\text{S}$	Dikalcijev silikat, belit
$3\text{CaO}\cdot\text{Al}_2\text{O}_3$	$\text{C}_3\text{A}$	Trikalcijev aluminat, aluminat
$4\text{CaO}\cdot\text{Al}_2\text{O}_3\cdot\text{Fe}_2\text{O}_3$	$\text{C}_4\text{AF}$	Tetrakalcijev aluminoferit, ferit
$\text{CaSO}_4 \times 2\text{H}_2\text{O}$	$\text{C}\bar{\text{S}}\text{H}_2$	gips

Faze prisutne u portlandskom cementu modificirane su u sastavu i kristalnoj strukturi zamjenom ionima koji su manje zastupljeni poput magnezija, natrija, kalija i sulfata. Identificirano je sedam različitih polimorfa alita i pet različitih polimorfa belita [H. F. W. Taylor, *Kemija cementa drugo izdanje*, London, Thomas Telford, 1997, str. 1 - 28]. Visokotemperturne modifikacije alita i belita mogu se izolirati na nižim temperaturama samo ako su stabilizirane većom količinom supstituirajućih iona. U industrijski proizvedenim portlandskim cementnim klinkerima prisutne su monoklinske modifikacije alita ( $\text{M}_1$  i  $\text{M}_3$ ) ili njihova smjesa. Belit se u industrijski proizvedenim portlandskim cementnim klinkerima najčešće nalazi u obliku  $\beta$  – polimorfa, a trikalcijev aluminat u kubičnom ili rompskom kristalnom sustavu. Ferit tvori niz čvrstih otopina općeg sastava  $\text{Ca}_2(\text{Al}_x\text{Fe}_{1-x})_2\text{O}_5$  gdje je  $0 < x < 0,7$ . Dio magnezija ugrađuje se u glavne faze (do 2 %), a dio kristalizira kao MgO, periklas. Slobodni kalcijev oksid rjeđe je prisutan u suvremenim portlandskim cementima. Obje faze imaju kubičnu strukturu. Alkalijski metali su prisutni u obliku dvostrukih sulfata ili se ugrađuju u alit i belit u slučajevima kada nema dovoljno sulfata [H. F. W. Taylor, *Kemija cementa drugo izdanje*, London, Thomas Telford, 1997, str. 1 - 28].

Fazni sastav cementa moguće je izračunati iz kemijskog sastava cementa upotrebom formula po Bogueu:

$$C_3S = 4.0710C - 7.6024S - 6.7187A - 1.4297F$$

$$C_4AF = 2.8675S - 0.7544C_3S$$

$$C_3A = 2.6504A - 1.6920F$$

$$C_4AF = 3.0432F \text{ [ R. H. Bogue, } \textit{Ind. Eng. Chem.} \textbf{1} \text{ (1929) 192 – 197].}$$

Bogueov izračun utemeljen je na pretpostavci da su četiri osnovne faze prisutne u klinkeru kemijski čiste, odnosno da sadrže samo CaO, SiO<sub>2</sub>, Al<sub>2</sub>O<sub>3</sub>, Fe<sub>2</sub>O<sub>3</sub> i SO<sub>3</sub>. Ovo je najveći izvor nesigurnosti Bogueovog izračuna, jer su faze prisutne u portlandskom cementu čvrste otopine čiji sastav odstupa od sastava čistih faza [G .L. Saoût, V. Kocaba i K. Scrivener *Cem. Concr. Res.* **41** (2011) 133 – 148]. Postojanje i drugih manje zastupljenih individualnih faza također utječe na točnost proračuna [G .L. Saoût, V. Kocaba i K. Scrivener *Cem. Concr. Res.* **41** (2011) 133 – 148].

Rendgenska difrakcija na prahu je jedina metoda kojom se može odrediti fazni sastav klinkera, cementa i hidratizirane cementne paste [H. F. W. Taylor, *Kemija cementa drugo izdanje*, London, Thomas Telford, 1997, str. 1 - 28]. Primjena rendgenske difrakcije na prahu moguća je jer svaka faza prisutna u cementu ima svoj specifični difraktogram. U primjeni rendgenske difrakcije na cementu postoje određeni izazovi koji proizlaze iz same metode i prirode materijala. Difraktogrami portlandskog cementa vrlo su kompleksni zbog mnogobrojnih preklapanja difrakcijskih maksimuma s difrakcijskim maksimumima alita kao najzastupljenijom fazom u portlandskom cementu [C. D. Lawrence, *Sastav i specifikacije portlandskog cementa*, u: P. C. Hewlett (ur.) *Lea – Kemija Cementa i Betona četvrto izdanje*, Oxford,, Oxford, Elsevier, 2005, str. 131 – 193 (engleski izvornik)]. Promjene u sastavu i strukturi svake od faza, značajno utječu na položaj i intenzitet pojedinih difrakcijskih maksimuma u difraktogramu. Glavni izvori sustavnih i slučajnih pogrešaka su: pomicanje uzorka, preferirana orijentacija i ograničena dubina interakcije rendgenskih zraka. Pomicanje uzorka uzrokuje pomicanje difrakcijskih maksimuma u difraktogramu i ne utječe značajnije na njihov intenzitet. Preferirana orijentacija utječe na intenzitet difrakcijskih maksimuma. Ako je područje neke faze usporedivo s dubinom prodiranja moguće je da jedna ili više faza dominiraju u uzorku [M. A. G. Aranda , A. G. De la Torre i L. León – Reina, *Rew. Mineral. Geochem.* **74** (2012) 169 - 209]. Sva tri izvora greške mogu se značajno reducirati smanjenjem veličine čestica u uzorku. Pogreške uzrokovane pomicanjem uzorka mogu se

smanjiti i upotrebom internog standarda kao što su rutil, silicij, kalijev bromid, kalcijev fluorid i korund [H. F. W. Taylor, *Kemija cementa drugo izdanje*, London, Thomas Telford, 1997, str. 1 - 28 (engleski izvornik); H. F. W. Taylor, *Adv. Cem. Res.* **2** (1989) 73 - 77]. Mljevenje je vrlo zahtjevno jer može rezultirati oštećenjem faza i smanjenjem kristaliničnosti što može utjecati na proširenje difrakcijskih maksimuma.

Snimanje i karakterizacija rendgenograma portlandskog cementa zahtjeva puno vještine i iskustva. Zbog toga se rendgenska difrakcija desetljećima primjenjivala za kvalitativnu, a ne za kvantitativnu analizu. Danas se za kvantitativnu analizu najčešće primjenjuje Rietveldova metoda koja je primjenjiva na klinkeru, cementu i hidratiziranoj cementnoj pasti [G. L. Saoût, V. Kocaba i K. Scrivener *Cem. Concr. Res.* **41** (2011) 133 – 148; A. I. Boikova, *Kemijski sastav sirovina kao glavni čimbenik odgovoran za sastav, strukturu i svojstva klinkerskih faza*, Zbornik radova Osmog međunarodnog simpozija o kemiji cementa, knjiga I, Rio de Janeiro, Brasil, 1986, str. 19 - 33 (engleski izvornik)]. Posebno razvijeni računalni programi olakšavaju primjenu Rietveldove metode. Rezultati dobiveni Rietveldovom metodom precizniji su, a moguće ju je primjeniti i u ispitivanjima trajnostnih svojstava [M. A. G. Aranda, A. G. De la Torre i L. León – Reina, *Rew. Mineral. Geochem.* **74** (2012) 169 - 209].

Primjena rendgenske difrakcije na hidratiziranim cementnim pastama ograničena je činjenicom da je glavni produkt hidratacije portlandskog cementa gotovo potpuno amorfan. No može se primijeniti na druge kristalinične faze poput portlandita, etringita, nehidratiziranih klinkerskih faza ili manje zastupljenih individualnih faza [I. G. Richardson, *Cem. Concr. Res.* **38** (2008) 137 - 158]. Rendgenska difrakcija *in-situ* uspješno je primijenjena tehnika koja omogućava praćenje hidratacije u vremenu bez utjecaja na uzorak.

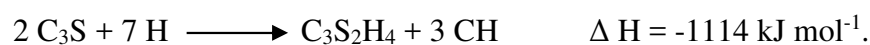
Svi elementi koji su u portlandskom cementu prisutni u koncentracijama manjim od nekoliko postotaka smatraju se elementima u tragovima [M. Achternbosch, K. R. Bräutigam, N. Hartliebe; C. Kupsch, U. Richers, P. Stemmermann, i M. Gleis., *Teški metali u cementu i betonu kao rezultat suspaljivanja otpada u cementnoj peći u odnosu na zakonske zahtjeve za upotrebu otpada*, FZK, Karlsruhe, **2003**, str. 15 – 105 (engleski izvornik)]. Povećana upotreba otpada kao sirovine ili goriva u proizvodnji cementa povećala je interes za elemente u tragovima koji se ugrađuju u portlandski cement. Neki od njih su toksični ili kancerogeni (arsen, kadmij, kobalt, krom, bakar, živa, nikal, olovo) ili predstavljaju značajan rizik u radu (krom, kobalt, nikal) [S. Bodaghpour, N. B. Joo i S. Ahamdi, *Int. J. Geol.* **6** (2012) 62 - 67]. Prijelazni metali (kobalt, krom, bakar, mangan, nikal, vanadij, titan, cink) imaju utjecaj na

---

proces nastajanja klinkera i svojstva konačnog proizvoda [C. J. Engelsen, *Utjecaj mineralizatora na proizvodnju cementa*, Concrete Innovation Centre, Trondheim, 2007, str. 4 - 15]. Elementi u tragovima mobiliziraju se u osnovnim fazama klinkera kada su prisutni u niskim koncentracijama. Kada im se koncentracija poveća, nastaju nove faze. Mehanizam ugradnje ovisi i o oksidacijskom stanju elementa koji je posljedica kemijskog sastava materijala i proizvodnih uvjeta [D. Herfort, G. K. Moir, V. Johansen, F. Sorrentino i H. Bollio - Arceo, *Adv. Cem. Res.* **22** (2010) 187 - 194].

## Hidratacija portlandskog cementa

Hidratacija portlandskog cementa uključuje sve reakcije između cementa i vode. Mješavina cementa i vode naziva se cementnom pastom, a uključuje i očvrslu materijal. Omjer vode i cementa ili vodocementni faktor određuje mnoga svojstva portlandske cementne paste [H.F.W. Taylor, *Kemija cementa drugo izdanje*, London, Thomas Telford, 1997, str.113 - 156]. Interpretacija složenih reakcija hidratacije portlandskog cementa moguća je jedino uz poznavanje hidratacije pojedinačnih faza klinkera. Složena reakcija hidratacije alita može se pojednostavljeno prikazati slijedećom jednažbom:



Glavni produkti koji nastaju ovom egzotermnom reakcijom su kalcijev hidroksid (CH) kojeg obično zovemo portlandit i kalcijev silikat hidrat obično označen kao C-S-H [A. Đureković, *Cement i cementni kompoziti i dodaci za beton*, Školska knjiga, Zagreb, 1996, str. 21 - 251]. Približno 70 % alita reagira unutar 28 dana, a gotovo sav za godinu dana [H. F. W. Taylor, *Kemija hidratacije cementa*, Zbornik Osmog međunarodnog simpozija o kemiji cementa, knjiga I, Rio de Janeiro, 1986, str. 82 - 110]. Kalcijev silikat hidrat je amorfan ili slabo kristaliničan. Crtece u njegovom imenu označavaju da je odnos između pojedinih komponenti (C/S i H/S) promjenjiv. Sastav ovisi o uvjetima nastajanja i mijenja se tijekom hidratacije [H.F.W. Taylor, *Kemija cementa drugo izdanje*, London, Thomas Telford, 1997, str.113 – 156; A. Đureković, *Cement i cementni kompoziti i dodaci za beton*, Školska knjiga, Zagreb, 1996, str. 21 - 251]. Kalcijevi silikati hidrati mogu se naći u prirodi, sintetizirati u laboratoriju ili nastati tijekom hidratacije portlandskog cementa [J. J. Chen, J. J. Thomas, H. F. W. Taylor i H. M. Jennings, *Cem. Concr. Res.* **34** (2004) 1499 - 1519]. Struktura i velika specifična površina C-S-H omogućava mu da zajedno s pornim otopinama stvara rigidan gel u kojem se pore mijenjaju od makroskopskih do nanometarskih. Izraz C-S-H gel koristi se samo



kada je nastao hidratacijom portlandskog cementa. Primarno je odgovoran za razvoj mehaničkih svojstava portlandske cementne paste. Rendgenski difraktogram C-S-H gela pokazuje nepostojanje uređene strukture [H.F.W. Taylor, *Kemija cementa drugo izdanje*, London, Thomas Telford, 1997, str. 113 – 156; A. Đureković, *Cement i cementni kompoziti i dodaci za beton*, Školska knjiga, Zagreb, 1996, str. 21 - 251]. Usporedbom strukture kristaliničnih hidrata 1,4-nm tobermorita i jenita prikupljeno je dosta podataka o nanostrukтури C-S-H gela [J .J. Chen, J. J. Thomas, H. F. W. Taylor i H. M. Jennings, *Cem. Concr. Res.* **34** (2004) 1499 - 1519]. Difraktogram C-S-H gela ne daje nam jednoznačan dokaz koja od dvije navedene strukture bolje odgovara strukturi C-S-H gela. Dokazi prikupljeni drugim metodama podupiru pretpostavku da je struktura C-S-H gela u početku hidratacije smjesa obje strukture, a s protekom vremena prevladava struktura jenita [H. F. W. Taylor, *J. Am. Ceram. Soc.* **69** (1986) 464 - 467]. Pretražnom elektronskom mikroskopijom potvrđeno je postojanje četiri morfološka oblika C-S-H gela:

- Tip I: vlaknasti materijal duljine do 2 μm dominantan u ranoj fazi hidratacije;
- Tip II: saćasti ili mrežasti materijal tipčan za ranu hidrataciju;
- Tip III: masivna ili dobro zbijena sferična zrna veličine do 300 nm uočena u starijim pastama;
- Tip IV: bezobličan i masivan produkt uočen u starijim pastama

[S. Diamond, *Mikrostruktura cementne paste – pregled na nekoliko nivoa: u Hidraulične cementne paste: struktura i svojstva*, Zbornik radova konferencije održane na Sveučilištu u Sheffieldu, 8 – 9 travnja 1976., Slough: Cement and Concrete Association; 1976. str. 2 – 30].

Hidratacijom belita nastaju isti produkti kao i hidratacijom alita. Samo 30 % belita reagira unutar 28 dana, a 90 % unutar godine. Reakcija hidratacije može se prikazati pojednostavljenom jednadžbom:



Iz jednadžbe je vidljivo da nastaje značajnije manja količina CH i da je relativni udio C-S-H gela veći. Nema razlike u rastu, morfologiji i sastavu C-S-H gela nastalog hidratacijom alita i belita [H. E. Petch, *Acta. Cryst.* **14** (1961) 950 – 957; R. J. Bartlett i G. D. Purvis, *Int. J. Quantum Chem.* **14** (1978) 561 – 581]. Kalcijev hidroksid ima slojevitú strukturu s oktaedarski koordiniranim atomima kalcija i tetraedarski koordiniranim atomima kisika [J.D. Bernal i H. D. Megaw, *Proc. Roy. Soc.* **A151** (1935) 384 – 420; H. E. Petch, *Acta. Cryst.* **14** (1961) 950 – 957]. Čisti C<sub>3</sub>A reagira trenutno s vodom, pri čemu se oslobađa velika

količina topline. Reakcijom nastaju kristalni produkti kao što su  $C_3AH_6$ ,  $C_4AH_{19}$  i  $C_2AH_8$  [H.F.W. Taylor, *Kemija cementa drugo izdanje*, London, Thomas Telford, 1997, str.113-156; A. Đureković, *Cement i cementni kompoziti i dodaci za beton*, Školska knjiga, Zagreb, 1996, str. 21 - 251]. Kada  $C_3A$  reagira s vodom u prisutnosti kalcijevog sulfata, nastaje etringit koji u daljnjoj reakciji stvara aluminat ferat monosulfatne faze (AFm faze). Reakcije se mogu prikazati slijedećim jednadžbama:



$C_3A + C_6A\bar{S}_3H_{32} + 4 H \longrightarrow 3 C_4A\bar{S}H_{12}$  [H.F.W. Taylor, *Kemija cementa drugo izdanje*, London, Thomas Telford, 1997, str.113 – 156].

Etringit ( $C_6A\bar{S}_3H_{32}$ ) je prvi kristalni hidrat koji nastaje u hidratiziranoj cementnoj pasti, približno 30 minuta od početka reakcije. U periodu od 24 do 48 sati, etringit reagira dalje i stvara AFm faze. Hidratacijom  $C_4AF$  nastaju produkti koji su slični onima koji nastaju hidratacijom  $C_3A$  [H.F.W. Taylor, *Kemija cementa drugo izdanje*, London, Thomas Telford, 1997, str.113 – 156]. Etringit pripada aluminat ferat trisulfatnim fazama (AFt faze) opće formule  $[Ca_3(Al,Fe)(OH)_6 \cdot 12H_2O]_2 \cdot X_3 \cdot xH_2O$  gdje je  $x$  normalno  $\leq 2$  i gdje  $X$  predstavlja jedan dvostruko nabijeni anion ili dva jednostruko nabijena aniona. Faza AFm u portlandskom cementu je slabo kristalinična i pomiješana sa C-S-H gelom. Opća formula AFm faze je  $CaAl(OH)_6 \cdot X \cdot nH_2O$  gdje  $X$  predstavlja jedan jednostruko nabijeni ili polovicu dvostruko nabijenog aniona. Hidratacija aluminatne i feritne faze vrlo je važna jer određuje vezivanje cementa, reološka svojstva svježje portlandske cementne paste i rano očvršćivanje.

Hidratacija portlandskog cementa je vrlo slična hidrataciji čistog  $C_3S$ . Osnovni produkti C-S-H gel i CH koji nastaju hidratacijom kalcijevih silikata i AFt i AFm faze koje nastaju hidratacijom aluminatne i feritne faze također su prisutni u hidratiziranoj portlandskoj cementnoj pasti. Klinkerske faze troše se različitim brzinama, kalcijevi sulfati obično nisu više prisutni nakon 24 sata. U difraktogramu praha difrakcijski maksimumi koji odgovaraju etringitu obično se uočavaju nakon nekoliko sati i dostižu svoj maksimum nakon 1 dana. Difrakcijski maksimumi koji odgovaraju AFm fazi pojavljuju se kasnije. Obično su vrlo široki što sugerira da je AFm faza slabo kristalinična [H. F. W. Taylor, *Kemija cementa drugo izdanje*, London, Thomas Telford, 1997, str. 187 - 225]. U cementnim pastama portlandskog cementa s visokim omjerom  $\bar{S}/A$  ili u pastama sulfatno otpornih cementa etringit je detektiran i nakon godine dana hidratacije. Karbonatizacija hidratizirane portlandske

cementne paste također izaziva nastajanje etringita u kasnijem periodu hidratacije [G. Strohmaier i H.J. Kuzel, *ZKG Int.* **41** (1988) 358 - 360].

### **Mikrostruktura očvrslje portlandske cementne paste**

Očvrsla portlandska cementna pasta ima svojstva rigidnog gela. To je čvrsta krutina visoke poroznosti. Očvrslu portlandsku cementnu pastu izgrađuju hidratacijski produkti, neizreagirana zrna cementa, kapilarne pore i vodena otopina zvana porna otopina [A. Đureković, *Cement i cementni kompoziti i dodaci za beton*, Školska knjiga, Zagreb, 1996, str. 21 – 251; H. F. W. Taylor, *Kemija cementa drugo izdanje*, London, Thomas Telford, 1997, str. 227- 259]. Vodu u očvrslj portlandskoj cementnoj pasti dijelimo na isparivu i neisparivu. Neispariva voda je ugrađena unutar hidratacijskih produkata i ponekad se koristi kao mjera za stupanj hidratacije. Ispariva voda ispunjava kapilarne pore i gel-pore u hidratacijskim produktima [T. C. Powers, *Fizička svojstva cementne paste*, Zbornik radova Četvrte međunarodne konferencije o kemiji cementa, knjiga 2, Washington, USA, 1960, str. 577 - 613. (engleski izvornik)]. Ukupna poroznost očvrslje cementne paste uključuje sve tipove pora: otvorene (prohodne i vrećaste) i zatvorene [A. Đureković, *Cement i cementni kompoziti i dodaci za beton*, Školska knjiga, Zagreb, 1996, str. 21 - 251]. Prema IUPAC-ovom prijedlogu pore u očvrslj portlandskoj cementnoj pasti dijele se na mikropore promjera manjeg od 2,6 nm, mezopore ili kapilarne pore promjera između 2,6 i 50 nm i makro pore promjena većeg od 50 nm [IUPAC Priručnik o simbolima i terminologiji, Dodatak 2, Dio 1, Koloidna i površinska kemija, *Pure Appl.Chem.*, **31** (1972) 578 - 638 (engleski izvornik)].

Veza između nekih svojstava koja opisuju poroznost i mehaničkih svojstava cementa opširno je proučavana. Powers je uspostavio vezu između tlačnih čvrstoća i odnosa između volumena hidratacijskih produkata i kapilarne poroznosti. Razvijeni su mikrostrukturni modeli koji povezuju mehanička svojstva i mikrostrukturu cementne paste. Vrlo malo istraživanja usmjereno je prema objašnjenju kako priroda hidratacijskih produkata utječe na mehanička svojstva cementne paste. Razlog su poteškoće u kvantifikaciji volumena kojeg različite hidratizirane faze zauzimaju u hidratiziranoj cementnoj pasti i nedostatku modela koji mogu povezati fazni sastav s mehaničkim svojstvima. Nedavno je utvrđeno da svi hidratacijski produkti ne pridonose tlačnim čvrstoćama. C-S-H gel ima kritičnu ulogu u odnosu na druge hidratacijske produkte. Ovo je objašnjeno činjenicom da je C-S-H gel pomiješan s porama odnosno da su druge faze samo umetnute u matriks kojeg čine C-S-H i

pore. [H.F.W. Taylor, *Kemija cementa drugo izdanje*, London, Thomas Telford, 1997, str.113 - 156].

Pretražna elektronska mikroskopija može dati vrlo važne informacije o mikrostrukтури očvrste cementne paste. Moguće je koristiti široki raspon povećanja od 20× do 10 000× što omogućava promatranje morfologije hidratacijskih produkata. Pretražni elektronski mikroskopi obično su opremljeni tako da mogu napraviti rendgensku mikroanalizu koja omogućava identifikaciju različitih mikrostrukturnih sastavnica [S. Diamond, *Cem. Concr. Comp.* **26** (2004) 919 – 933; K. L. Scrivener, *Cem. Concr. Comp.* **26** (2004) 935 – 945].

Nakon hidratacije, elementi u tragovima iz nehidratiziranog cementa prelaze u hidratacijske produkte. Struktura i sastav hidratacijskih produkata potiče ugradnju elemenata u tragovima različitim mehanizmima: kemisorpcijom, taloženjem, stvaranjem površinskih produkata, inkluzijom i kemijskom ugradnjom [D. L. Coke i M. Y. A. Mollah, *J. Hazard. Mater.* **24** (1990) 231 - 253]. Mnogi elementi u tragovima prisutni su u hidratiziranoj portlandskoj cementnoj pasti u obliku individualnih faza: hidroksida, karbonata i miješanih nitratnih soli [F. K. Cartledge, L. G. Butler, D. Chalasani, H. Eaton, F. P. Frey, E. Herrera, M. T. Tittlebaum i S. Yang, *Environ. Sci. Technol.* **24** (1990) 867 - 873]. Manji dio elemenata u tragovima otopljeno je u pornoj otopini prisutnoj u kapilarnim porama hidratizirane cementne paste.

Porna otopina je osnovni, ali vrlo često zanemareni sastojak hidratizirane cementne paste. Sastav porne otopine odražava kemijske procese i interakciju između čvrste i tekuće faze. Kemijski sastav porne otopine može biti koristan za razumijevanje mehanizma i kinetike hidratacije cementa kao i za termodinamičko modeliranje hidratacije [A. Vollpracht, B. Lothenbach, R. Snellings i J. Haufe, *Mater. Struct.* **49** (2016) 3341 - 3367]. Porna otopina odgovorna je za transport tvari unutar portlandske cementne paste i služi kao ulaz za tvari izvana. Zbog toga se sastav porne otopine može koristiti za vrednovanje različitih destruktivnih djelovanja povezanih s trajnošću [R. D. Hooton, M. D. A. Thomas i T. Ramlochan, *Adv. Cem. Res.* **22** (2010) 203 - 210]. Porna otopina smatra se otopinom alkalijskih hidroksida jer su najzastupljeniji ioni u pornoj otopini hidroksidni ioni, ioni kalija, natrija, kalcija, ortosilikatni i aluminatni ion.

Koncentracija iona natrija i kalija u pornoj otopini raste s vremenom zbog procesa hidratacije i oslobađanja elemenata ugrađenih u osnovne faze klinkera. Maksimalnu koncentraciju dosežu oko 7 dana hidratacije. Nakon maksimuma, koncentracija oba elementa

---

malo opada dok ne dosegnu konstantnu vrijednost koju dugoročno zadržavaju. Koncentracija alkalija u pornoj otopini ovisi o ukupnom sadržaju alkalija u cementu i vodocementnom faktoru. Koncentracija hidroksidnih iona povezana je s koncentracijom alkalija. Obično se izražava u obliku vrijednosti pH. Povećanjem koncentracije alkalijskih iona povećava se i vrijednost pH. Koncentracija hidroksidnih iona ovisi o vodocementom faktoru. Koncentracija iona kalcija i sulfatnih iona ovisi o produktu topljivosti faza prisutnih u određenom hidratacijskom vremenu. Dugoročno, koncentraciju kalcijevih iona određuje topljivost portlandita, pa zbog efekta zajedničkog iona ona ovisi o vrijednosti pH otopine. Etringit ograničava topljivost iona sulfata koja značajnije ne ovisi o pH vrijednosti otopine [A. Vollpracht, B. Lothenbach, R. Snellings i J. Haufe, *Mater. Struct.* **49** (2016) 3341 - 3367]. Ispitivanja sadržaja elemenata u tragovima u pornim otopinama slabo su dostupna.

### **Proizvodnja portlandskog cementa**

Portlandski cement se proizvodi nizom međusobno povezanih operacija jednim od četiri moguća procesa: mokri proces, polumokri proces, polusuhi proces i suhi proces.

Osnovna razlika među procesima je u načinu pripreme sirovine. U polusuhom i suhom procesu, sirovine se suše i melju u praškasti materijal, nazvan sirovinsko brašno. U polumokrom i mokrom procesu sirovina se pretvara u emulziju. Suhi proces je pogodniji jer je energetski učinkovitiji zbog toga što ne zahtijeva energiju za isparavanje vode iz emulzije tijekom proizvodnje [Institute for Prospective Technological Studies, Sustainable Production and Consumption Unit, European IPPC Bureau, *Najbolje primjenjive tehnike*, Referentni dokument za proizvodnju cementa, vapna i magnezija, 2013]. Jeftini materijali kao što su vapnenac, lapor, dolomit, glina i pijesak obično se koriste za pripremu sirovine. Ponekad je potrebno dodati boksit ili rudu željeza da bi se osigurale količine aluminijske i željezne potrebne za stvaranje kalcijevih aluminata ili alumoferita [H. F. W. Taylor, *Kemija cementa drugo izdanje*, London, Thomas Telford, 1997, str. 1 – 28; G. J. Verbeck i R. H. Helmuth, *Struktura i fizička svojstva cementne paste*, Zbornik radova s Petog međunarodnog simpozija o kemiji cementa, knjiga I, Tokyo, Japan, 1968, str. 1 - 32]. Sirovinsko brašno (ili emulzija) zagrijevaju se na 1450 °C u rotacijskoj peći pri čemu nastaju tamne kuglice portlandskog cementnog klinkera. Potrebna toplinska energija osigurava se sagorijevanjem fosilnih goriva. Alternativna goriva dobivena iz industrijskih izvora kao što su gume, otpadna ulja, plastika, otapala i mnogi drugi materijali mogu se koristiti kao zamjena za fosilna goriva. Proizvedeni

klinker melje se uz dodatak nekoliko postotaka gipsa u portlandski cement. Cement se distribuira kupcima u rasutom stanju ili u vrećama kamionskim prijevozom, vlakom ili brodom.

Glavni izvori emisije CO<sub>2</sub> u proizvodnji su dekarbonatizacija, sagorijevanje goriva i indirektna emisija. Preko 50 % emisija CO<sub>2</sub> u proizvodnji cementa otpada na dekarbonatizaciju, jednostavnu reakciju transformacije vapnenca u vapno:



[[https://cembureau.eu/media/1500/cembureau\\_2050roadmap\\_lowcarboneyconomy\\_2013-09-01.pdf](https://cembureau.eu/media/1500/cembureau_2050roadmap_lowcarboneyconomy_2013-09-01.pdf) (pristup 28. veljače 2019)].

Smanjenje emisije CO<sub>2</sub> iz dekarbonatizacije najizazovnije je zadatak u proizvodnji portlandskog cementa. Ako cjelokupan kalcij dolazi iz vapnenca, za proizvodnju 1 t portlandskog cementnog klinkera potrebno je 1,26 t vapnenca pri čemu se oslobodi približno 526 t CO<sub>2</sub> [L. Bacarello, J. Kline, G. Walenta i E. Gartner, *Mater. Struct.* **47** (2014) 1055 – 1065]. Tradicionalni pristupi smanjenju dekarbonatizacijskog CO<sub>2</sub> ograničeni su na povećanje hidrauličke aktivnosti portlandskog cementa i proizvodnju miješanih cementa [C. D. Lawrence, *Proizvodnja nisko – energetske cemenata*, u: P. C. Hewlett (ur.) *Lea – Kemija Cementa i Betona četvrto izdanje*, Oxford, Elsevier, 2005, str. 421 - 470 (engleski izvornik)]. Dodavanje nekih elemenata poput fluorida (F<sup>-</sup>) u malim količinama sirovini za proizvodnju klinkera može poboljšati hidrauličku aktivnosti cementa i omogućiti upotrebu manjih količina portlandskog cementa u proizvodnji betona. U proizvodnji miješanog portlandskog cementa dio klinkera zamjenjuje se materijalima koji imaju slična svojstva poput: prirodnih pucolana, letećeg pepela, granulirane zgure visoke peći, silikatne prašine ili vapnenca. Upotreba zamjenskih materijala je utemeljena na mnogobrojnim znanstvenim istraživanjima. CO<sub>2</sub> otisak pojedinih klinkerskih faza opada u nizu C<sub>3</sub>S > C<sub>3</sub>A > C<sub>2</sub>S > C<sub>4</sub>AF [L. Bacarello, J. Kline, G. Walenta i E. Gartner, *Mater. Struct.* **47** (2014) 1055 – 1065]. Alternativna rješenja uključuju proizvodnju klinkera upotrebom sustava utemeljenih na sulfoaluminatima, sulfoferitima i fluoroaluminatima.

### **Kalcijev sulfoaluminatni cement**

Glavna karakteristika kalcijevog sulfoaluminatnog cementa (CSA cement) je visok sadržaj tetrakalcijevog aluminat sulfata (C<sub>4</sub>A<sub>3</sub>S̄) poznatog kao jelimit ili Kleinova sol. Ovaj tip cementa potječe iz Kine gdje je razvijen početkom 1970-ih [L. Zhang, M. Su i Y. Wang, *Adv.*

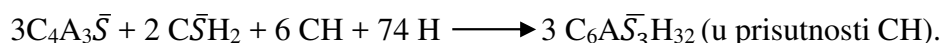
*Cem. Res.* **11** (1999) 15 – 21; T. Sui and Y. Yao, *Suvremeni napredak u posebnim cementima u Kini*, Zbornik radova Jedanaestog međunarodnog kongresa o kemiji cementa, knjiga 4, Durban, South Africa, 2003, str. 2028 - 2032 (engleski izvornik)]. Druge osnovne faze prisutne u CSA cementu su  $C_2S$  i  $C\bar{H}_2$  i neke manje zastupljene kao što su  $CA$ ,  $C_3A$ ,  $C_4AF$ , majanit i gelenit [J. Péra i J. Ambroise, *Cem. Concr. Res.* **34** (2004) 671 - 676.; D. Gastaldi, F. Canonico i E. Boccaleri, *J. Mater. Sci.* **44** (2009) 5788 - 5794., W. Lan and F.P. Glasser, *Adv. Cem. Res.* **8** (1996) 127 - 134].

Nema europske norme za cemente koje sadrže jelimit, pa se CSA cementi mogu podijeliti u tri različite grupe ovisno o ukupnom sadržaju jelimita:

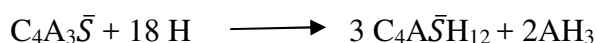
- kalcijev sulfoaluminatni cement s visokim sadržajem jelimita;
- belitni kalcijev sulfoaluminatni cement;
- alitni kalcijev sulfoaluminatni cement

[M. A. G. Aranda i A .G. Dela Torre, *Sulfoaluminatni cementi*, u: F. Pacheco – Torgal, S. Jalali i J. Labrinda (ur.) *Eko -učinkovitost betona*, Cambridge, Woodhead Publishing Limited, 2013, str. 488 - 522].

Hidratacija CSA cementa je složena, no ključne su reakcije stvaranja i transformacije etringita. Etringit nastaje brzom hidratacijom jelimita prema slijedećim jednadžbama:



Ako nema gipsa reakcije teku prema slijedećim jednadžbama:



Reakcije hidratacije  $C_2S$ ,  $C_4AF$  i drugih faza odgovaraju onima u portlandskom cementu. Osnovne kristalne faze koje nastaju hidratacijom CSA cementa su etringit i monosulfat. C-S-H koji nastaje hidratacijom  $C_2S$  i aluminijev hidroksid ( $AH_3$ ) koji nastaje hidratacijom jelimita su gelovi [J. Péra and J. Ambroise, *Cem. Concr. Res.* **34** (2004) 671 - 676]. CSA cement ima manji negativan utjecaj na okoliš pa je zbog toga vrlo zanimljiv za proučavanje. Jedna trećina  $CO_2$  ispuštenog za proizvodnju  $C_3S$  ispušta se za proizvodnju  $C_4A_3\bar{S}$  (približno  $220 \text{ kg t}^{-1}$ ). Temperatura proizvodnje je približno  $200 \text{ }^\circ\text{C}$  niža od temperature potrebne za proizvodnju portlandskog cementnog klinkera. Različiti industrijski poluproizvodi ili otpadni materijali poput granulirane zgure visoke peći, crvenog mulja ili fosfogipsa mogu se koristiti kao sirovine za proizvodnju kalcijevog sulfoaluminatnog cementa [Beretka, B. De Vito, L.

Santoro, N. Sherman i G. L. Valenti, *Cem. Concr. Res.* **23** (1993) 1205 – 1214; S. Sahu i J. Majling, *Cem. Concr. Res.* **24** (1994) 1065 – 1072; J. Majling i J. Strigac, *Adv. Cem. Res.* **11** (1999) 27 – 34; P. Arjunan, M. Silsbee i D. M. Roy, *Cem. Concr. Res.* **29** (1999) 1305 - 1311]. Upotreba kalcijevog CSA cementa u Europi je vrlo ograničena zbog nedostataka odgovarajućih normi.

## Izluživanje

Hidratacijski produkti u portlandskoj cementnoj pasti su u dinamičkoj ravnoteži s pornom otopinom čiji se sastav mijenja s hidratacijom [H. F. W. Taylor, *Kemija cementa drugo izdanje*, London, Thomas Telford, 1997, str. 187 - 225]. Kad je portlandska cementna pasta izložena djelovanju kemijski agresivnog okoliša kemijski sastav hidratacijskih produkata i porne otopine se mijenja, što dovodi do urušavanja i ponovnog uspostavljanja ravnoteže, nestajanja čvrstih produkata i stvaranja novih. Ovo može imati negativan utjecaj na mehanička svojstva portlandske cementne paste, uzrokovati njenu degradaciju i konačno smanjiti njen vijek uporabe i uzrokovati lošu trajnost. Deionizirana voda koja sadrži male koncentracije otopljenih iona uzrokuje dekalifikaciju [F. Adenot i M. Buil, *Cem. Concr. Res.* **22** (1992) 489 – 496; M. Mainguy, C. Tognazzi, J. M. Torrenti i F. Adenot, *Cem. Concr. Res.* **30** (2000) 83 - 90]. Proces se naziva izluživanje. Smanjenje koncentracije iona kalcija i hidroksidnih iona u pornoj otopini izaziva hidrolizu i izluživanje hidratacijskih produkata koji sadrže kalcij [T. H. Wee, J. Zhua, H. T. Chua i S. F. Wong, *ACI. Mater. J.* **98** (2001) 184 – 193; S. Kamali, B. Gerrard i M. Moranville, *Cem. Concr. Compos.* **25** (2003) 451 - 458]. Osjetljivost prema deioniziranoj vodi opada u slijedu CH, AFm, AFt, C-S-H [M. Mainguy, C. Tognazzi, J. M. Torrenti i F. Adenot, *Cem. Concr. Res.* **30** (2000) 83 - 90]. Otapanje portlandita smanjuje pH vrijednost porne otopine i uzrokuje povećanje makro poroznosti cementne paste. Otapanje C-S-H postepeno smanjuje C/S odnos i uzrokuje povećanje mikro poroznosti. Izluživanje alkalijskih metala nema negativan utjecaj na mehanička svojstva portlandske cementne paste. U izluženoj portlandskoj cementnoj pasti dolazi do sekundarnog taloženja AFm, AFt i kalcita [F. Adenot i M. Buil, *Cem. Concr. Res.* **22** (1992) 489 – 496; T. H. Wee, J. Zhua, H. T. Chua i S. F. Wong, *ACI. Mater. J.* **98** (2001) 184 – 193; S. Kamali, B. Gerrard i M. Moranville, *Cem. Concr. Compos.* **25** (2003) 451 – 458; J. Jain i N. Neithalath, *Cem. Concr. Comps.* **31** (2009) 176 – 185; F. P. Glasser, J. Marchand i E. Samson, *Cem. Concr. Res.* **38** (2008) 226 – 246; R. D. Hooton, M. D. A. Thomas i T. Ramlochan, *Adv. Cem.*



---

*Res. 22* (2010) 203 - 210]. Povećanje poroznosti i propusnosti i gubitak čvrstoće su ključne posljedice procesa izluživanja [C. Carde, R. Francois i J. M. Torrenti, *Cem. Concr. Res.* **26** (1996) 1257 – 1268; F. H. Heukamp, F. J. Ulm i J. T. Germaine, *Cem. Concr. Res.* **31** (2001) 767 – 774; G. J. Verbeck i R. H. Helmuth, *Struktura i fizička svojstva cementne paste*, Zbornik radova s Petog međunarodnog simpozija o kemiji cementa, knjiga I, Tokyo, Japan, 1968, str. 1 - 32]. Izluživanje može utjecati na imobilizaciju elementa u tragovima, njihovu koncentraciju u pornim otopinama i mogući rizik za okoliš. Izluživanje se javlja u portlandskim cementnim pastama izloženim djelovanju pare, magle, kišnice ili podzemne vode. Izraženo je u građevinama kao što su brane, spremišta vode, cjevovodi, a posebno u skladištima nuklearnog otpada [R. D. Hooton, M. D. A. Thomas i T. Ramlochan, *Adv. Cem. Res.* **22** (2010) 203 – 210; P. K. Mehta i P. J. M. Monteiro, *Beton: Mikrostruktura, Svojstva i Materijali*, New York, McGraw-Hill, 2006, str. 203 - 251(engleski izvornik)].

---

## MATERIJALI I METODE

Ispitivanje je provedeno prema planu ispitivanja navedenim u tablici I.III.

Tablica I. III. Plan ispitivanja

Oznaka uzorka	Razdoblje hidratacije (izluživanja)	Svojstva
CEM I CEM III CSA cement	nehidratizirani	kemijski i fazni sastav, sastav*
deionizirana voda	-	električna vodljivost, pH, elementi u tragovima, kalcij i magnezij, tvrdoća, ukupno otopljene krutine
CEM I – CP**		čvrstoća (na savijanje, na tlak), modul elastičnosti,
CEM III – CP	dani: 2, 7, 28, 56, 90, 180, 360	fazni sastav, kemijski sastav, dimenzionalna stabilnost, gubitak mase
CSA cement – CP		
CEM I – CP CEM III – CP CSA cement – CP	28 dana (samo sadržaj zračnih pora) 365 dana	kapilarno upijanje vode, plinopropusnost, SEM, sadržaj zračnih pora
CEM I – CP CEM III – CP CSA cement – CP	sati: 1-48 dani: 7,14,28	<i>in – situ</i> fazni sastav
CEM I – PS*** CEM III – PS CSA cement – PS	dani: 2, 7, 28, 56, 90, 180, 360	pH, kemijski sastav, elementi u tragovima
* samo za CEM I i CEM III	** CP – cementna pasta	*** PS – porna otopina

Ispitivanja su provedena normiranim metodama ili dobro poznatim nenormiranim metodama koje se primjenjuju za karakterizaciju portlandskog cementa, morta ili betona uz neke manje modifikacije koje se odnosile na pripremu uzoraka ili vrijeme hidratacije. Metode su primijenjene i na kalcijev sulfoaluminatni cement jer posebne normirane metode za ispitivanje ovog tipa cementa nisu razvijene.

Istraživanje je provedeno na cementnim pastama pripremljenim iz portlandskog cementa CEM I 42,5R (dalje: CEM I) proizvođača Cemex, Hrvatska, sulfatnootpornog metalurškog cementa niske topline hidratacije CEM III/A 52,5 N SR LH (CEM III) proizvođača Schwenk Zement KG Njemačka i kalcijevog sulfoaluminatnog cementa Alipre® (dalje: CSA cement) proizvođača Italcementi, Italija. CEM I i CEM III odgovaraju normi HRN EN 197-1: 2012 Cement – 1 dio: Sastav, specifikacije i kriteriji sukladnosti cementa opće namjene.

Ispitivanja kemijskog sastava nehidratiziranog cementa obuhvatila su svojstva i provedena su metodama navedenim u tablici I.IV.

Tablica I.IV. Metode određivanja kemijskog sastava CEM I, CEM III i CSA cementa

Svojstvo	Točka norme HRN EN 196-2:2013
Gubitak žarenjem (950 ± 50)°C	4.4.1
Netopljivi ostatak u HCl i Na <sub>2</sub> CO <sub>3</sub>	4.4.3
Netopljivi ostatak u HCl i KOH	4.4.4
CaO	4.4.5
MgO	4.5.15
SiO <sub>2</sub>	4.5.6
Al <sub>2</sub> O <sub>3</sub>	4.5.8
Fe <sub>2</sub> O <sub>3</sub>	4.5.11
SO <sub>3</sub>	4.5.10
S <sup>2-</sup>	4.4.2
Cl	4.4.5
CO <sub>2</sub>	4.5.16
MnO	4.5.17
K <sub>2</sub> O	4.4.6
Na <sub>2</sub> O	4.5.19.4.1
Na <sub>2</sub> O <sub>ekvivalent</sub>	4.5.19.4.1
	4.5.19.6.2

Sadržaj odabranih elemenata u tragovima u polaznim cementima određen je spektrometrijom masa s induktivno spregnutom plazmom (Agilent 7800, Agilent, Santa Clara, CA, USA). Uzorci su prevedeni u otopinu mikrovalnom digestijom upotrebom smjese

nitratne kiseline, klorovodične kiseline i tetrafluoroboratne kiseline. Provedena je slijedeća procedura digestije: 20 minuta zagrijavanja do 220 °C i 15 minuta na 220 °C uz snagu od 1800 W uređaja za mikrovalnu digestiju. Određen je sastav cementa CEM I i CEM III normiranom metodom (HRI CEN/TR 196-4:2017 Metode ispitivanja cementa – 4 dio: Kvantitativno određivanje sastojaka). Za CSA cement korišteni su podaci proizvođača o sastavu jer nema metode za određivanje sastava CSA cementa. Fazni sastav cementa određen je rendgenskom difrakcijom na prahu.

Deionizirana voda pripremljena je u Laboratoriju za veziva i ekologiju primjenom sustava za čistu vodu (Direct Q UV, Merck Milipore, Njemačka). Deionizirana voda upotrijebljena je za izradu paste i njegovanje u uvjetima izluživanja. Vodljivost, ukupne otopljene krutine, pH i sadržaj kalcija, magnezija i elemenata u tragovima u deioniziranoj vodi određeni su normiranim metodama navedenim u tablici I.V. Tvrdoća je dobivena računski primjenom slijedeće formule:

$$\text{Tvrdoća} = 2.497 [\text{Ca}, \text{mgL}^{-1}] + 4.118 [\text{Mg}, \text{mg}^{-1}]$$

Tablica I.V. Metode ispitivanja deionizirane vode

Svojstvo	Norma
pH	HRN EN ISO 10523:2008
električna vodljivost	Kvaliteta vode – održavanje pH vrijednosti HRN EN 27888:2008 Kakvoća vode – Određivanje električne vodljivosti
ukupne otopljene krutine	HRN EN 15216:2008 Karakterizacija otpada – Određivanje ukupno otopljenih krutina (TDS) u vodi i eluatima
kalcij, magnezij, elementi u tragovima	HRN EN ISO 17294-2:2016 Kvaliteta vode – Primjena spektrometrije masa s induktivno spregnutom plazmom – 2 dio: određivanje odabranih elemenata uključujući uranijeve izotope

Uzorci cementnih pasti pripremljeni su miješanjem cementa i vode u kontroliranim uvjetima (temperatura  $(20 \pm 2)$  °C, vlažnost veća od 50 %). U standardnoj miješalici za mort pripremljene su cementne paste s vodocementnim faktorom 0,5 modificiranom standardnom procedurom opisanom u normi HRN EN 196-1: 2016 Metode ispitivanja cementa – 1 dio: Određivanje čvrstoće. Modifikacija se odnosila na količinu cementa (upotrijebljeno je 1000 g cementa) i količinu vode koja je prilagođena vodocementnom faktoru 0,5. Nakon procedure miješanja, pripremljena cementna pasta ugrađena je u kalupe za izradu prizmatičnih ili cilindričnih uzoraka ili u držače za *in-situ* rendgenska mjerenja. Standardni kalupi upotrebljeni su za izradu prizmatičnih uzoraka dimenzija  $40 \times 40 \times 160$  mm. Cementne paste ugrađene su u kalup bez dodatnog sabijanja i vibracije uz uklanjanje zračnih mjehurića samo nježnim udarcima. Ista vrsta kalupa s ugrađenim graničnicima iskorištena je za pripremu uzoraka za određivanje volumne stabilnosti. Ispunjeni kalupi njegovani su u komori na temperaturi  $(20,0 \pm 1,0)$  °C i relativnoj vlažnosti većoj od 90 % tijekom 24 sata. Nakon raskalupljivanja, prizmatični uzorci su smješteni u spremnike s deioniziranom vodom na način da je omjer površine uzorka i volumena bio 1:10. Voda u kojoj su se prizme njegovale mijenjana je tri puta tjedno (ponedjeljkom, utorkom, petkom) kako bi se osiguralo stalno agresivno djelovanje deionizirane vode na cementnu pastu. Prizmatični uzorci korišteni su za ispitivanja čvrstoće (na savijanje i na tlak), modula elastičnosti, dimenzionalne i masene stabilnosti, kemijskog i faznog sastava. Cilindrični kalupi upotrijebljeni su za pripremu cilindričnih uzoraka dimenzija  $100 \times 200$  mm. Paste su pripremljene i njegovane na istovjetan način kao i paste za prizmatične uzorke. Cilindrični uzorci korišteni su za pripremu poduzoraka za ispitivanja pretražnim elektronskim mikroskopom, ispitivanja sadržaj zračnih pora, kapilarnog upijanja i plinopropusnosti. Porne otopine su pripremljene istiskivanjem pod tlakom.

Čvrstoća (na savijanje i tlak), modul elastičnosti, dimenzionalna stabilnost, sadržaj zračnih pora, kapilarno upijanje i plinopropusnost cementne paste određeni su normiranim metodama navedenim u tablici I.VI.

---

Tablica I.VI. Ispitivanja fizičkih i mehaničkih svojstava cementne paste

Svojstvo	Norma
čvrstoća (na savijanje, na tlak)	HRN EN 196-1: 2016 Metode ispitivanja cementa – 1 dio: Određivanje čvrstoće
modul elastičnosti	HRN EN 12390-13: 2013 Ispitivanje očvrslog betona – 13 dio: Određivanje sekantnog modula elastičnosti pri tlaku
dimenzionalna stabilnost	HRN EN 12617-4: 2003 Proizvodi i sustavi za zaštitu i popravak betonskih konstrukcija – Ispitne metode- 4 dio: Određivanje skupljanja i bubrenja
sadržaj zračnih pora	Dodaci betonu i mortu za injektiranje – Ispitne metode – 11 dio: Određivanje značajka zračnih pora u očvrslom betonu
kapilarno upijanje	HRN EN 15418: 2004 Značajke građevnih materijala i proizvoda s obzirom na toplinu i vlagu – Određivanje koeficijenta vodoupojnosti pri djelomičnom uranjanju
plinopropusnost	HRN EN 993-4: Metode ispitivanja ne prozirnih vatrostalnih proizvoda – 4 dio: Određivanje propusnosti na plinove

Podaci o mikrostrukturi prikupljeni su i pretražnom elektronskom mikroskopijom. Promjena mase određena je vaganjem pod vodom. Kemijski sastav cementnih pasti i pornih otopina određen je normiranim metodama navedenim u tablici I.IV. pH pornih otopina izmjeren je normiranom metodom navedenom u tablici I.V. Za praćenje promjena u faznom sastavu cementnih pasti primijenjena je metoda rendgenske difrakcije na prahu i rendgenska *in-situ* difrakcija.

## REZULTATI I RASPRAVA

Sadržaj glavnih i sporednih oksida u portlandskim cementima CEM I i CEM III je različit. Gubitak žarenjem ovisi o sadržaju materijala koji nisu prošli obradu na visokim temperaturama prije dodavanja cementu. To su najčešće prirodni gips ili vapnenac. Veći maseni udio gubitka žarenjem u cementu CEM I u odnosu na CEM III ukazuje na veći maseni udio prirodnog kalcijevog sulfata (gipsa) ili prisutnost vapnenca. Veći maseni udio sulfata i CO<sub>2</sub> u CEM I također odgovara tom rezultatu. Osnovni minerali klinkera: alit, belit, aluminati i ferit potvrđeni su rendgenskom difrakcijom na prahu u cementu CEM I i CEM III. Prisutnost vapnenca nije potvrđena. U difraktogramu praha CEM I uočen je difrakcijski maksimum kod 51,7° s dodatkom (ramenom) na 51,9° koji je karakterističan za monoklinski M<sub>1</sub> polimer. Struktura ovog polimera nije poznata, pa je za Rietveldovu analizu upotrebljen difraktogram strukturno vrlo sličnog M<sub>3</sub> polimera. Kvantitativnom rendgenskom difrakcijom utvrđeno je da su alit i belit dominantne faze u cementu CEM I.

Veći maseni udio netopljivog ostataka u CEM III odgovara većem masenom udjelu ukupnog silicija i upućuje na prisutnost staklastog materijala koja je potvrđena difraktogramom praha. Danas se smatra da suvremeni klinkeri sadrže stalastu fazu samo u rijetkim slučajevima. Granulirana zgura visoke peći sadrži između 50 % do 90 % masenog udjela staklaste faze. Kristalne faze prisutne u cementu CEM I potvrđene su i u cementu CEM III. Visok šum odgovara amorfnoj fazi koja je rezultat dodavanja granulirane zgure visoke peći.

Kemijski sastav CSA cementa znatno se razlikuje u usporedbi s CEM I i CEM III. Niži maseni udio CaO i SiO<sub>2</sub> i viši maseni udio Al<sub>2</sub>O<sub>3</sub> upućuje na to da su primarni spojevi koji izgrađuju ovaj cement kalcijevi aluminosulfati za razliku od kalcijevih silikata koji su osnovni spojevi u CEM I i CEM III. Viši maseni udio sulfata i manji maseni udio gubitak žarenjem također podupiru ovaj rezultat koji je potvrđen i faznom analizom. Jelimit, glavna faza u CSA cementu uz belit i druge manje zastupljene faze potvrđena je rendgenskom difrakcijom na prahu. Kvantitativni fazni sastav cementa određen Rietveldovom analizom dan je u tablici I.VII. Faze s manjim masenim udjelom (<1,8 %) nisu navedene.

---

Tablica I.VII. Fazni sastav CEM I, CEM III i CSA cement

Mineral	w / %		
	CEM I	CEM III	CSA cement
C <sub>3</sub> S	71.8	41.0	0
C <sub>2</sub> S	12.8	3.7	13.5
C <sub>3</sub> A	3.2	3.2	3.4
C <sub>4</sub> AF	3.7	8.1	0
C <sub>4</sub> A <sub>3</sub> Š	0	0	70.7
C <sub>2</sub> AS	0	0	2.5
C <sub>12</sub> A <sub>7</sub>	0	0	2.6
anhidrit	0.5	0	1.8
kalcit	4.8	2.2	0
periklas	0	0	2.4
Staklaste faze	0	38.0	0

Rezultati kemijske analize pokazuju da je razlika glavnih i sporednih oksida u cementu CEM I i CEM III posljedica dodatka granulirane zgure visoke peći. Zamjena 64 % klinkera granuliranom zgurom visoke peći utvrđena je analizom sastava u cementu CEM III. Prisutnost vapnenca u cementu CEM III nije potvrđena.

Koncentracija elemenata u tragovima, osim žive i olova, niža je u cementu CEM I u usporedbi s cementnom CEM III. Ovi podaci odgovaraju rezultatima drugih autora dobivenih za iste tipove cementa [M. Achternbosch, K. R. Bräutigam, N. Hartliebe; C. Kupsch, U. Richers, P. Stemmermann, i M. Gleis, *Teški metali u cementu i betonu kao rezultat suspaljivanja otpada u cementnoj peći u odnosu na na zakonske zahtjeve za upotrebu otpada*, FZK, Karlsruhe, 2003, str. 15 – 105. (engleski izvornik)]. Zamjena klinkera granuliranom zgurom visoke peći povećava sadržaj elementa u tragovima u CEM III. Elementi u tragovima mogu se podijeliti u dvije grupe: elementi s koncentracijom iznad 5 mg kg<sup>-1</sup> (Co, Cr, Cu, Ni, Sb, Zn and V) i elementi koncentracije ispod 5 mg kg<sup>-1</sup> (As, Cd, Hg and Pb). Niža koncentracija nekih elemenata povezana je s njihovom hlapljivošću. Arsen, kadmij, živa i olovo smatraju se lako hlapljivim elementima koji se zadržavaju u sustavu rotacijske peći za proizvodnju klinkera. Oni se teško stabiliziraju u portlandskom cementnom klinkeru, dok se



drugi elementi koji su uključeni u ovo istraživanje smatraju manje hlapljivim, dobro se ugrađuju u faze klinkera i zbog toga su zastupljeniji u cementu [M. Achternbosch, K. R. Bräutigam, N. Hartliebe; C. Kupsch, U. Richers, P. Stemmermann, i M. Gleis., *Teški metali u cementu i betonu kao rezultat suspaljivanja otpada u cementnoj peći u odnosu na na zakonske zahtjeve za upotrebu otpada*, FZK, Karlsruhe, 2003, str. 15 – 105 (engleski izvornik)].

Znatno viša koncentracija hlapljivog arsena i posebno olova prisutna je u CSA cementu u odnosu na CEM I i CEM III. Niža temperatura nastajanja kalcijevog sulfoaluminatnog klinkera i veće količine industrijskog otpada koje se mogu koristiti kao sirovina u proizvodnji pogoduju ugradnji veće količine ovih elemenata tijekom proizvodnje u CSA klinker. Niže vrijednosti koncentracije antimona, kadmija i žive u CSA vjerojatno su posljedica manjih vrijednosti u sirovinama i gorivima. Zastupljenost drugih elemenata u tragovima u CSA cementu nalazi se unutar vrijednosti zabilježenih za CEM I i CEM III.

Čisti sastojci cementa, klinker, gips i zgura kao ni sirovinski materijali upotrijebljeni u proizvodnji klinkera i cementa nisu bili dostupni za ovo istraživanje. Zbog toga, dublja analiza izvora pojedinih elemenata u tragovima u cementu nije moguća. Istraživanja sadržaja elemenata u tragovima u CSA cementu su slabo dostupna u literaturi.

Električna vodljivost, vrijednosti pH, tvrdoća i sadržaj TDS u deioniziranoj vodi upotrijebljenoj za pripremu i njegovanje uzoraka cementne paste zadovoljavaju zahtjeve za vrlo meku vodu. Izlužujuća svojstva deionizirane vode dodatno su potvrđena malim sadržajem odabranih elementa u tragovima, kalcija i magnezija.

Difraktogrami su izvor vrijednih informacija, usproks ograničenjima u primjeni rendgenske difrakcije na hidratiziranim cementnim pastama. Difraktogrami CEM I paste pokazuju da se alit potroši tijekom 365 dana hidratacije. Kristalinične faze koje možemo pratiti tijekom hidratacije i izluživanja mogu nam dati dragocijene informacije. Nakon 1, 5 dana hidratacije u difraktogramu je vidljiv portlandit čija količina, kao i količina etringita raste do 7 dana hidratacije. Nije vidljiv značajniji prirast portlandita i etringita do 28 dana hidratacije. Smanjenje etringita javlja se u periodu od 56 do 365 dana hidratacije. Rezultati odgovaraju smanjenju čvrstoće zabilježenom za 365 dana hidratacije. Vrlo mali difrakcijski maksimum pri  $9,9^\circ 2\theta$  odgovara monosulfatu. Stvaranje kalicta uslijed karbonatizacije vidljivo je za period 365 dana hidratacije.

Visok šum prisutan je u difraktogramima na početku hidratacije cementa CEM III što je posljedica dodatka granulirane zgure visoke peći. Kristalini portlandit nastaje nakon 1, 5 dana

zajedno s etringitom. Smanjenje etringita prisutno u CEM I pasti uočeno i u CEM III pasti u istom hidratacijskom vremenu, odgovara ponašanju čvrstoće. Kalcit raste s hidratacijom, a alit je gotovo potpuno potrošen unutar 365 dana.

Uzorak CSA cementa reagira s vodom puno brže jer etringit nastaje već nakon 12 sati, a dominantna faza jelimit je u potpunosti potrošen tijekom 7 dana hidratacije. Etringit i stratlingit su glavne kristalinične faze nastale hidratacijom CSA cement. Nastajanje kalcita raste hidratacijom.

Difraktogrami za XRPD *in-situ* mjerenja pokazuju da je karbonatizacija dominantan proces na površini uzoraka jer difraktogram kalcita dominira difraktogramima svih cementnih pasta. Ovaj rezultat ukazuje da XRPD *in-situ* mjerenja nisu prikladna za ispitivanje izluživanja zbog stvaranja kalicta na površini uzoraka.

Konačne čvrstoće na savijanje i tlak za CEM I, CEM III i CSA cementnu pastu smanjuju se uslijed izluživanja. U periodu od 28 dana nije zabilježeno smanjenje čvrstoća što ukazuje na to da izluživanje u tom periodu ne utječe na hidrataciju sva tri tipa cementa. Prvo smanjenje čvrstoće na savijanje i tlak uočeno je za CSA cementnu pastu nakon 56 dana hidratacije. Smanjenje čvrstoće nastavlja se u periodu do 365 dana s konačnim smanjenjem čvrstoće na savijanje za 70 % i čvrstoće na tlak za 13 %.

Smanjenje čvrstoće na savijanje cementne paste CEM III za 53 % uočeno je nakon 180 dana. Čvrstoća na tlak za CEM III smanjuje se za 61 %, a za CEM I za 13 % nakon 365 dana izluživanja. CEM I pasta izgubi 53 % čvrstoće na savijanje. Smanjenje čvrstoće na savijanje i tlak posljedica je dugotrajnog izluživanja. Rezultati upućuju na to da osjetljivost prema izluživanju opada u slijedu CSA > CEM III > CEM I.

Gubitak čvrstoće kao posljedica izluživanja ili nekog drugog degradacijskog procesa obično je popraćena smanjenjem modula elastičnosti. U periodu do 365 dana nije uočen pad modula elastičnosti za CEM I, CEM III i CSA cementnu pastu. U suprotnosti, zabilježen je porast modula elastičnosti za sva tri tipa cementne paste. Modul elastičnosti je usko povezan s poroznošću cementne paste. Porastom poroznosti modul elastičnosti opada. Rezultati upućuju da izluživanjem nije povećana poroznost CEM I, CEM III i CSA i da je smanjenje čvrstoće posljedica promjene kemijskog sastava hidratacijskih produkata. Bubrenje i skupljanje portlandskih cemenata kao i CSA cementa je uobičajeno. Nema značajnije promjene mase u periodu od 365 dana. Dimenzionalna i masena stabilnost, potvrđuje izostanak nastajanja ekspanzivnih produkata pod utjecajem dugotrajnog izluživanja.

---

Pretražnom elektronskom mikroskopijom, u mikrostrukturi CEM I cementne paste uočavaju se područja pločastog CH i grudastog C-S-H gela s igličastim etringitom. U CEM III cementnoj pasti, portlandit je izmiješan s C-S-H gelom i nije vidljiv pločasti CH. Najveća količina etringita uočena je u CSA cementnoj pasti. Nekoliko manjih pora vidljivo je u CEM I, CEM III i CSA cementnoj pasti. Mikrostruktura i morfologija hidratacijskih produkata ne pokazuju posljedice propadanja uslijed izluživanja. Mikrostruktura odgovara prije uočenom porastu modula elastičnosti za sva tri tipa cementa.

Sadržaj zračnih pora u CEM I, CEM III i CSA cementu pokazuje promjene u periodu 365 dana hidratacije. Najmanje povećanje sadržaja pora od 7 % opaženo je za CEM I cementnu pastu, a najviše od 60 % za CEM III cementnu pastu. CSA cementna pasta bilježi povećanje sadržaja zračnih pora za 33%. Rezultati se u potpunosti slažu s rezultatima smanjenja tlačne čvrstoće. Mikroskopsko određivanje sadržaja zračnih pora uključuje određivanje pora promjera između 0 i 4000  $\mu\text{m}$ .

Poroznost cementnih materijala dobro se može procijeniti određivanjem apsorpcije vode uslijed kapilarnog upijanja. Materijali s većom apsorpcijom vode uslijed kapilarnog upijanja su porozniji. Osjetljivost prema izluživanju raste s povećanjem poroznosti. Rezultati istraživanja pokazuju da poroznost, a time i osjetljivost prema izluživanju opada u nizu CSA > CEM I > CEM III.

Nije bilo moguće odrediti plinopropusnost za CEM I, CEM III i CSA cementnu pastu zbog raspada uzorka. Vjerojatan uzrok raspada uzoraka je sušenje koje je neophodno provesti prije mjerenja, iako je primijenjen modificirani postupak sušenja na nižoj temperaturi. Sušenje uzrokuje razgradnju hidratacijskih produkata i raspad uzoraka.

Cementne paste CEM I, CEM III i CSA pokazuju smanjenje sadržaja kalcija, natrija i kalija s vremenom. Rezultati odgovaraju izluživanju i u skladu su s rezultatima prethodnih istraživanja. Cementna pasta CSA ima najveći gubitak kalcija. Najmanji gubitak zabilježen je za CEM III cementu pastu što odgovara manjoj količini CH i C-S-H u pasti tog tipa nakon 2 dana hidratacije. Ovo je posljedica manjeg sadržaja  $\text{C}_3\text{S}$  u usporedbi s cementom CEM I. Natrij i kalij također izlužuju iz cementne paste. Sadržaj alkalijskih elemenata u cementnoj pasti i pornoj otopini nije povezan s ukupnim sadržajem u nehidratiziranom cementu. Nehidratizirani CEM I i CEM III pasta u hidratacijskom periodu od 2 dana sadrže najviše koncentracije kalija. Rezultati upućuju da je kalij u cementu CEM III uglavnom ugrađen unutar klinkerskih faza, a u cementu CEM I kao i u CSA cementu većinom je dostupan u obliku lako topljivih

---

sulfatnih soli. Natrij je u cementu CEM I i CEM III glavninom ugrađen unutar faza klinkera, a u CSA cementu prisutan u obliku lako topljivih soli sulfata. Izluživanje natrija je izraženije u CSA pasti, a zatim u CEM III i CEM I što upućuje da otpornost prema izluživanju raste u ovom nizu. Koncentracija aluminija i željeza se ne mijenja s vremenom, dok koncentracija silicija i magnezija malo raste. Navedeni rezultati upućuju na to da izluživanje ne utječe na hidratizirane faze koje sadrže aluminij i željezo.

Alkalitet CSA porne otopine znatno je niži u odnosu na cement CEM I i CEM III. Opadanje pH vrijednosti s vremenom uočeno je u svim pornim otopinama i u skladu je s opadanjem koncentracije alkalija i kalcija. Rezultati ispitivanja kemijskog sastava cementne paste i pornih otopina ukazuju da je otpornost CEM I i CEM III cementne paste znatno bolja u odnosu na CSA cementu pastu u danim eksperimentalnim uvjetima.

Koncentracija topljivih elemenata u tragovima u pornim otopinama podupire njihovu slabu topljivost i dobru imobilizaciju u visoko alkalnim cementnim pastama. Koncentracija bakra, kroma i vanadija je najviša u CSA pornim otopinama što je u skladu s visokom zastupljenošću ovih elemenata u nehidratiziranom cementu. Ekstremno niske koncentracije arsena, kadmija, žive i olova odgovaraju njihovoj niskoj zastupljenosti u nehidratiziranom cementu CEM I i CEM III. Niska zastupljenost kadmija u nehidratiziranom cementu također rezultira niskom i konstantnom koncentracijom ovog elementa u CSA pornim otopinama. Ekstremno niska koncentracija olova u pornim otopinama nije u skladu s njegovom visokom zastupljenošću u CSA cementu. Ovaj rezultat upućuje na dobru imobilizaciju olova u CSA cementnoj pasti. Ponašanje ostalih elemenata u tragovima (Co, Cr, Cu, Hg, Ni, Sb i V) osim cinka u CSA pasti je istovjetno. Vrlo visoke koncentracije nakon 2 dana hidratacije (posebno za Cr i V) značajno opadaju s vremenom. Samo koncentracija cinka pokazuje vrlo mali rast. Mobilnost odabranih elemenata u tragovima u CSA cementu ne raste sa smanjenjem pH vrijednosti. Izluživanje ne utječe na imobilizaciju elementa u pornim otopinama. Visok sadržaj AFm i AFt faze vjerojatno je odgovaran za dobru imobilizaciju elemenata u tragovima u CSA cementnoj pasti.

Elementi u tragovima prisutni u cementu CEM I i CEM III nemaju istovjetno ponašanje kao kod CSA cementa. Živa se u CEM I i CEM III pastama ponaša slično kadmiju i olovu ali ima najveću topljivost među svim elementima u tragovima uključenima u ovo istraživanje. Više koncentracije žive ugrađene u klinkerske faze portlandskog cementa mogu predstavljati potencijalni rizik za okoliš. Mali rast u koncentraciji arsena odgovara smanjenju sadržaja CH

---

u CEM I i CEM III cementnoj pasti. Veći sadržaj arsena u portlandskoj cementnoj pasti može predstavljati potencijalni rizik za okoliš. Niže koncentracije antimona na početku hidratacije rastu s vremenom u CEM i CEM III pornoj otopini. Imobilizacija antimona ovisi o vrijednosti pH i koncentraciji kalcija. Povećanje topljivosti antimona podupire izluživanje kalcija iz CEM I i CEM III cementne paste. Antimon ugrađen u klinkerske faze može potencijalno predstavljati rizik za okoliš. Rast koncentracije bakra u CEM I i CEM III pornim otopinama nakon 7 dana hidratacije upućuje na degradaciju C-S-H gela i potencijalni rizik za okoliš. Visoke koncentracije cinka u CEM I i CEM III pornim otopinama smanjuju se s protekom vremena. Mobilnost cinka povećava se u otopinama s pH vrijednošću ispod 7. Ponašanje cinka u CEM I i CEM III pornim otopinama ne upućuje na štetne reakcije. Opadanje koncentracije nikla u skladu je sa smanjenjem pH vrijednosti. Promjena koncentracije nikla upućuje na degradaciju cementne paste CEM I i CEM III uslijed izluživanja. Koncentracija kroma i vanadija pokazuje nejasan trend rasta. Koncentracija kobalta u CEM I i CEM III pornim otopinama pokazuje velike varijacije i razlike u ponašanju između CEM I i CEM III pastama. Ovo upućuje na različite načine imobilizacije kroma, vanadija i kobalta unutar hidratiziranog i nehidratiziranog CEM I i CEM III. Nije moguće povezati koncentracije ovih elemenata s degradacijom cementne paste uslijed izluživanja. Ponašanje ovih elementa treba pažljivo uzeti u obzir prilikom procjene rizika za okoliš zbog izraženih varijacija u koncentraciji.

---

## ZAKLJUČAK

Nastajanje kristaliničnih hidratacijskih produkata, portlandita i etringita i njihova zastupljenost nakon 28 dana hidratacije ukazuju da portlandske cementne paste nisu pogođene izluživanjem. Smanjenje etringita u periodu od 56 do 365 dana hidratacije odgovara smanjenju čvrstoće portlandskih cementnih pasta u ovom periodu. Sastav hidratizirane portlandske cementne paste ne podržava otapanje hidratacijskih produkata koji sadže aluminij (npr. etringit). Rezultati upućuju da je mogući uzrok smanjenja etringita jednostavna transformacija etringita u monosulfat. Zastupljenost kristaliničnih faza nastalih hidratacijom kalcijevog sulfoaluminatnog cementa, ne upućuje na izluživanje u 365 dana hidratacije ovog tipa cementne paste. Izluživanje kalcija i alkalijских metala iz svih cementnih pasta i njihovih otopina, praćeno smanjenjem bazičnosti, upućuje na promjene u sastavu C-S-H ili količini CH. Portlandit nije potvrđen u CSA cementnoj pasti. Karbonatizacija se pojavljuje u svim uzorcima cementnih pasta s protekom vremena. Ona je značajna samo za rendgensku difrakciju *in-situ*, jer se javlja na površini uzoraka. Karbonatizacija ne utječe na stvaranje dodatnog etringita u kasnijem dobu hidratacije.

Mikrostuktura i morfologija hidratacijskih produkata nakon 365 dana hidratacije ne upućuje na razaranje uzoraka uslijed izluživanja. Povećanje zatvorenog volumena pora u periodu od 56 do 365 dana hidratacije upućuje na promjene u sustavu pora i odgovara smanjenju čvrstoće.

Manja kapilarna poroznost portlandskih cementnih pasta u usporedbi s kalcijevom sulfoaluminatnom cementnom pastom nakon 365 dana hidratacije smanjuje osjetljivost portlandskih cementnih pasta prema izluživanju. Povećanje modula elastičnosti u hidratacijskom periodu ukazuje da nema značajnijeg porasta ukupne poroznosti s protekom vremena. Difraktogrami cementnih pasta pokazuju da nema nastajanja ekspanzivnih spojeva uslijed izluživanja, što odgovara volumnoj i masenoj stabilnosti.

Čvrstoće, najvažnije svojstvo cementne paste, pogođene su izluživanjem. Dugotrajno izluživanje u danim eksperimentanim uvjetima smanjuje čvrstoću na savijanje i tlak nakon 56 dana ili više. Prema rezultatima čvrstoće, cement utemeljen na kalcijevim sulfoaluminatnim spojevima je osjetljiviji prema izluživanju nego portlandski cement utemeljen na kalcijevim silikatnim i kalcijevim aluminatnim spojevima. Brzina izluživanja ovisi o tipu cementa. Cementna pasta s višim sadržajem C-S-H je manje osjetljiva prema izluživanju.

---

Rezultati istraživanja ukazuju da se kemijski sastav i struktura C-S-H gela mijenja što rezultira gubitkom čvrstoće. Ove promjene treba potvrditi budućim istraživanjima.

Imobilizacija elemenata u tragovima u kalcijevoj sulfoaluminatnoj cementnoj pasti nije pogodena izluživanjem, što onemogućava upotrebu koncentracija elemenata u tragovima u pornim otopinama u ispitivanjima izluživanja. Porast koncentracije arsena, žive, antimona i bakra i smanjenje koncentracije nikla u pornim otopinama portlanskog cementa podupire kemijsko razaranje uslijed izluživanja. Ponašanje kroma, vanadija i kobalta ne može se povezati s procesima razaranja zbog uočenih varijacija u koncentraciji.

Dugotrajna ispitivanja izluživanja, najmanje 365 dana ili duže, potrebna su kako bi se jednoznačno odredio utjecaj izluživanja na cementnu pastu. Moguće je korigirati nezrele cementne paste u ispitivnjima što može skratiti potrebno vrijeme za ispitivanje. Rendgenska difrakcija *in-situ* nije prikladna metoda za ispitivanje izluživanja zbog stvaranja kalicta na površini uzoraka.

Cement koji je utemeljen na kalcijevim sulfoaluminatnim spojevima nije preporučljiv za primjenu u konstrukcijama koje su izložene izluživanju, ali je vrlo pogodan za imobilizaciju metala u tragovima. Novi, održivi cement mogao bi biti utemeljen na smjesi kalcijevih silikata, kalcijevih aluminata i kalcijevih sulfoaluminata. Prikladne omjere pojedinih spojeva treba odrediti daljnjim istraživanjem.

---

## § 1. INTRODUCTION

### 1.1. Problem statement

Portland cement production accounts for around 5 to 8 % of anthropogenic CO<sub>2</sub>. Thus, the sustainability has become one of the two main drivers for innovation in Portland cement industry together with improving of properties.<sup>1</sup>

Different possibilities for achieving a substantial reduction in CO<sub>2</sub> emissions have been developed.<sup>1,2,3</sup> The traditional solutions present improvements of common Portland cements based on calcium silicates or calcium aluminates. More innovative solutions include formulation of novel cements based on sulfoaluminate, sulfoferrite or fluoroaluminate.<sup>3</sup>

Portland cement production is closely tied to construction and it is appropriate to apply a holistic approach for evaluation of new cement solutions. The concept of holistic approach, originally developed for concrete, shown in Figure 1.1, is also suitable for evaluation of new cement solutions.<sup>4</sup>

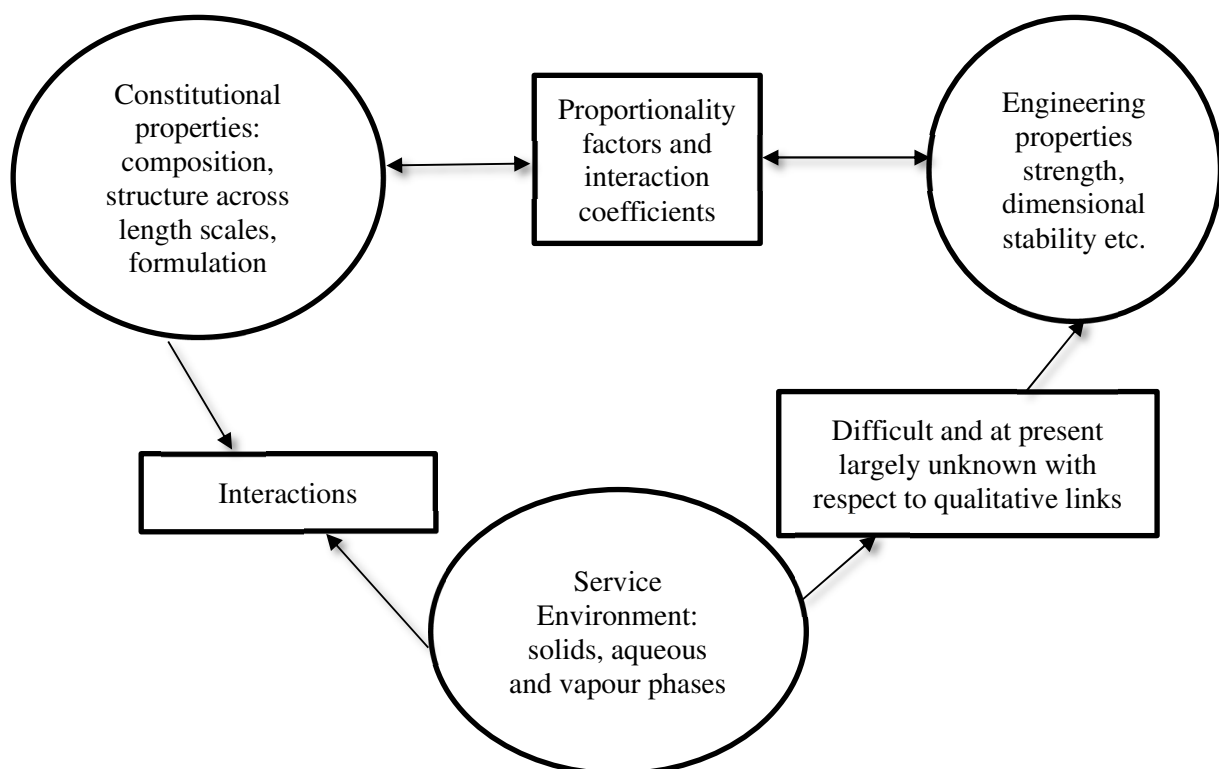


Figure 1.1. Holistic approach for the new cement solution according to F.P. Glasser<sup>4</sup> originally developed for concrete



The modern construction is based on design codes and standards which are very conservative since their objective is to minimize the possibility for catastrophic failure and loss of life.<sup>1</sup> Introducing the new material into codes and standards requires durability data. Durability is an abstract term usually understood as a demonstration of performances over long time scale.<sup>4</sup> Wide range of methods for determination of chemistry, physics, mineralogy and structure of Portland cement system are available.<sup>5</sup> Tests of engineering properties are performed by well-established standard methods. The critical element of this approach is deficiency of standard test methods for durability assessment. Researches on closed systems (with respect to transport of matter) are simple and give good starting data. However, common degradation processes mostly occur in open or partly open systems. Open systems are more complicated and require different sets of methods to be applied.<sup>4</sup> This makes durability testing time and labour consuming which is in conflict with legal requirements for rapid CO<sub>2</sub> emissions decrease.

Portland cement composite have the good durability in normal service life up to 70 years or more.<sup>6</sup> During the service life the Portland cement paste may be exposed to weathering and degradation and may exhibit a reduced service life. Deionized water containing a low concentration of dissolved ions in contact with the Portland cement paste induces decalcification.<sup>7,8</sup> The process is called leaching. The increased porosity and permeability and loss of strength are the key consequences in the structures exposed to leaching.<sup>9-12</sup>

Leaching appears in Portland cement pastes exposed to steam, fog, rainwater or groundwater.<sup>13</sup> This is a significant issue for structures constantly exposed to soft or acid waters such as dams, water tanks, pipes or nuclear waste storages.<sup>9</sup> It is also very important for the waste solidification and stabilization by Portland cement.<sup>14</sup>

Generic approach to testing of Portland cement paste resistance towards leaching has not been developed yet. Initial tests were done by immersing solid samples in water to characterize this process.<sup>8,15-17</sup> Later, tests on milled samples were developed.<sup>18,19</sup> Particular deficiency has been observed in tests in which the changes in the chemical and mineralogical composition are related to the changes in engineering properties such as strength, modulus of elasticity, dimensions, etc. The absence of a general approach leads to inconsistency in collected data, making them difficult to compare with each other and resulting in impossibility to quantitatively define the relationship between chemical and mineralogical properties of the cement paste and associated mechanical and physical properties. The

inability for reliable assessment of durability of Portland cement pastes exposed to leaching prevents introduction of new cements into construction codes and standards.

## 1.2. Objectives, hypothesis and methods of research

The final objectives of the research are:

- determination of the changes in the chemical and phase composition and the microstructure of immature cement pastes with different initial chemical and phase compositions exposed to leaching by deionized water, without stopping hydration;
- determination of changes of physical and mechanical properties: strength, modulus of elasticity, dimensional and mass stability caused by leaching;
- determination of the effect of initial composition of the cement on the leaching process and the impact of leaching on the hydration process;
- determination of the possibility to use incorporated trace elements in leaching researches;
- determination of the possibility to use immature cement pastes in a partly opened system of leaching research.

The basic hypothesis is that resistance of cement paste to the action of deionized water depends on the properties of all constituents of cement paste: hydration products, pore solution and pore system. These properties are determined by the phase composition of anhydrous cement and curing conditions in which hydration reactions are carried out. X-ray diffraction is used to determine phase composition of anhydrous cements and to observe changes in the phase composition of hydrated cement pastes in the course of time. Bulk composition (major, minor and trace elements) of cement, cement pastes and pore solutions are determined by wet chemistry methods or by inductively coupled plasma mass spectrometry. The changes in pore system are observed by scanning electron microscopy, determination of air voids content, water absorption due to capillary action and permeability to gasses. The chemical resistance of cement pastes to the action of deionized water is monitored by determination of performance properties: strength, modules of elasticity, volume stability and loss of mass. The knowledge on the interdependence of cement phase composition, microstructure of cement paste, curing conditions and resistance of cement paste to the action of deionized water may facilitate design of new cement solutions with lower environmental footprint.

## § 2. LITERATURE REVIEW

### 2.1. Portland cement

Cement is usually defined as an adhesive element in composite material, generally in concrete, mortar or cement paste.<sup>20</sup> It is a powder material which in contact with water transfers to a hardened cement paste by chemical reactions and physical processes.<sup>21</sup> Portland cement is produced by milling Portland cement clinker with a few percentages of gypsum.

Portland cement was invented at the beginning of 19<sup>th</sup> century partly supported by construction knowledge from Antique, Greece and Rome.<sup>22</sup> Since then, it has made the great contribution to the quality of life. Today, Portland cement is in the form of the final product – concrete, the most widely used material of modern construction.<sup>13</sup> Construction of roads, bridges, buildings, dams, plants, skyscrapers etc. would not be possible without it. The availability of raw materials, common production and relatively low prices has increased the Portland cement mass production. The estimated world production of Portland cement in 2016 was 4.6 billion tones with China producing 52% of total world production (Figure 2.1).<sup>23</sup> Portland cement industry plays an important role in the economic, social and environmental development. It significantly contributes to the creation of employment, wealth and progress of the local and wider communities.

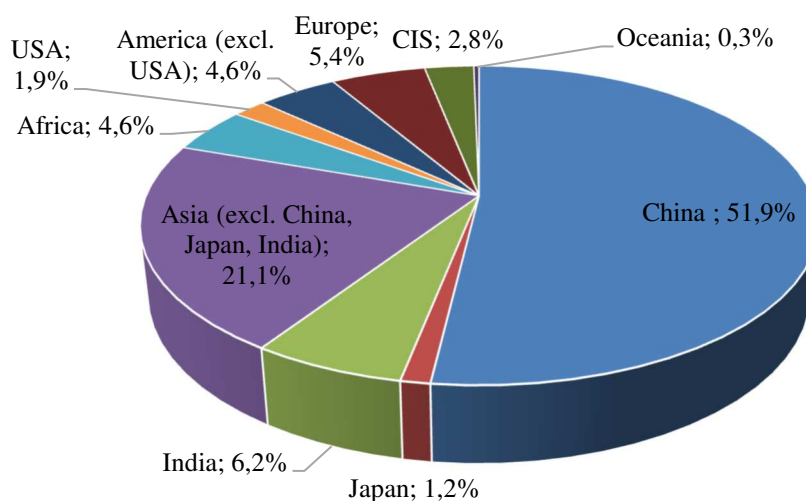


Figure 2.1. World Portland cement production in 2016

Source: CEMBUREAU, Activity report 2017<sup>23</sup>

## 2.2. Portland cement composition

### 2.2.1. Bulk composition of Portland cement

Portland cement is composed of different calcium compounds. The routine chemical analysis of Portland cement is commonly reported in terms of mass fraction of oxides of the present elements. Oxides of calcium (CaO), silicon (SiO<sub>2</sub>), aluminium (Al<sub>2</sub>O<sub>3</sub>) and iron (Fe<sub>2</sub>O<sub>3</sub>) determine the bulk composition of Portland cement. Portland cement chemists commonly use a form of notation to simplify the formula. This notation is given in Table 2.1.<sup>13</sup>

Table 2.1. Portland cement oxide notation

Oxide	Notation
CaO	C
SiO <sub>2</sub>	S
Al <sub>2</sub> O <sub>3</sub>	A
Fe <sub>2</sub> O <sub>3</sub>	F
MgO	M
SO <sub>3</sub>	$\bar{S}$
Na <sub>2</sub> O	N
K <sub>2</sub> O	K
H <sub>2</sub> O	H

Titrimetric methods are used to estimate oxide composition of Portland cement. Complexing agent 2,2',2''2'''-(ethane-1,2-diyldinitrilo)tetraacetic acid (EDTA) in the form of disodium salt is used to determine CaO, MgO, Al<sub>2</sub>O<sub>3</sub> and Fe<sub>2</sub>O<sub>3</sub> in Portland cement. EDTA forms octahedral complexes with many metal ions. Selectivity is controlled by pH and by masking interfering elements by suitable reagents. Silica is determined by traditional method of treating the sample with hot strong hydrochloric acid (HCl) containing ammonium chloride (NH<sub>4</sub>Cl) to dissolve other species. The dissolution is followed by titration and ignition. Well know method of precipitation with barium chloride (BaCl<sub>2</sub>) followed by weighing of the dry precipitate is used to determine sulfate.<sup>24</sup>

Some minor elements such as sodium, potassium, chloride or manganese are also incorporated in Portland cement. Alkaline elements are determined by flame photometry and spectrophotometric methods are commonly applied for manganese determination. Chloride is

determined by reacting the digested sample with silver nitrate solution and back titrating with ammonium thiocyanate.<sup>24</sup>

The oxide composition of Portland cement is not related to its mechanical properties such as strength and no final conclusion about Portland cement can be made from oxide analysis.<sup>24</sup> Phases formed by series of chemical reactions over a range of temperatures during Portland cement clinker production determine key properties of Portland cement.<sup>5,13,24</sup> Typical oxide composition of Portland cement clinker according Taylor is given in Table 2.2.<sup>5</sup>

Table 2.2. Typical Portland cement clinker composition

Oxide	w / %
CaO	67
SiO <sub>2</sub>	22
Al <sub>2</sub> O <sub>3</sub>	5
Fe <sub>2</sub> O <sub>3</sub>	3
Other components	3

### 2.2.2. Portland cement phase composition

Portland cement has complex mineralogy, which is consequence of thermodynamic relationship existing between different compounds during Portland cement clinker production.<sup>24</sup>

Alite, belite, aluminate and ferrite are four major phases detected in Portland cement. Cement notation for principal phases is given in Table 2.3. Some minor phases such as alkaline sulfates, calcium oxide (free lime) and magnesium oxide (periclase) are also incorporated.<sup>5</sup>

Table 2.3. Portland cement phase notation

Phase	Notation	Phase name
3CaO·SiO <sub>2</sub>	C <sub>3</sub> S	tricalcium silicate, alite
2CaO·SiO <sub>2</sub>	C <sub>2</sub> S	dicalcium silicate, belite
3CaO·Al <sub>2</sub> O <sub>3</sub>	C <sub>3</sub> A	tricalcium aluminate, aluminate
4CaO·Al <sub>2</sub> O <sub>3</sub> ·Fe <sub>2</sub> O <sub>3</sub>	C <sub>4</sub> AF	tetracalcium aluminoferrite, ferrite
CaSO <sub>4</sub> ·2H <sub>2</sub> O	C $\bar{5}$ H <sub>2</sub>	gypsum

Chemical composition of Portland cement phases is not exactly what is expressed by commonly used formulas or notations. Compounds are modified in composition and crystal structure by ion substitution with small amounts of impurities such as magnesium, sodium, potassium or sulfate. Seven different alite polymorphs has been confirmed and phase transformation is given in Figure 2.2.<sup>5</sup>

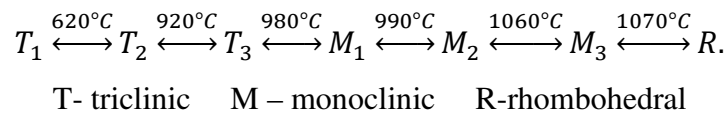


Figure 2.2. Temperature phase transformations of pure  $\text{C}_3\text{S}$  after Taylor<sup>5</sup>

Higher temperature  $\text{C}_3\text{S}$  polymorphs require higher substitution by  $\text{MgO}$ ,  $\text{Al}_2\text{O}_3$  and  $\text{Fe}_2\text{O}_3$  oxides. In industrially produced Portland cement alite incorporates 3 % to 4 % of substituent oxides and at room temperature is mainly present in form of  $M_1$  or  $M_3$  polymorph, rarely as  $T_2$ .<sup>25-29,39</sup>  $\text{C}_3\text{S}$  crystallizes as the R polymorph at  $1450^\circ\text{C}$  and inverts to lower temperature polymorphs by cooling. The content of magnesium oxide ( $\text{MgO}$ ) and sulfate ( $\text{SO}_3$ ) determine whether transformation to  $M_1$  or  $M_3$  polymorph occurs. Mixture of  $M_1$  and  $M_3$  is also possible. High  $\text{MgO}$  content favours  $M_3$  and high  $\text{SO}_3$  has an opposite effect.<sup>31,32</sup> The formation of  $T_2$  polymorph is possible only in low substituted and slowly cooled Portland cement clinkers. The superstructure of alite is built from silica tetrahedra, calcium and oxygen ions. Coordination of oxygen ions around calcium is irregular with oxygen atoms being concentrated on one side of each calcium ion. The large structural holes are formed which increase lattice energy and reactivity of alite towards water.<sup>13</sup>

Belite has five different polymorphs given in Figure 2.3.<sup>34-36</sup>

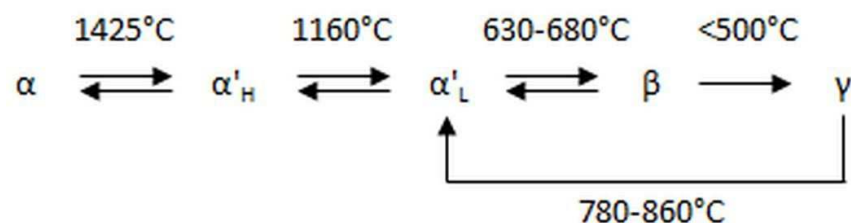


Figure 2.3. Temperature phase transformations of pure  $\text{C}_2\text{S}$  after Taylor<sup>5</sup>

Higher temperature polymorphs must be stabilized with substitute ions to be kept on lower temperatures. In industrially produced Portland cement, belite is almost entirely present in form of  $\beta$ -C<sub>2</sub>S with 4 % to 6 % of substituting oxides, mainly Al<sub>2</sub>O<sub>3</sub> and Fe<sub>2</sub>O<sub>3</sub>.<sup>5</sup> The structure of belite in industrially produced Portland cements is irregular but with less interstitial holes than alite, which accounts for less reactivity of belite compared to alite. The structure observed for  $\gamma$ -belite accounts for its nonreactivity with water.

Pure calcium aluminate does not exhibit polymorphism. It has a cubic crystal cell built from Ca<sup>2+</sup> ions and six AlO<sub>4</sub> tetrahedra.<sup>37</sup> In industrially produced Portland cement, aluminate is present in cubic or orthorhombic form alone or in a mix.<sup>5</sup> Both phases are stabilized with substituting oxides, with the cubic polymorph incorporating about 13 % and orthorhombic about 20 % of substituting oxides. Orthorhombic phase is formed in rapid cooled Portland cement clinker with sufficient alkali content.<sup>38</sup>

Ferrite phase is closely mixed with cubic aluminate in industrially produced Portland cement.<sup>39</sup> In the pure system ferrite forms series of solid solutions with the formula Ca<sub>2</sub>(Al<sub>x</sub>Fe<sub>1-x</sub>)<sub>2</sub>O<sub>5</sub> where 0 < x < 0.7. In this series C<sub>4</sub>AF is the only possible composition for which x is 0.5. The series members are not isostructural since space group changes when x = 0.33.<sup>40</sup> Ferrite composition significantly differs from C<sub>4</sub>AF. It is much lower in Fe<sub>2</sub>O<sub>3</sub> and incorporates about 10% of substituent oxides. It corresponds to Ca<sub>2</sub>AlFe<sub>0.6</sub>Mg<sub>0.2</sub>Si<sub>0.15</sub>Ti<sub>0.05</sub>O<sub>5</sub> which reflects substitution of Fe<sup>2+</sup> by Mg<sup>2+</sup> and Si<sup>4+</sup> by Ti<sup>4+</sup>.<sup>5</sup> Microanalysis has shown that there is much variation in ferrite composition between Portland cement clinkers and within the clinker.<sup>41</sup>

The part of MgO in Portland cement is incorporated within major phases (up to 2 %) and the rest occurs as crystalline MgO, periclase. Uncombined or free calcium oxide is rarely present in significant amounts in modern Portland cement. Both MgO and CaO have cubic structures with calcium or magnesium ions surrounded with oxygen atoms in a regular octahedron. Both phases react slowly with water and can cause unsoundness of Portland cement, thus both phases are undesirable. Magnesium is the smaller ion thus well packed with oxygen. Calcium is larger causing oxygen ions to force apart. This is the reason why periclase is much less reactive than free lime.<sup>13</sup>

Alkaline originating from clay component of raw material are commonly expressed as Na<sub>2</sub>O equivalent. In Portland cement they form double sulfates of alkalis such as langbeinite

( $2\bar{C}\bar{S}\cdot\bar{N}\bar{S}$ ) or aphythitalite ( $3\bar{N}\bar{S}\cdot\bar{K}\bar{S}$ ). When there is no sufficient amount of sulfate available from raw mix or fuel, alkalis are incorporated within alite or belite.<sup>5</sup>

### 2.2.3. Calculation of phase composition

When chemical composition of Portland cement is known, it is possible to estimate quantitative phase composition using the following calculations developed by Bogue:

$$C_3S = 4.0710C - 7.6024S - 6.7187A - 1.4297F$$

$$C_4AF = 2.8675S - 0.7544C_3S$$

$$C_3A = 2.6504A - 1.6920F$$

$$C_4AF = 3.0432F.<sup>42</sup>$$

Calculations have been refined by Taylor with intention to reduce deviation of the estimated phase assemblage from reality.<sup>43</sup> The Bogue calculation assumes that for major phases ( $C_3S$ ,  $C_2S$ ,  $C_3A$  and  $C_4AF$ ) are chemically pure and thus only CaO, SiO<sub>2</sub>, Al<sub>2</sub>O<sub>3</sub>, Fe<sub>2</sub>O<sub>3</sub> and SO<sub>3</sub> content are used in calculation. This is the major uncertainty source of Bogue calculation since the phases in cement are actually solid solutions with composition deviating from pure phases.<sup>44</sup> The difference between the assumed and actual composition also arises from the absence of equilibrium during clinkerization and cooling reactions. The existence of other minor individual phases also affects accuracy of calculation.<sup>44,45</sup> The modified Bogue calculations based on more realistic phase compositions are still not commonly applied in Portland cement production.<sup>46,47</sup>

## 2.3. X-ray diffraction

X-ray powder diffraction (further: XRPD) is the only physical method suitable to determine phase composition of Portland cement clinker, Portland cement and Portland cement paste.<sup>5</sup> The XRPD Portland cement phase determination is possible due to the fact that each cement phase has a unique diffraction pattern independent of others. The intensity of each pattern is proportional to the concentration of the phase in the mix. There are certain challenges in XRPD Portland cement phase determination arising from the nature of material and from the method itself. The patterns of Portland cement clinker or cement are very complex with many overlaps especially from alite since it is the most abundant Portland cement phase.<sup>24</sup> The peak positions and relative intensities are affected by variations in composition and structural variation of each phase. Peak broadening due to compositional zoning and imperfect crystallinity has been observed especially for the ferrite phase.<sup>5</sup>



The XRD patterns of alite polymorphs, particularly in industrial clinkers, are very similar and many peaks overlap those of other phases. The patterns depend on the polymorphs present and also on the nature and amount of substitute ions incorporated in alite. The principal difference in diffraction patterns are observed in fine structure of certain peaks.<sup>28,29,30</sup> The diffraction pattern of M<sub>1</sub> alite has almost a singlet peak at  $2\theta$  51.7°. This peak transforms to a doublet for M<sub>3</sub> alite and into a triplet for all three triclinic phases. The differences in diffractograms of alite polymorphs are shown in Figure 2.4.<sup>5</sup> There are also differences in the peaks in the  $2\theta$  range 32 – 33° but they are less useful because of the overlaps with other phases.

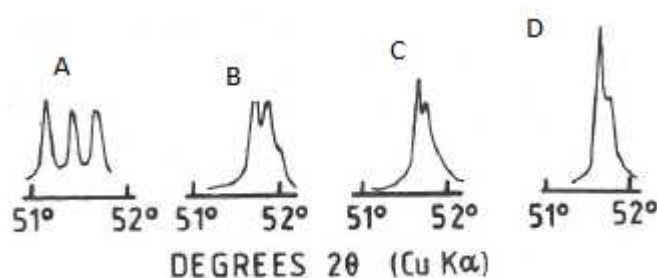


Figure 2.4. XRPD patterns of alite modifications after Taylor<sup>5</sup>

(A) T<sub>1</sub> modification of alite; (B) M<sub>3</sub> modification of alite; (C) (M<sub>1</sub> + M<sub>3</sub>) modification of alite; (D) M<sub>1</sub> modification of alite

Characterization of belite polymorphs is difficult due to similarities between the powder patterns shown in Figure 2.5. Additional difficulties arise from overlaps with alite peaks.<sup>48</sup>

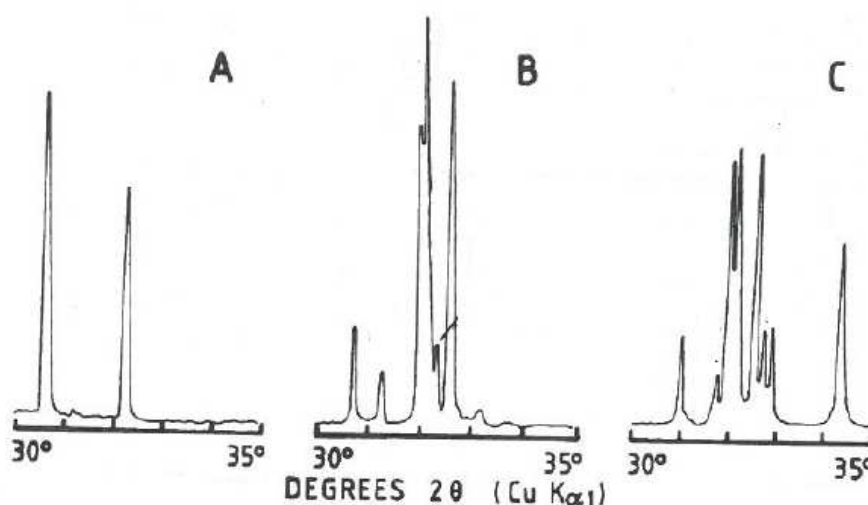


Figure 2.5. XRPD powder patterns of belite modifications from Taylor<sup>5</sup> after Regourd *et al.*<sup>36</sup>

(A)  $\alpha$ -C<sub>2</sub>S at 1500 °C (B)  $\alpha'$ -L-C<sub>2</sub>S (C)  $\beta$ -C<sub>2</sub>S

The powder patterns of cubic and orthorhombic aluminate phase differ in the peak at  $2\theta$   $33.3^\circ$  (Figure 2.6).<sup>36</sup> The cubic phase is characterized by a strong single peak while for the orthorhombic phase this peak is split into a strong singlet at  $33.2^\circ$  and a weak doublet in the  $2\theta$  range of  $32.9\text{--}33.0^\circ$ .

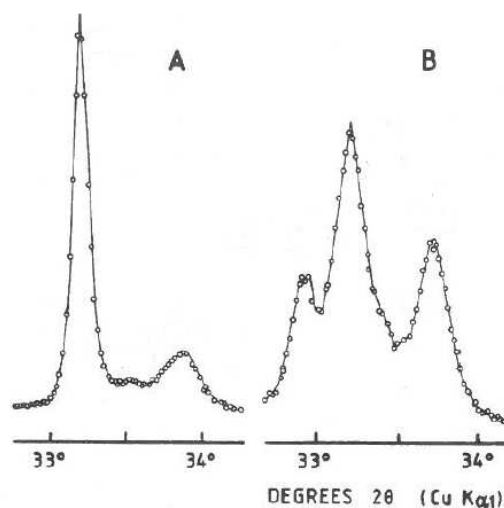


Figure 2.6. XRD powder patterns of aluminate from Taylor<sup>5</sup> after Regourd *et al.*<sup>36</sup>  
(A) cubic and (B) orthorhombic phase

The XRD patterns of ferrite from industrially produced Portland cement clinker are strongly affected by the cooling rate. Rapid cooling causes poor crystallinity of the ferrite phase and, as a consequence, disappearance of many peaks and broadening of the peaks.<sup>49</sup>

The major sources of systematic and random errors in XRPD are: sample displacement, preferred orientation and limited interaction depth of the X-ray beam.<sup>50</sup> The sample displacement causes systematic shift in observed peaks but it does not affect the peak intensities significantly. The preferred orientation affects the relative peaks intensities for a given phase. The oversampling of one or more Portland cement phases is possible if the phase domains are comparable with interaction depth of X-ray beam.<sup>51</sup> Reduction of particle size by grinding can significantly reduce all three of these errors. The anisometric particles are crushed by grinding into smaller, more random shapes with reduced tendency for preferred orientation. It is not possible to completely avoid the preferred orientation for alite, calcite and gypsum due to the strong cleavage planes characteristic for these phases. The better packing is

produced with finely ground powder resulting in smoother surfaces and reduced sample displacement. Internal standard is also used to minimize the error of the sample displacement. The commonly used internal standards are rutile ( $\text{TiO}_2$ ), silicon (Si), potassium bromide (KBr), calcium fluoride ( $\text{CaF}_2$ ) and corundum ( $\text{Al}_2\text{O}_3$ ).<sup>5,48</sup> Corundum is a very suitable internal standard since it gives no overlaps with important cement peaks up to  $2\theta = 60^\circ$ .<sup>5</sup> Grinding improves representative phase sampling by reducing the average phase domain size.<sup>50</sup> Reduction of particle size to about 10 microns or less would be ideal to reduce this source of possible errors. Wet grinding with an inert solvent such as benzene, isopropyl alcohol or cyclohexane is recommended.<sup>48</sup> The grinding is very challenging since it may result in damage to the phases, reduced crystallinity and as a consequence peak broadening.

Collection and characterization of complex Portland cement powder diffractograms requires much skill and experience. Thus, the XRPD studies have been for more decades more qualitative than quantitative. The quantitative X-ray powder diffraction (further: QXRPD) can be obtained by number of methods.<sup>50</sup> Nowadays it is mainly based on Rietveld method and has become the most appropriate quantification method of the crystalline phases in Portland cement, clinker and hydrated cement paste.<sup>44,50</sup> The Rietveld method is the whole powder pattern fitting method which uses a least squares approach to refine theoretical pattern to match the best possible the measured powder diffractogram. It does not require calibration curve or internal standard but the crystal structures of all crystalline constituents must be known.<sup>51</sup> The Rietveld method of QXRPD is carried out by one of several specially developed computer programs.<sup>51</sup> The method has significantly improved the precision of QXRPD cement phase determination and shows to be useful in Portland cement durability studies.<sup>50,52,53</sup>

Unfortunately, implementation of XRPD on hydrated cement paste is limited mostly due to the fact that the principal hydration phase of Portland cement is nearly amorphous. It can be successfully implemented on other crystalline phases in Portland cement paste such as: portlandite, ettringite, unreacted Portland cement phases or some minor hydrated phases.<sup>54</sup> The X-ray diffraction *in-situ* is successfully implemented technique that offers the possibility for time dependent observation of the Portland cement phase composition and in combination with the Rietveld method, quantitative determination of present phases without influencing the sample by further preparation.

## 2.4. Minor elements in Portland cement

The term trace element is generally used in analytical chemistry for any element having average concentration less than  $100 \text{ mg kg}^{-1}$ . In Portland cement it is applied to elements with concentration above this limit to distinguish them from the main elements reaching concentrations in the percentage range.<sup>55</sup> The increased waste utilization as a partial substitution of primary raw materials and fuels in Portland cement production has increased interest for trace elements incorporated in Portland cement. Some of these elements are toxic or carcinogenic (arsenic, cadmium, cobalt, chromium, copper, mercury, nickel, lead) or present an important occupational risk (chromium, cobalt, nickel).<sup>56</sup> Transition metals (cobalt, chromium, copper, manganese, nickel, vanadium, titanium, zinc) also have influence on the process reaction during clinkerization and on the properties of the final product.<sup>57</sup> The quantity of the trace elements present in Portland cement determines the mechanism and place of immobilization.<sup>58</sup> The immobilization in the principal clinker phases ( $\text{C}_3\text{S}$ ,  $\text{C}_2\text{S}$ ,  $\text{C}_3\text{A}$ ,  $\text{C}_4\text{AF}$ , free lime and periclase) is dominant at low concentration. When the concentration of trace element exceeds the threshold limit, new phases are formed.<sup>58</sup> The binding mechanism of the specific trace element depends on the oxidative state of the element which is a function of raw materials chemistry and production conditions.<sup>59,60</sup>

Oxidative states of chromium in Portland cement clinker are +3, +4, +5 and +6.<sup>61</sup> At high temperatures and in an oxidizing atmosphere during production the oxidative state +3 is the most stable one. Chromium in this oxidative state is concentrated in  $\text{C}_4\text{AF}$  due to its replacement with  $\text{Fe}^{3+}$ . Chromium ions in higher oxidative states (+4,+5) are smaller and replacement for Al and Si in  $\text{C}_3\text{S}$  and  $\text{C}_2\text{S}$  is possible.<sup>60</sup> The existence of individual phases of chromium in different oxidative states has been also confirmed.<sup>61</sup> The oxidative states +2 and +3 have been confirmed for cobalt in Portland cement clinker, being concentrated in  $\text{C}_4\text{AF}$ .<sup>57,58,62</sup> Copper and nickel are mainly incorporated in  $\text{C}_4\text{AF}$ , followed by  $\text{C}_3\text{S}$ ,  $\text{C}_3\text{A}$  and  $\text{C}_2\text{S}$ .<sup>63</sup> Formation of a copper solid solution in free lime has been confirmed for higher uptakes.<sup>64,65</sup> Nickel can form an individual compound ( $\text{MgNiO}_2$ ) with magnesium.<sup>66</sup> Vanadium in Portland cement clinker is present in the form of  $\text{V}_2\text{O}_5$  and has preferential partition towards  $\text{C}_2\text{S}$ .<sup>67,63</sup> Bolio-Arceo *et al.* have confirmed that most of the zinc is present in form of a solid solution based on  $6\text{CaO}\cdot 3\text{ZnO}\cdot 2\text{Al}_2\text{O}_3$ .<sup>67</sup> A small amount of the zinc is partitioned into the solid solution of the main clinker phases.<sup>63,68</sup> Cadmium is incorporated in  $\text{C}_3\text{S}$ ,  $\text{C}_2\text{S}$  and free lime. Belite has higher ability to incorporate cadmium than alite.<sup>69</sup>

Metalloids, arsenic and antimony are present as individual phases, both in the oxidative state +5.<sup>70-72</sup> Incorporation of mercury and lead within the clinker phases has not been researched well. These elements are difficult to stabilize within the Portland clinker due to their volatility. They are concentrated in the filter dust or off gases.<sup>55</sup>

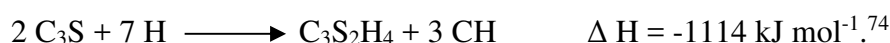
## 2.5. Portland cement hydration

Hydration of Portland cement includes all changes that occur in reactions between Portland cement composite and water.<sup>73</sup> Products that possess setting and hardening characteristic are formed through these complex reactions.<sup>73,74</sup> Setting usually occurs within a few hours from mixing and no significant development of compressive strength is observed within this period. Significant development of compressive strength is a slower process called hardening. The mixture of cement and water in proportions enabling setting and hardening to occur is called cement paste. Water to cement ratio (further: w/c) in the cement paste determines many its properties. The term also includes the hardened material. Curing samples of cement pastes, mortar or concrete means storage under conditions such that hydration occurs.<sup>73</sup>

The interpretation of complex hydration reactions of Portland cement is not possible without deep understanding of hydration reactions of each individual Portland cement phase.<sup>74</sup>

### 2.5.1. Hydration of alite

The rather complex hydration of C<sub>3</sub>S can be simplified and described by the following equation:



In the exothermic reaction two main products are formed: calcium hydroxide (CH) usually called portlandite and calcium silicate hydrate usually denoted as C-S-H. Around 70 % of alite present in Portland cement reacts within 28 days and virtually all within the 1-year period.<sup>73,75</sup>

The phase C-S-H is amorphous or poorly crystalline calcium silicate hydrate. The dashes in this generic name indicate that relation between components (C/S and H/S) is not constant and no particular composition is implied. The composition depends on formation condition and is altered during the hydration reactions.<sup>73,74</sup> Calcium silicate hydrates can be found in nature, synthesized in laboratory or formed during the hydration of Portland cement. More than 30 of them are crystalline.<sup>73,76</sup> Due to its structure and large specific surface, C-S-H together with pore solution forms a rigid gel in which pores range in size from macroscopic to

nanometer dimensions. The term C-S-H gel is used only for calcium silicate hydrate formed during hydration of Portland cement. It is primary responsible for development of mechanical properties of Portland cement paste.<sup>73,74</sup> The XRPD pattern of C-S-H gel shows that there is no long-range order in its structure. Thus, determination of nanostructure is a more appropriate term for the C-S-H gel than determination of the crystal structure. The structural comparisons with crystalline silicate hydrates usually 1.4-nm tobermorite ( $C_5S_6H_9$ ) and jennite ( $C_9S_6H_{11}$ ) has given much knowledge about the nanostructure of C-S-H gel.<sup>76</sup> Both minerals have layer structure and on heating lose interlayer water and undergo unidimensional lattice shrinkage.<sup>73,77,78</sup> They belong to the group of nature minerals having a silicate dreierketten structure that is built of a central Ca–O layer bordered on both sides by chains of tetrahedral silicates. The interlayer distance, distance between two Ca–O layers is usually filled with calcium atoms and molecules of water. Schematic drawing of a dreierketten structure is given in Figure 2.7.<sup>79</sup>

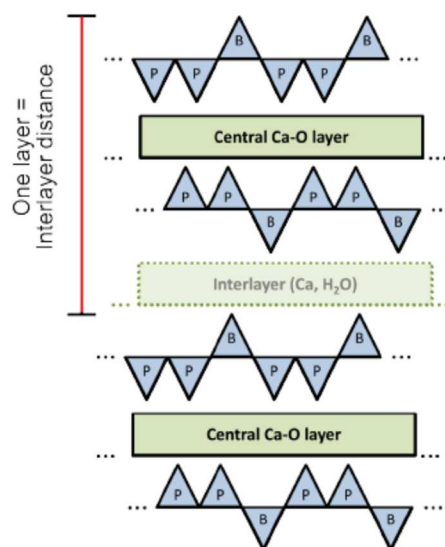


Figure 2.7. Schematic drawing of a dreierketten structure showing the central Ca–O layer and chains of tetrahedral silicates with paired tetrahedra (P) and bridging tetrahedra (B)<sup>79</sup>

The structures of 1.4-nm tobermorite (Figure 2.8) and jennite (Figure 2.9) have been recently completely resolved.<sup>80,81</sup> The C/S ratio in 1.4-nm tobermorite is 0.83 and the prefix 1.4-nm refers to the interlayer thickness. Two oxygen atoms from paired tetrahedra in 1.4-nm tobermorite are coordinated to the central calcium ions. In jennite, only one oxygen atom from paired tetrahedra is coordinated to the central calcium ion. The second oxygen atom is

provided by the hydroxide ion. Thus, jennite has a more corrugated structure in which every other dreierketten is replaced with a row of hydroxyl groups. The C/S ratio in jennite is 1.50.<sup>76,79</sup>

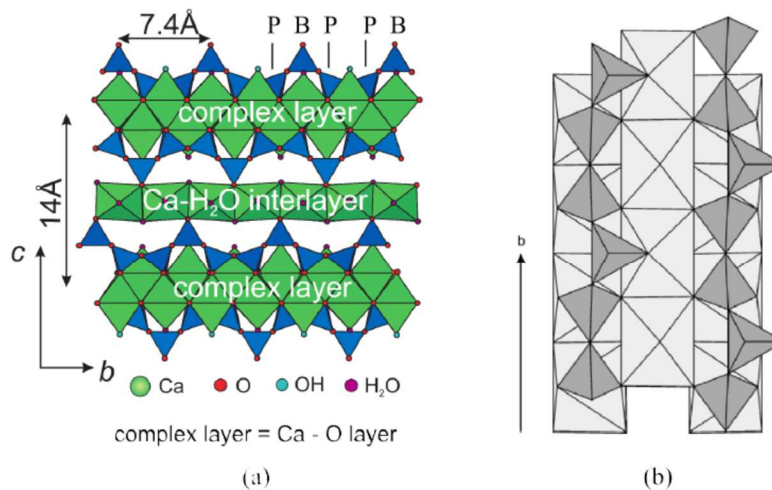


Figure 2.8. Structure of 1.4-nm tobermorite (a) The structure as seen along [100], with two Ca–O layers separated 1.4 nm apart<sup>82</sup> (b) Connection of silicate chains (dark grey) to the layer of calcium polyhedra (light grey), as seen down [100]<sup>83</sup>

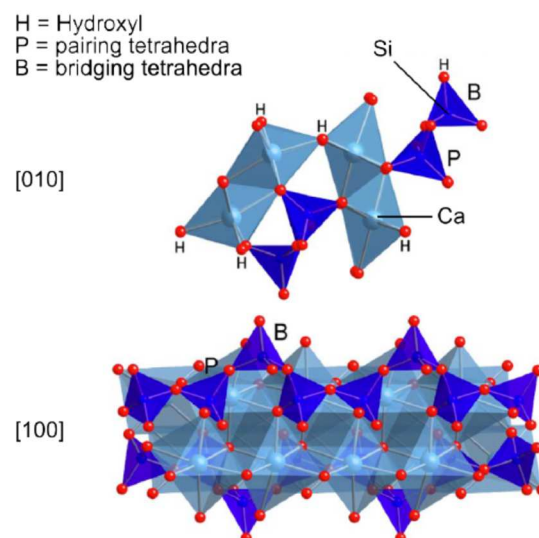


Figure 2.9. Structure of jennite as seen along [010] (top) and [100] (bottom). “H” indicates hydroxyl groups. Reproduced from Richardson who used data from Bonaccorsi<sup>81,84</sup>

Both 1.4-nm tobermorite and jennite have ability to vary in composition, degree of polymerization and extent of crystallinity while maintaining the essential features of the composite layer structure. The variations of the C/S ratio, the silicate structure and contents of Si–OH and Ca–OH in C-S-H are correlated.<sup>76</sup>

The XRPD pattern of C-S-H gel does not give unambiguous evidence which structure, 1.4-nm tobermorite or jennite, better approximates the nanostructure of C-S-H gel. The C/S ratio 1.7 to 1.8 has been determined for the C-S-H gel by determination of the CH content, residual C<sub>3</sub>S content and microanalysis using microprobe or transmission electron microscopy (further: TEM).<sup>85-92</sup> These observations together with other evidences support the hypothesis that C-S-H gel is initially a mixture of 1.4-nm tobermorite and jennite-like structures with later becoming dominant with age.<sup>93</sup>

The researches of microstructural development of calcium silicate pastes by scanning electron microscopy (further: SEM) has confirmed the existence of massive and almost structureless C-S-H gel formed from the larger anhydrous grains called inner product. The outer product formed in the water filled space forms columns or fibres radiating from the anhydrous grain.<sup>94-97</sup> Further SEM investigations have confirmed four morphological types of the C-S-H gel:

- Type I: fibrous material with fibres up to 2 µm long dominant at early ages of hydration;
- Type II: honeycombs or reticular networks form as a normal early product;
- Type III: massive formed of tightly packed spherical grains up to 300 nm across observed in older pastes;
- Type IV: more featureless and massive, inner-like product observed in older pastes.<sup>95</sup>

The three principal stages of product development have been distinguished in C<sub>3</sub>S pastes:

- Early product formed during the first 4 hours;
- middle product formed between 4 and 24 hours;
- late product formed subsequently.<sup>98</sup>

The early product is characterized as consisting of foils, flakes and honeycombs and being very similar to Type I.<sup>99,100</sup> Rapid formation of the C-S-H gel and CH is characteristic for the middle stage of hydration.<sup>91</sup> Type I C-S-H is dominant but also the outer like product has been observed. In the late stage Types III and IV C-S-H are formed together with more CH.<sup>98</sup>



Calcium hydroxide has a layer structure with calcium atoms octahedrally and the oxygen atoms tetrahedrally coordinated.<sup>101,102</sup> There are no experimental evidences that some of the CH in calcium silicate pastes is amorphous.<sup>73</sup>

#### 2.5.2. Hydration of belite

The hydration of C<sub>2</sub>S is similar to C<sub>3</sub>S hydration but the reaction is slower. Only 30% of belite reacts within 28 days and 90% in 1 year.<sup>73</sup> The hydration of C<sub>2</sub>S can be simplified and described by the following equation:



The equation shows that a significantly lower amount of CH is formed by hydration of C<sub>2</sub>S than by C<sub>3</sub>S and the relative portion of C-S-H in the final product is higher for C<sub>2</sub>S. There are no differences in the growth, morphology and composition of C-S-H formed by hydration of belite and alite.<sup>103,104</sup>

#### 2.5.3. Experimental considerations

The susceptibility of C-S-H to carbon dioxide, organic solvent and heating makes the experimental research on Portland cement more complicated.<sup>73</sup>

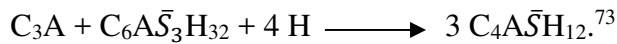
C-S-H reacts with atmospheric CO<sub>2</sub> with formation of CaCO<sub>3</sub>. This reaction decreases the C/S ratio in the C-S-H gel. It is usually important to know how much CO<sub>2</sub> is present in the Portland cement paste or to conduct experiments in CO<sub>2</sub>-free atmosphere. It can be determined by simple and accurate method based on decomposition with dilute acid and absorption of the liberated CO<sub>2</sub> in Ba(OH)<sub>2</sub> solution which is then back titrated with HCl. The XRPD method and thermogravimetry (further: TG) can be applied but less accuracy can be achieved.<sup>73</sup>

Polar organic liquids such as methanol, propan-2-ol or acetone are usually used to stop hydration before further experimental determinations. It is undesirable since removal of organic liquids from Portland cement paste can cause seriously alternations.<sup>73</sup> Acetone can undergo aldol condensation at room temperature and methanol reacts with CH.<sup>105,106</sup> Heating at 105 °C or equilibration to constant mass at low relative humidity partially dehydrates the C-S-H or decomposes other hydrated phases.<sup>73</sup>

#### 2.5.4. Hydration of aluminate and ferrite phase

Pure C<sub>3</sub>A reacts with water immediately, liberating a large amount of heat of hydration. Crystalline hydrates such as C<sub>3</sub>AH<sub>6</sub>, C<sub>4</sub>AH<sub>19</sub> and C<sub>2</sub>AH<sub>8</sub> are formed by this reaction.<sup>73,74</sup> When C<sub>3</sub>A reacts with water in the presence of calcium sulfate, ettringite is formed which

reacts further to form aluminato ferrate monosulfate (further: AFm) phases. The reactions can be described by further equations:



Ettringite ( $\text{C}_6\text{A}\bar{\text{S}}_3\text{H}_{32}$ ) is the first crystal hydrate formed in the Portland cement paste, within 30 minutes from contact between Portland cement and water. In the period 24 – 48 hours, ettringite reacts further to form AFm phases. The hydration products formed by hydration of  $\text{C}_4\text{AF}$  are essentially similar to those formed by  $\text{C}_3\text{A}$  hydration.<sup>73</sup>

Ettringite  $[\text{Ca}_3(\text{Al,Fe})(\text{OH})_6 \cdot 12\text{H}_2\text{O}]_2 \cdot (\text{SO}_4)_3 \cdot 2\text{H}_2\text{O}$  or  $\text{C}_6\text{A}\bar{\text{S}}_3\text{H}_{32}$  belongs to the family of AFt phases having the general constitutional formula  $[\text{Ca}_3(\text{Al,Fe})(\text{OH})_6 \cdot 12\text{H}_2\text{O}]_2 \cdot \text{X}_3 \cdot x\text{H}_2\text{O}$  where  $x$  is normally  $\leq 2$  and  $\text{X}$  represents one doubly charged anion or two singly charged anions. It also occurs as a natural mineral. Ettringite and other AFt phases form hexagonal prismatic or acicular crystals. There are two distinct structural components: columns of  $[\text{Ca}_6(\text{Al}(\text{OH})_6)_2 \cdot 24\text{H}_2\text{O}]^{6+}$  and channels with  $[(\text{SO}_4)_3 \cdot 2\text{H}_2\text{O}]^{6-}$ . Figure 2.10 illustrates the structure of ettringite.<sup>73</sup>

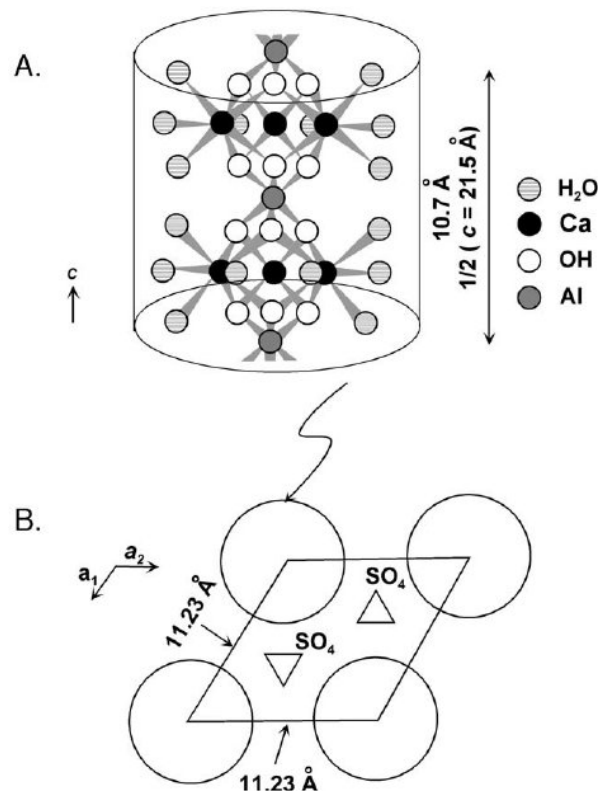


Figure 2.10. Schematic structure of ettringite after Taylor<sup>107</sup>

The AFm phases may be prepared from aqueous solutions containing ions necessary for this formation or by the hydration of Portland cement. AFm form can form hexagonal crystals but in Portland cement paste much is poorly crystalline and intimately mixed with C-S-H. General formula of AFm phase is  $\text{CaAl}(\text{OH})_6 \cdot \text{X} \cdot n\text{H}_2\text{O}$  where X represents a single charged or half a double charged anion. AFm has a layer structure derived from CH composed of two layers: positively charged rigid layer  $[\text{Ca}_2\text{Al}(\text{OH})_6]^+$  and negatively charged  $[\text{X} \cdot n\text{H}_2\text{O}]^-$ . Different anions ( $\text{OH}^-$ ,  $\text{SO}_4^{2-}$ ,  $\text{CO}_3^{2-}$ ,  $\text{Cl}^-$ ) and a number of water molecules can be present in the interlayer region.<sup>73,108</sup>

The hydration of aluminate and ferrite phases is very important since it determines setting behaviour, rheology of fresh Portland cement paste and early hardening.

#### 2.5.5. Portland cement hydration

Hydration of Portland cement is very similar to hydration of  $\text{C}_3\text{S}$ . The principal products formed the C-S-H gel, and CH formed by hydration of calcium silicate, and AFt and AFm phases formed by hydration of aluminate and ferrite are also present in hydrated Portland cement paste. Amorphous CH was confirmed in hydrated Portland cement pastes in contrast with the pure  $\text{C}_3\text{S}$  pastes.<sup>109,110</sup> Clinker phases are consumed at different rates and calcium sulfate phases are usually no longer detectable after 24 hours. In the XRD pattern ettringite is observed early, within few hours and usually reaches its maximum at about 1 day. Peaks corresponding to AFm are observed subsequently. They are usually broad thus suggesting that AFm is poorly crystalline.<sup>107</sup> The appearance of AFm peaks usually corresponds to decrease of  $\text{SO}_4^{2-}$  concentration in solution that favours formation of monosulfate instead of ettringite. In some cases, in Portland cement with a high  $\bar{S} / A$  ratio or sulfate resisting cement, ettringite can be detected up to one year. Carbonatization of hydrated Portland cement paste also causes ettringite formation in the late period of hydration.<sup>111</sup>

#### 2.5.6. Hydration kinetics and mechanism of hydration

It is difficult to resolve the individual mechanisms of Portland cement hydration or the parameters that determine their rates due to the complexity and interdependence of chemical and microstructural processes. Portland cement hydration processes fall into one of the following categories: (1) dissolution / dissociation, (2) diffusion, (3) growth, (4) nucleation, (5) complexation and (6) adsorption.<sup>112</sup> These processes are carried out in series, parallel or in some more complex combination. Unfortunately, the application of chemical kinetics models based on fundamental chemistry and physics is not efficient because of difficulties in isolating

individual chemical processes for further studies. Thus, the present models of cement hydration are more empirical, less mechanistic. The overall hydration can be divided into four stages: (1) initial reaction, (2) the period of slow reaction (3) acceleration period and (4) deceleration period. The initial period corresponds to early product formation, while the middle product is formed during acceleration and deceleration period.<sup>112</sup>

Two mechanisms of Portland cement hydration have been proposed: through–solution hydration and solid–state hydration. Through–solution hydration involves dissolution of anhydrous compounds to ionic constituents, formation and precipitation of hydration products. In the solid–state hydration mechanism reaction takes place on the surface of the anhydrous cement phases without ions dissolving in the solution. Through–solution mechanism is dominant at early hydration and solid–state take place at later ages when the mobility of ions in solution is restricted.<sup>13</sup>

## **2.6. Microstructure of hardened Portland cement paste**

Hardened Portland cement paste has properties of a rigid gel. It is strong solid of high porosity and internal surface area. Hardened Portland cement paste is built of hydration products, unreacted cement grains, capillary pores and water solution called pore solution.<sup>74,113</sup> Water in hardened Portland cement paste can be categorized as: evaporable and non - evaporable water. Non – evaporable water is incorporated within hydration products and sometimes is used as measure of the degree of hydration.<sup>114</sup> Evaporable water occupies capillary pores and partly so-called gel pores within hydration products. Total porosity of hardened Portland cement paste includes all types of pores shown in Figure 2.11: closed (isolated), opened (passable and baggy).<sup>74</sup>

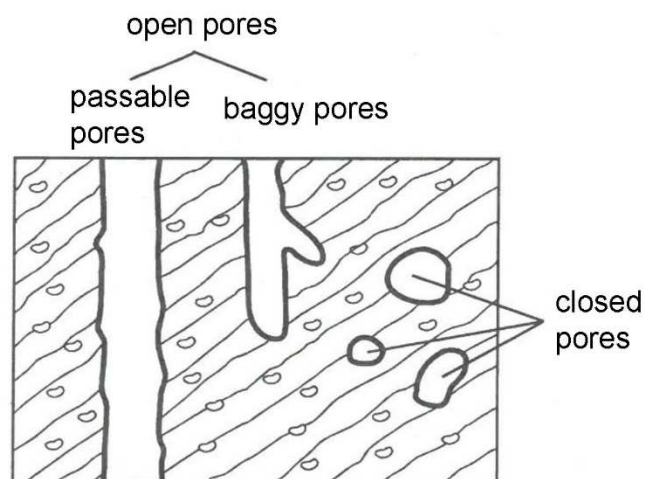


Figure 2.11 Schematic diagrams of pore types in hardened Portland cement paste after Đureković<sup>74</sup>

According to the IUPAC proposal pores in hardened Portland cement paste are classified as: micro pores in gel with the diameter less than 2.6 nm; capillary pores or mezzo pores with the diameter between 2.6 and 50 nm and macro pores with the diameter larger than 50 nm.<sup>115</sup> Portland cement type, water to cement ratio and hydration condition largely determine features of the pore system in the hardened Portland cement paste.

The link between some microstructural descriptors such as porosity has been studied extensively. Powers has established a connection between compressive strength and the ratio of the volume of hydration products and capillary porosity. Microstructural models have also been developed to link mechanical properties to microstructure of the material. Little has been done to explain how the nature of hydration products impacts the mechanical properties of cement. This is consequence of difficulties to quantify the volumes of the different phases in the system and the lack of models to relate mineral assemblage to mechanical properties. Recently it was determined that all hydrates do not contribute in the same way to compressive strength. The C-S-H gel has a critical role compared to other hydrates in contributing to the compressive strength of the cement paste. This is explained by the fact that C-S-H is intermixed with porosity and other phases are just inclusions in C-S-H and porosity matrix.

#### 2.6.1. Scanning electron microscopy

Scanning electron microscopy (further: SEM) can give important information about the microstructure of hardened Portland cement paste.<sup>116</sup> It is possible to use a wide range of

magnifications usually  $20 \times$  to  $10\,000 \times$  and thus observe morphology of the hydration products. The scanning electron microscope is usually equipped to do X-ray microanalysis which enables determination of the composition of the features in the SEM image and thus enables identification of different microstructural constituents.<sup>117</sup> Secondary electron imaging (further: SEI) or backscattered electron image (further: BSEI) are commonly recorded depending on the type of detector used with microscope. The interaction of incident electron beam with the sample generates different signals among which secondary electrons, backscattered electrons and X-rays are commonly used for microstructural identification. Energy dispersive X-ray spectrometry (further: EDS) can be usually done with the same instrument. Different signals generating from different regions (Figure 2.12) are picked up by different detector types, converted to electrical signal and used for imaging.<sup>11</sup>

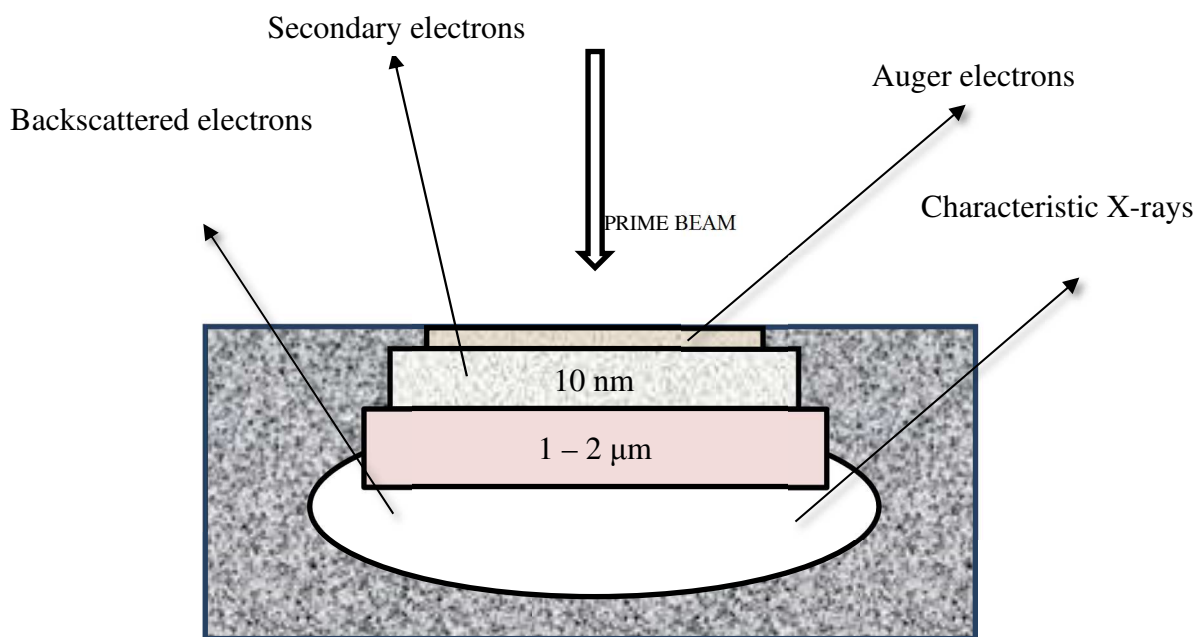


Figure 2.12. Schematic diagram of SEM signals generation

Compositional contrast as a result of different average atomic numbers of different features. Hydration products appear less bright in BSE images due to their lower average atomic number and present a strong contrast to bright unreacted Portland cement clinker phases with higher average atomic numbers. Topographic contrast in SEI and BSE images enables

imagination of size, shape and texture of different features present in hardened Portland cement paste.<sup>116,117</sup>

### 2.6.2. Distribution of the trace elements in hydrated Portland cement paste

Following the primary hydration, trace elements from anhydrous cement are transferred to the hydration products in the Portland cement paste. The structure and chemistry of hydration products favour immobilization of trace elements by multiple mechanisms: chemisorption, precipitation, formation of surface compounds, inclusion and chemical incorporation.<sup>118</sup> Ettringite acts as a host to a number of ions. Immobilization of  $\text{Cd}^{2+}$ ,  $\text{Co}^{2+}$ ,  $\text{Pb}^{2+}$  and  $\text{Zn}^{2+}$  within the AFt phase at the  $\text{M}^{2+}$  site has been reported.<sup>55,119,120</sup> Elements present in the oxidative state +3 (chromium, cobalt, nickel) can substitute  $\text{Al}^{3+}$  ions in AFt.<sup>119,121,122</sup> Substitution of the sulfate ion in AFt with vanadate ( $\text{VO}_4^-$ ), chromate ( $\text{CrO}_4^{2-}$ ) and arsenate ( $\text{AsO}_4^{3-}$ ) has been experimentally confirmed as well as physical encapsulation of mercury.<sup>119,123,124</sup> Immobilization within the AFm phases is not so well researched mainly due to the assumption that all ions immobilized in the AFt phases are transferred to the AFm phases in the later period of hydration.<sup>55</sup> Immobilization mechanisms of the trace elements within C-S-H include: sorption (Co, Ni, Zn, As), substitution (Cu, Cr) and phase mixing (nickel hydroxide, cadmium hydroxide).<sup>55,121,122,125-128</sup> Many trace elements are present in the form of individual phases. Cadmium, lead and zinc also precipitate in the form of hydroxide, carbonate and nitrate mixed salts.<sup>119,129</sup> Cadmium hydroxide provides the nucleation sites for precipitation of calcium hydroxide and the C-S-H gel.<sup>129,130</sup> Formation of Ni-Al layered double hydroxides has been confirmed in the Portland cement paste.<sup>131,132</sup> For higher zinc concentrations precipitation of  $\beta\text{-Zn}(\text{OH})_2$  and calcium zincate,  $\text{Zn}_2\text{Ca}(\text{OH})_6 \cdot 2\text{H}_2\text{O}$ , has been reported.<sup>123,133</sup> Precipitation of magnesium and calcium arsenate in the amorphous rather than in the crystalline form has been confirmed.<sup>71,134</sup> Precipitation of calcium antimonate in the Portland cement paste is not supported due to its pH independent solubility.<sup>135</sup> Cornelis *et al.* have shown that antimonate forms a solid solution predominantly with AFm and the C-S-H gel. For the higher concentrations of antimony (1000 mg/kg), the formation of romeite with a general formula  $\text{Ca}_{1+x}\text{Sb}_2\text{O}_6\text{OH}_{2-2x}$  has been proposed.<sup>136</sup> The composition and the structure of romeite changes with pH and the concentration of available calcium ions.<sup>137</sup> Substitution of  $\text{Ca}^{2+}$  by  $\text{Pb}^{2+}$  ions in all hydrated phases was suggested by different authors.<sup>120,138</sup> Small fractions of trace elements are dissolved in pore solutions within the capillary pores of hydrated Portland cement pastes.

### 2.6.3. Pore solution chemistry

Pore solution is essential but often the overlooked part of hydrated Portland cement paste. The composition of pore solution reflects the chemical processes and interactions between the solid and liquid phases. It can be useful in understanding of the mechanism and kinetics of cement hydration as well as the thermodynamic modelling of hydration.<sup>139</sup> The pore solution is mainly responsible for transport of substances within Portland cement paste and also serve as entry channels for external substances. Thus, the composition of the pore solution can be used to evaluate different destructive reactions in the Portland cement paste related to durability.<sup>140</sup>

Vacuum filtration or centrifugation can be used to extract the pore solution from the hydrated Portland cement during the first hours of hydration.<sup>141,142</sup> The high-pressure device firstly described by Longet *et al.* is commonly used for pore solution expression from hardened Portland cement paste. Pressures up to 250 MPa are usually applied since data indicate that the composition of the pore solution does not change with pressure up to this value.<sup>143,144</sup>

The pore solution has been considered as an alkali hydroxide solution with hydroxide ions, sodium, potassium, calcium, sulfate, silicon and aluminium as the principle dissolved ions. Sodium and potassium are usually present in the form of ready soluble alkali sulfates in Portland cement and are partly incorporated within the main clinker phases. Alkali sulfates dissolve within the first minute when water is added. A part of alkalis is bound in the C-S-H gel.<sup>145,146</sup> Concentration of sodium and potassium increases in the course of time due to hydration processes and release of alkalis incorporated in the main clinker phases. Their concentrations increase until reaching the maxima at about 7 days hydration period. A decline is then observed until reaching constant values present for a long time. Concentration of alkalis in the pore solution depends on total  $K_2O$  and  $Na_2O$  content in Portland cement and w/c ratio of hydrated cement paste.<sup>139</sup> The average pore solution concentrations of sodium and potassium in pure Portland cement pastes obtained by statistical evaluation of data from numerous researches are given in Figure 2.13.



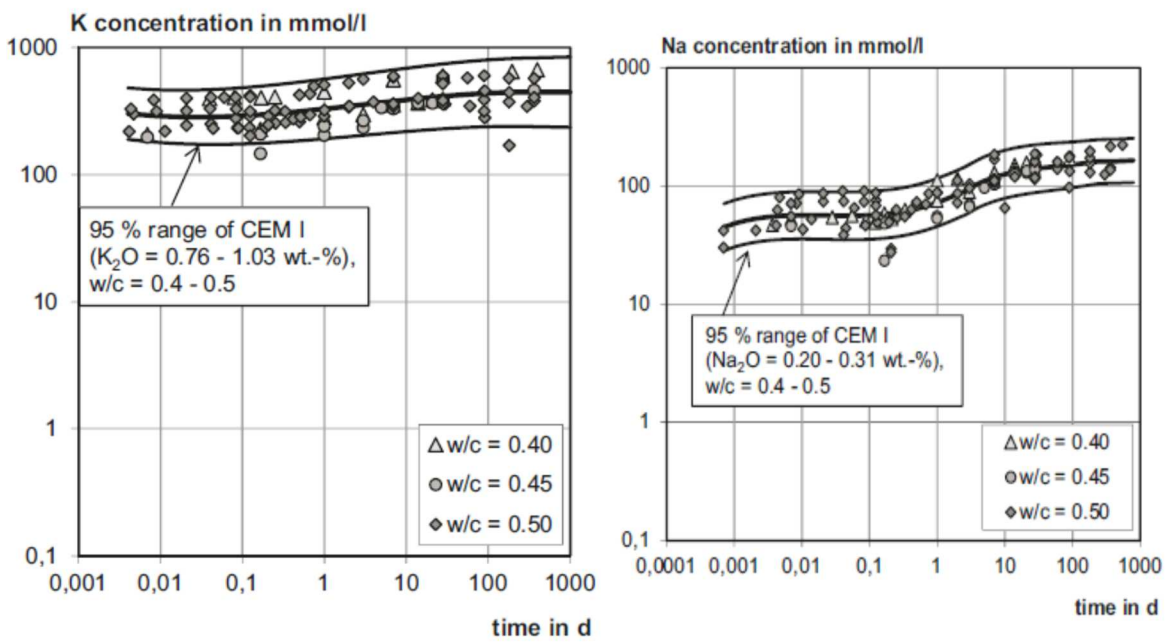


Figure 2.13. Average pore solution concentrations of potassium and sodium in pure Portland cement pastes with K<sub>2</sub>O content between 0.76 % - 1.03 % and Na<sub>2</sub>O content between 0.20 % - 0.31 %, after Vollpracht *et al.*<sup>139</sup>

The concentration of hydroxyl ions ( $\text{OH}^-$ ) is correlated with concentration of alkalis in the pore solution. Usually it is expressed in the form of pH value. Common practice in experimental research of pore solution is to calculate the pH value from the  $\text{OH}^-$  concentration or vice versa. The increase of alkalis concentration causes increase of the pH value (concentration of  $\text{OH}^-$ ). The w/c ratio also determines concentration of hydroxyl ions. For higher w/c ratio, dilution is higher and thus the pH value lower. The average pore solution concentrations of  $\text{OH}^-$  ions in pure Portland cement pastes obtained by statistical evaluation of data from numerous researches are given in Figure 2.14.

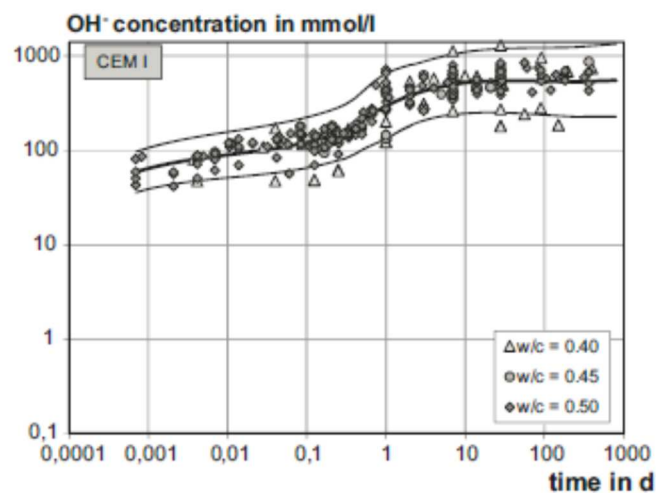


Figure 2.14. Average pore solution concentrations of  $\text{OH}^-$  ions of pure Portland cement pastes after Vollpracht <sup>139</sup>

Calcium and sulfate concentration in the pore solutions depend on the solubility of the phases present at the particular hydration time. The w/c ratio has a small impact, although the pH values influence the calcium concentration. Higher concentrations of calcium and sulfate are observed in the early period of hydration where they follow the gypsum ( $\text{CaSO}_4 \cdot 2\text{H}_2\text{O}$ ) and anhydrite solubility. Decrease in the concentration corresponds with the acceleration period of hydration and formation of ettringite. Within a longer period the concentration of calcium is determined by the solubility of portlandite and thus depends on the pH value due to the common ion effect. It decreases with an increase of the pH value. Ettringite limits the concentration of sulfate ion on the long-term scale and the influence of the pH value is very small. The average pore solution concentrations of calcium and sulfate in pure Portland

cement pastes obtained by statistical evaluation of data from numerous researches are given in Figure 2.15

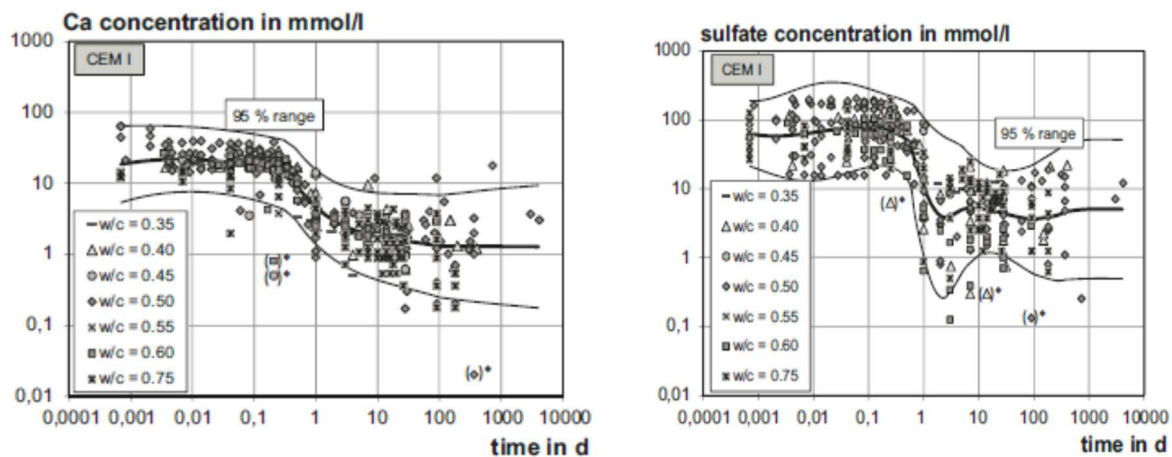


Figure 2.15. Average pore solution concentrations of calcium and sulfate of pure Portland cement pastes after Vollpracht <sup>139</sup>

Concentrations of silicon and aluminium are below 1 mmol / L and slightly increase with the pH value. The addition of granulated blast furnace slag (further: GBFS), slightly lowers the alkali concentrations and pH values of pore solutions. The stronger influence on alkalinity has been observed for the higher GBFS amounts (>75%). The effect on the other ions is relatively small.

Investigation of the trace elements in the pore solution is less often encountered in the literature. Kempel *et al.* have reported the total content of the selected trace elements (lithium, barium, strontium, iron, aluminium and silicon) in hydrated and carbonated Portland cement pastes.<sup>147</sup> The research of Díez *et al.* on immobilization of cadmium in the Portland cement paste has shown a low concentration of cadmium in the pore solution.<sup>59</sup> Vollpracht *et al.* have investigated development of the concentrations of selected elements (antimony, barium, chromium, lead, molybdenum and vanadium) in pore solutions of Portland cement pastes exposed to leaching throughout a 28 days period.<sup>148</sup> These researches were mainly focused on mechanisms and places of the trace elements binding and less or not at all to deleterious processes in Portland cement pastes.

## 2.7. Portland cement production

### 2.7.1. Production process

Portland cement is manufactured in a series of operations using one of four available process routes:

- wet process;
- semi dry process;
- semi wet process;
- dry process.<sup>148</sup>

The principal difference between the four routes is the raw material preparation. In the dry and semi dry processes, the raw materials are dried and ground together in defined and controlled proportions to form a flowable powder. The slurry is created from the raw materials in the wet process and the semi wet process. The resulting materials are called raw meal (dry and semi dry process) or raw slurry (wet or semi wet process). The dry process is favourable since it is more energy efficient because it does not require energy for evaporation of water from the raw slurry. Only about 2.5 % of European production in 2007 originated from the wet process kilns and around 7.5 % from semi dry/semi wet processes. The remainder, around 90 %, accounts for the dry processes.<sup>148</sup> The following sub-processes are common to all process types:

- quarrying, raw materials storage and preparation;
- fuel storage and preparation;
- control and preparation of waste materials used as raw materials and/or fuels;
- clinker burning with emission reduction;
- cement grinding;
- cement dispatch.

The flow diagram of the dry process of the Portland cement production is shown in Figure 2.16.<sup>148</sup>

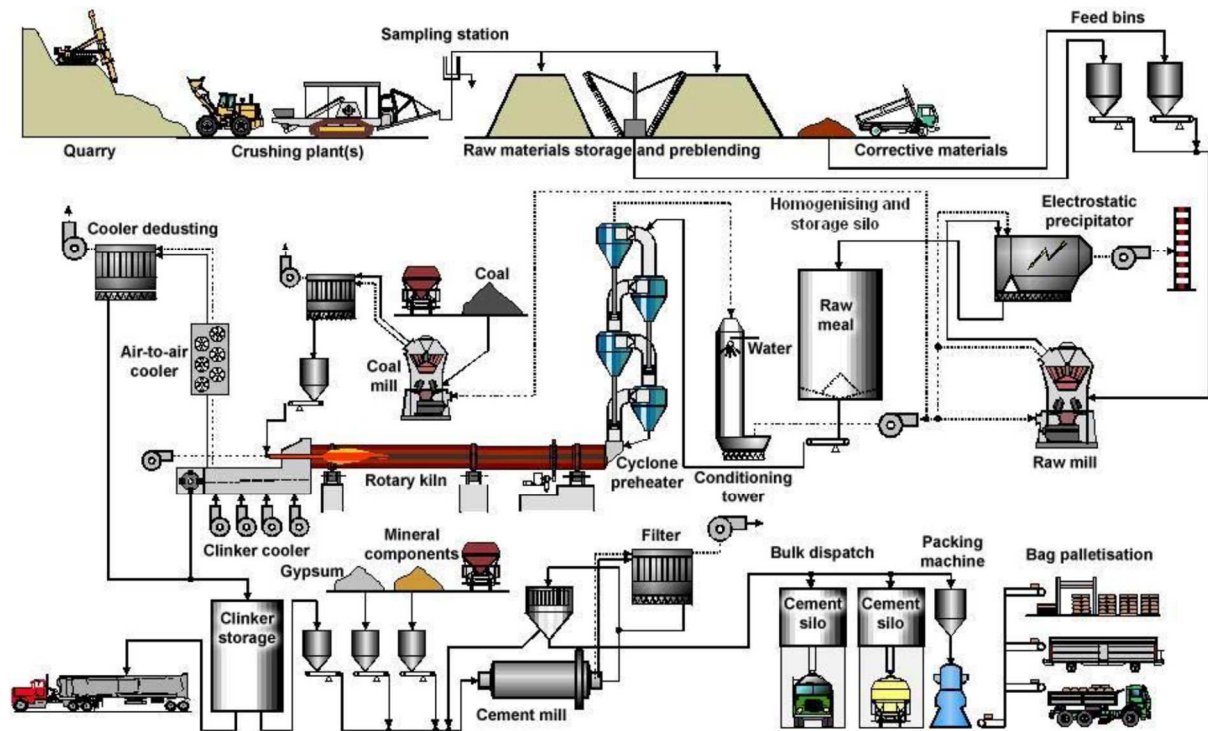


Figure 2.16. General overview of the cement manufacturing process (dry process) after BAT reference document for the production of cement, lime and magnesium oxide<sup>148</sup>

Since calcium silicates are the primary constituents of Portland cement, the raw materials used for Portland cement production must provide calcium and silica for its productions. Cheap, naturally occurring materials such as limestone, chalk, marl, dolomite, clay and sand are commonly used materials. Sometimes addition of bauxite or iron ore to the raw materials are necessary to assure the required levels of aluminium or iron for the formation of calcium aluminates or aluminoferrites.<sup>5,13</sup>

The raw meal (or raw slurry) is heated at about 1450°C in a cement kiln to produce black nodular material, Portland cement clinker. The combustion of fossil fuels assures the required high inputs of thermal energy necessary for Portland cement clinker production. Non fossil fuels derived from industrial sources such as tyres, waste oil, plastics, solvents and many more are commonly used as substitute fuels today.<sup>148</sup> Finally, Portland cement clinker is underground with a few percentages of gypsum to produce Portland cement. It is dispatched packed in bags or as a bulk by road, rail or ships.

### 2.7.2. CO<sub>2</sub> emission in Portland cement production

The key sources of CO<sub>2</sub> emissions in cement industry are emissions from decarbonatization, burning fuels and indirect emissions (electricity consumption and transport).<sup>149</sup> The contribution of different sources of emission to the overall CO<sub>2</sub> emission from the Portland cement production is reported in Figure 2.17. Over 50% of all CO<sub>2</sub> emissions from cement production accounts for decarbonatization, the simple transformation of limestone to lime:

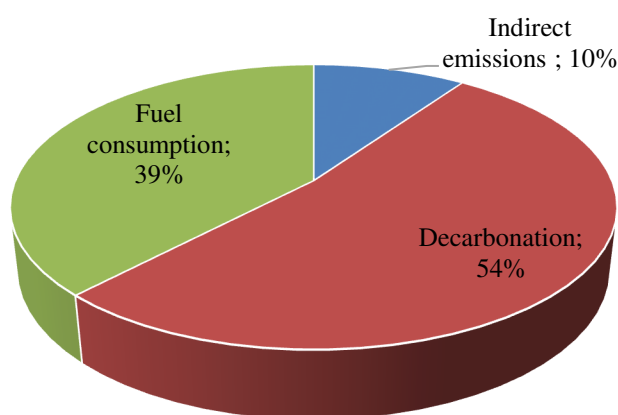
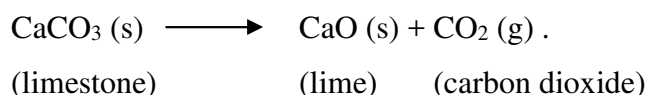


Figure 2.17. Contribution of different sources to CO<sub>2</sub> emissions from Portland cement production<sup>149</sup>

The reduction of released CO<sub>2</sub> due to reduced thermal energy requirements by more efficient technology or by usage of alternative fuels is the traditional approach. It has limitations and does not radically change the chemical composition and the required quantity of decarbonated CaCO<sub>3</sub>.

The reduction of CO<sub>2</sub> emission due to decarbonatization is the most challenging task in Portland cement production. A typical Portland cement contains around 67% of calcium expressed as oxide (CaO).<sup>5</sup> If all calcium comes from limestone, production of one ton of Portland cement clinker requires roughly 1.2 tonnes of limestone which releases about 526 kg of CO<sub>2</sub>.<sup>150</sup>

Traditional approaches for decarbonated CO<sub>2</sub> reduction are limited to improvement of hydraulic activity of Portland cement clinker and to production of blended Portland cement

types.<sup>2</sup> The addition of some elements such as fluoride (F<sup>-</sup>) in a minor percentage to the raw meal may improve the hydraulic activity of Portland cement clinker and can thus enable the reduction of total cement content in concrete. In blended Portland cement a part of Portland cement clinker is substituted by supplementary cementitious materials (further: SCMs). The production of blended cements is a very well established approach to reduce the CO<sub>2</sub> footprint of Portland cement. Different SCMs such as natural pozzolana, fly ash, granulated blast furnace slag, silica fume or finely ground limestone are traditionally used.<sup>2</sup> Usage of SCMs is based on numerous scientific investigations which enabled finding of materials that can give similar properties to cement but have a much lower amount of embodied CO<sub>2</sub>. Blended Portland cement are a well established solution recognized by the European standard for commonly use Portland cements.<sup>151</sup>

Currently the average clinker content in European cements is less than 80% and estimation is that it can be reduced to 70%.<sup>149</sup> The implementation of traditional solutions is not sufficient to reduce even half the total required CO<sub>2</sub>.<sup>150</sup> Further reduction requires more radical solution such as a reduction in the CaO content of the Portland cement.<sup>2,152</sup>

The CO<sub>2</sub> footprint of clinker phases decrease in order C<sub>3</sub>S > C<sub>3</sub>A > C<sub>2</sub>S > C<sub>4</sub>AF. CO<sub>2</sub> emissions for clinker phases are reported in Table 2.4.<sup>150</sup>

Table 2.4. CO<sub>2</sub> emissions from raw materials (RM), fuel and total CO<sub>2</sub> emission for four main Portland cement clinker phases. The mass of CO<sub>2</sub> is per ton of clinker.

Clinker phase	m(RM CO <sub>2</sub> )/ kg	m(fuel CO <sub>2</sub> )/kg	m(sum CO <sub>2</sub> )/ kg
C <sub>3</sub> S	578	282	860
C <sub>2</sub> S	511	204	715
C <sub>3</sub> A	489	298	787
C <sub>4</sub> AF	362	208	570
free lime	785	486	1271

RM CO<sub>2</sub> = emission from raw materials, decarbonatization

Fuel CO<sub>2</sub> = emission from combustion of fuel

The production of Portland cement clinker and Portland cement containing more C<sub>2</sub>S than C<sub>3</sub>S is possible but not favourable. Belite Portland cements achieve significantly lower early strengths which do not correspond to the modern requirement for quick construction work

progress. The usage of larger quantities of SCMs as clinker substitute in belite cement would be impossible due to the decreasing impact of some SCMs to early strength.<sup>152</sup>

Alternative to production of belite clinker is sintering clinkers using chemical systems based on sulfoaluminate, sulfoferrite and fluoroaluminate.<sup>2</sup>

## 2.8. Calcium sulfoaluminate cement

Calcium sulfoaluminate cement (further: CSA cement) is characterized by high amounts of tetracalcium trialuminate sulfate ( $C_4A_3\bar{S}$ ) also known as Ye'elimite or Klein's salt. It originates from China where it was developed by China Building Materials Academy in the 1970s.<sup>153,154</sup> Other principal phases in the CSA clinker are  $C_2S$  and  $C\bar{S}H_2$  and some minor phases such as CA,  $C_3A$ ,  $C_4AF$ , mayenite and gehlenite.<sup>155-157</sup> CSA cements have a very variable phase composition. Ye'elimite crystallizes as the sodalite type structure with the general composition  $Na_8[Al_6Si_6O_{24}]$ . Initially, three polymorphs (cubic, tetragonal and orthorhombic) have been reported for pure Ye'elimite.<sup>158-161</sup> The recent researches have confirmed that the orthorhombic structure is the most stable one and that the cubic structure can exist at room temperature only if dopant ions are available to stabilize it.<sup>162,163</sup> Incorporation of different ions in the crystal structure of the solid solution leads to formation of pseudo cubic or cubic Ye'elimite.<sup>164,165</sup>

In Europe, there is no standard for Ye'elimite containing cements thus, they can be classified into three different groups according to their  $C_4A_3\bar{S}$  content:

- calcium sulfoaluminate cements with high Ye'elimite content;
- belite calcium sulfoaluminate cements;
- alite calcium sulfoaluminate cements.<sup>166</sup>

Calcium sulfoaluminate cements with high  $C_4A_3\bar{S}$  content (above 50 %) are usually prepared from CSA clinker with addition of calcium sulfate (typically from 10 % to 25 %). The addition of calcium sulfate determines the properties of CSA cement, thus the source and quantity have to be customized for the specific application.<sup>167</sup>

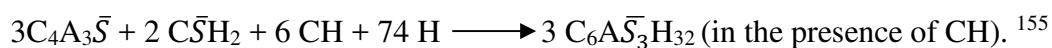
In belite calcium sulfoaluminate cements  $\beta$ - $C_2S$  is the main phase with abundance higher than 40%. Ye'elimite content is moderate, up to 30 %.<sup>168</sup> The main disadvantage of this cement type is lower early strength due to slower belite hydration. Two different formulations with different phase composition are possible within this group: iron-rich and aluminium-rich belite CSA cement.<sup>169,170</sup> Aluminium-rich CSA cement may contain  $C_{12}A_7$  or CA phases



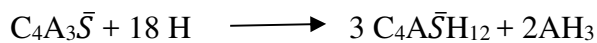
as main clinker phases, while in the iron-rich cement they are substituted by  $C_4AF$ . It is possible to produce belite CSA cement in which high temperature  $\alpha$ - $C_2S$  is stabilized with borax. This type of belite CSA cement shows significant improvement of early strengths.<sup>171</sup>

Alite CSA cements are characterized by the simultaneous presence of two major phases  $C_3S$  and  $C_4A_3\bar{S}$  in combination with other phases usually present in clinkers such as  $C_2S$  and  $C_3A$ . It is very hard to produce this cement type since optimum temperatures for two major phases are considerably different. It can be produced by addition of small amounts of compounds such as calcium fluoride ( $CaF_2$ ), copper or titanium oxide ( $CuO$  or  $TiO_2$ ) to the raw meal. The content of  $C_4A_3\bar{S}$  may be higher compared to  $C_3S$ .<sup>168,172</sup>

Hydration of CSA cement is complicated, but the most important reactions are the formation and transformation of ettringite. Ettringite is formed rapidly by hydration of  $C_4A_3\bar{S}$  according the following equations:



If gypsum is absent the following reactions occur:



Hydration reaction of  $C_2S$ ,  $C_4AF$  and other phases are the same as in Portland cement. The main crystal phases formed by hydration of CSA cement are ettringite and monosulfate. C-S-H formed by  $C_2S$  hydration and aluminium hydroxide ( $AH_3$ ) produced by Ye'elinite hydration are gel products.

The group of CSA cements are very attractive for research mainly due to reduced environmental impact and some improved properties. Only one third of the  $CO_2$  mass released by the production of  $C_3S$  is released during production of  $C_4A\bar{S}H_{12}$  (around  $220 \text{ kg t}^{-1}$  compared to  $860 \text{ kg t}^{-1}$ ).<sup>166</sup> The production temperature for CSA clinker is approximately  $200 \text{ }^\circ\text{C}$  lower than that for the Portland cement clinker. Natural raw materials limestone, bauxite, iron ores and gypsum are used to prepare the raw meal for CSA clinker production. Various industrial by-products such as fly ash, blast furnace slag, red mud or phosphogypsum may be used for raw meal preparation also.<sup>173-176</sup> Ye'elinite containing clinkers are easier to grind than Portland cement clinkers.

The usage of CSA cement in Europe is very limited due to the lack of standards and codes. CSA cement cannot be used for preparation of structural concrete. It is mainly used in blends with Portland cement for quick repairs, pre-cast products and floor concrete.<sup>166</sup>

## 2.9. Leaching

Hydration products in hydrated Portland cement paste are in dynamic equilibrium with the pore solution, thus the ion composition of pore solution varies as hydration proceeds.<sup>107</sup> When hydrated Portland cement paste is exposed to chemically aggressive environment chemical compositions of solid products and pore solution change, causing disruption and re-establishment of equilibrium, disappearance of solid products or precipitation of new ones. This can have adverse consequence on engineering properties of Portland cement paste causing its degradation and finally resulting in reduced service life and poor durability.

Water is involved both in creation and destruction of the Portland cement paste. It is crucial for different forms of physical or chemical deterioration such as crystallization of salts in pores, frost action, acidic solution attack, sulfate attack, alkali – aggregate reaction or steel corrosion.<sup>177</sup> In these processes water serves as transport media for aggressive ions but itself can also be a source of chemical degradation. Soft water containing a low concentration of dissolved ions in contact with Portland cement paste induces decalcification.<sup>178,179</sup> This process is called leaching. A decrease of calcium and hydroxide ions in the pore solution induces hydrolysis and leaching of the calcium containing hydration products.<sup>180,181</sup> Solid products are dissolved depending on their solubility. The susceptibility towards soft water decreases in the order CH, AFm, AFt, C-S-H.<sup>182</sup> Dissolution of portlandite reduces the pH value of the pore solution and induces macro-porosity of the cement paste.<sup>181,183,184</sup> Decalcification of the C-S-H gel gradually decrease C/S ratio and induces micro-porosity.<sup>181,183,185</sup> In the leached Portland cement paste, the secondary precipitation of AFm, AFt and calcite appears.<sup>186,187</sup> The increased porosity and permeability and loss of mechanical strength are the key consequences in the structures exposed to leaching.<sup>185,188-190</sup> Alkali metals are readily leached but without adverse effect on the Portland cement paste.<sup>184</sup> Leaching may affect immobilization of the trace elements and their concentration in the pore solution, especially on the long-term scale. The increased mobility of the trace elements may increase the possible environmental risk.

Leaching appears in Portland cement pastes exposed to steam, fog, rainwater or groundwater.<sup>184</sup> This is a significant issue for structures constantly exposed to soft or acid

waters such as dams, water tanks, pipes and especially to nuclear waste storage.<sup>185</sup> It is also very important for the waste solidification and stabilization by Portland cement.<sup>191</sup>

It is not easy to develop methods to perform leaching experiments in such a way that conditions normally present in real life are simulated in a laboratory. Immersion tests with mineralized or deionized water are the most frequently used methods in leaching research.<sup>8,15,16</sup> Methods performed on ground material have been developed too.<sup>192,193</sup> Procedures in which leaching is accelerated with a strongly acidified solution (such as ammonium nitrate), organic acids or by applying an electrical potential are also used in leaching process investigations.<sup>194,195,196,197</sup>

## § 3. MATERIALS AND METHODS

### 3.1. Introduction

The methods, procedures and results on characterization of starting materials (Portland cements, CSA cement, deionised water), cement pastes and pore solutions are described in this section.

Most of the analysis were carried out in the Institute IGH d.d., Zagreb, Department for materials and structures, Laboratory for binders and ecology and Laboratory for materials. The X-ray powder diffraction (XRD) and in-situ XRD were carried out in Pliva Croatia d.o.o., Research and Development Department. SEM analyses were carried out in the Institute Ruđer Bošković, Zagreb, Division of Materials Physics, Laboratory for Molecular Physics and Synthesis of New Materials.

### 3.2. Materials and methods

The research was performed in accordance with the research plan comprising sample designation, determination of properties and hydration ages. The research plan is given in Table 3.1.

The standard methods commonly applied to determine properties of Portland cement, mortar or concrete were mainly applied within this research with some minor modifications mainly concerning sample preparation or hydration ages. These methods as well as non-standardised methods are well known with established accuracy and precision. The methods were also applied to the CSA cement since there are no corresponding standards for this cement type.

Table 3.1. The research plan

Sample designation	Hydration age	Properties
CEM I CEM III CSA cement	anhydrous	chemical composition, phase composition, composition*
deionized water	-	electric conductivity, pH, trace elements, calcium and magnesium, hardness, TDS
CEM I – CP** CEM III – CP CSA cement – CP	days: 2, 7, 28, 56, 90, 180, 360	strength (flexural, compressive), secant modulus of elasticity, phase composition, chemical composition, dimensional stability, mass loss
CEM I – CP CEM III – CP CSA cement – CP	28 days (air voids content only) 365 days	water absorption due to capillary action, permeability to gasses, SEM, air voids content
CEM I – CP CEM III – CP CSA cement – CP	hours: 1-48 days: 7,14,28	<i>in – situ</i> phase composition
CEM I – PS*** CEM III – PS CSA cement – PS	days: 2, 7, 28, 56, 90, 180, 360	pH, chemical composition, trace elements concentration
* only for CEM I and CEM III	** CP - cement paste	*** PS – pore solution

### 3.2.1. Cement

Portland cement CEM I 42.5R (further: CEM I) according to the standard HRN EN 197-1:2012 produced by Cemex Croatia, Portland blast furnace cement CEM III/A 52.5N SR LH (further: CEM III) according to the same standard produced by Schwenk Zement KG Germany and CSA cement Alipre<sup>®</sup> produced by Italcementi were used.<sup>151</sup>

The following criteria were used for the selection of cements:

- composition of hydration products in hydrated cement paste;
- CO<sub>2</sub> emissions per ton of anhydrous cement;
- content of the selected trace elements levels.

#### 3.2.1.1. Cement bulk composition

Standard wet chemistry methods described in the standard HRN EN 196-2:2013 were applied to determine the major (CaO, SiO<sub>2</sub>, Al<sub>2</sub>O<sub>3</sub>, Fe<sub>2</sub>O<sub>3</sub>) and minor oxides (MgO, SO<sub>3</sub>, Na<sub>2</sub>O, K<sub>2</sub>O, MnO, CO<sub>2</sub> and inclusion of Cl).<sup>198</sup> The loss on ignition (further: LOI) and insoluble residue were also included within the chemical analysis. The standard method applied for determination of each property is reported in Table 3.2.

Table 3.2. Methods applied to determine chemical composition of CEM I, CEM III and CSA cement

Property	Article of standard HRN EN 196-2:2013
Loss on ignition (950 ± 50)°C	4.4.1
Insoluble residue in HCl and Na <sub>2</sub> CO <sub>3</sub>	4.4.3
Insoluble residue in HCl and KOH	4.4.4
CaO	4.4.5
MgO	4.5.15
	4.5.6
SiO <sub>2</sub>	4.5.8
	4.5.11
Al <sub>2</sub> O <sub>3</sub>	4.5.10
Fe <sub>2</sub> O <sub>3</sub>	4.4.2
SO <sub>3</sub>	4.4.5
S <sup>2-</sup>	4.5.16
Cl	4.5.17
CO <sub>2</sub>	4.4.6
MnO	4.5.19.4.1
K <sub>2</sub> O	4.5.19.4.1
Na <sub>2</sub> O	4.5.19.6.2
Na <sub>2</sub> O <sub>equivalent</sub>	

Term trace element in analytical chemistry is used for a element with an average concentration below 100 mg kg<sup>-1</sup> ppm.<sup>200</sup> In the cement chemistry it is applied to all elements that do not reach concentrations in the percentage range.

Levels of the selected trace elements (As, Cd, Co, Cr, Cu, Hg, Ni, Pb, Sb, V and Zn) in anhydrous CEM I, CEM III and CSA cement were measured by ICP-MS (Agilent 7800, Agilent, Santa Clara, CA, USA). Anhydrous cement (0.2000 ± 0.0001) g was subjected to digestion (ETHOS UP Milestone laboratory microwave) using the mixture of concentrated nitric (2.0 ± 0.1 mL), hydrochloric (6.0 ± 0.1 mL), phosphoric (1.0 ± 0.1 mL) and tetrafluoroboric acid (1.0 ± 0.1mL). The acid mixture actually contains *aqua regia* with the addition of tetrafluoroboric acid to dissolve silicates, aluminium and iron oxide.<sup>201</sup> The

digestion program included 20 min heating to 220 °C and 15 min at 220 °C. The applied power of the digestion device was 1800 W. The digestion temperature, time program and acid mixture were adjusted to ensure complete decomposition of the samples and provide a clear solution.

The whole fully digested volume from the pressure vessel was transferred to a volumetric flask and filled up with ultra-pure water to 50.0 mL volume. The samples were fully digested without any solid residue. The digested cement samples were analysed on the ICP-MS device with collision cell and using He mode to minimize the possible matrix and isobaric interferences. Additionally, the high matrix introduction plasma mode with 1:8 dilutions was used.

Ultrapure water taken through the entire sample preparation including digestion was used as method blank. The calibration curves were created using a method blank and seven calibration solutions. Composition of seven calibration solutions and QC solutions are reported in Table 3.3.

Table 3.3. Composition of calibration solutions and QC solutions used for determination of the trace elements in CEM I, CEM III, CSA cement by ICP-MS

Element	Concentration* / $\mu\text{g mL}^{-1}$							
	Cal.1	Cal.2	Cal.3	Cal.4	Cal.5	Cal.6	Cal.7	QC
As, Cd, Co, Cr, Cu, Hg, Ni, Pb, Sb, V, Zn	1.0	5.0	10.0	50.0	100.0	250.0	500.0	50.0
Hg	0.01	0.02	0.5	1.0	1.5	2.0	5.0	1.0

\*Concentration of each specified element

All calibration solutions were prepared by mixing stock solution A and stock solution C, nitric acid and hydrochloric acid. Ultra-pure water was used to fill up to total volume. Steps for calibration solution and QC solutions preparation are reported in Table 3.4.



Table 3.4. Volumes of calibration solutions for the determination of trace elements in CEM I, CEM III and CSA cement by ICP-MS

Calibration solution	Stock solution A	Stock solution C	HNO <sub>3</sub>	HCl	Inter. Stand. Sol.1	Total volume
Cal.1	50 µL	25 µL	0.25 mL	0.30 mL	250 µL	50 mL
Cal.2	250 µL	50 µL	0.25 mL	0.30 mL	250 µL	50 mL
Cal.3	0.5 mL	1.25 mL	0.25 mL	0.30 mL	250 µL	50 mL
Cal.4	2.5 mL	2.50 mL	0.25 mL	0.30 mL	250 µL	50 mL
Cal.5	5 mL	3.75 mL	0.25 mL	0.30 mL	250 µL	50 mL
Cal.6	1.25 mL	5.0 mL	0.25 mL	0.30 mL	250 µL	50 mL
Cal.7	2.50 mL	12.5 mL	0.25 mL	0.30 mL	250 µL	50 mL
QC	2.5 mL <sup>1</sup>	-	0.25 mL	0.30 mL	250 µL	50 mL

<sup>1</sup>Stock solution A' was used

Stock solution A, stock solution A' and stock solution C were prepared by mixing standard solution, nitric acid and hydrochloric acid. Ultra-pure water was used to fill up to total volume. Steps for stock solutions preparation are reported in Table 3.5.

Table 3.5. Volumes of components for stock A, stock A', stock B and stock C preparation

Stock solution	Standard solution 1	Standard solution 2	Standard solution 3	HNO <sub>3</sub>	HCl	Stock solution A	Total volume
A	5 mL	-	-	0.25 mL	0.30 mL	-	50 mL
B	-	-	-	0.25 mL	0.30 mL	0.5 mL	50 mL
A'	-	5 mL	-	0.25 mL	0.30 mL	-	50 mL
C	-	-	0.1 mL	0.25 mL	0.30 mL	-	50 mL

The equal portions of internal standard solution were added to method blank, calibration solutions, QC solutions and sample solution. For each of the analysed elements the appropriate internal standard was selected (see Table 3.6).

Table 3.6. Elements and internal standards used for ICP-MS determination

Element	Internal standard	Limit of determination / $\mu\text{g L}^{-1}$
As	Ge <sup>72</sup>	0.030
Cd	In <sup>115</sup>	0.006
Co	Sc <sup>45</sup>	0.008
Cr	Sc <sup>45</sup>	0.056
Cu	Sc <sup>45</sup>	0.203
Hg	Bi <sup>209</sup>	0.009
Ni	Sc <sup>45</sup>	0.042
Pb	Bi <sup>209</sup>	0.080
Sb	In <sup>115</sup>	0.005
V	Sc <sup>45</sup>	0.020
Zn	Ge <sup>72</sup>	1.06
Ca	Sc <sup>45</sup>	0.013 mg L <sup>-1</sup>
Mg	Sc <sup>45</sup>	0.003 mg L <sup>-1</sup>

The method blank, the calibration verification standard and QC solutions were used for the quality control during batch analysis. All samples, calibration solutions, method blank, calibration verification standard and QC solution were measured in triplicate and the final result was given as an average. The detection limit for each element was calculated from the average of ten-time repeated blank analysis plus the standard deviation. The sensitivity data, the resolution/axis data and the lens parameters were checked by the tuning before the batch with tune solution. The clear sampler and skimmer cone were used for each batch analysis. The operating conditions of the instrument are reported in Table 3.7.

Table 3.7. Operating parameters for Agilent 7800 for CEM I, CEM III and CSA cement analysis

Parameter	Value
Plasma mode	HMI
RF forward power / W	1600
Sampling depth / mm	10
Carrier gas flow / L min <sup>-1</sup>	0.33
Spray chamber temperature / °C	2
Extraction lens 1 / V	0
Kinetic energy discriminator / V	5
He cell gas flow / mL min <sup>-1</sup>	5

#### 3.2.1.2. Cement composition

The composition of Portland cement is one of two criteria (the second is based on performance criteria) commonly used to classify cements. The permitted cement composition is defined within specifications given in a relevant standard. The different cement standards are used worldwide but two major contributions to the cement classification has been done in Europe by European Committee for Standardization (CEN) and in the USA through the American Society for Testing and Materials (ASTM). The supporting standards for test methods and assessment of conformity are also included in the well-defined framework for Portland cement. No corresponding standards for classification, testing or assessment of conformity of CSA cement has been developed till today.

The compositions of CEM I and CEM III were determined by the standard wet chemistry method according HRI CEN/TR 196-4:2017.<sup>202</sup> Portland cements CEM I and CEM III have different main constituents. The substitution of 35 – 65 % of clinker with granulated blast furnace slag in CEM III is allowed by standard HRN EN 197-1.1 The maximum allowed clinker replacement for CEM I given by the same standard is 5 %. Composition of CEM I and CEM III are reported in Table 3.9. Composition data declared by the manufacturer were used for CSA cement since an appropriate method for determination of CSA cement composition was not available.

### 3.2.1.3. Cement phase composition

Crucial cement properties such as 28 days strength are mainly determined by its phase (mineralogic) composition.<sup>203</sup>

The diffraction patterns for CEM I, CEM III and CSA cement were recorded by the X-ray powder diffraction method (further: PXRD) on a Panalytical X'pert MPD PRO diffractometer in Bragg-Brentano geometry with CuK $\alpha$ 1 radiation ( $\lambda = 1.5406 \text{ \AA}$ ). The Rietveld method was used for quantitative phase analysis using the Panalytical HighScore Software Suite.<sup>204</sup>

### 3.2.2. Deionised water

Dissolved ions in water can be determined by a set of different analytical methods. The overall concentration of dissolved ions can be estimated by measuring at least one of the three so called *sum parameters*: electric conductivity, total dissolved solids (further: TDS) or ionic strength. These parameters depend on concentration of all dissolved ions present in water and are related to each other.

The electric conductivity of water is measure of the ability of water to conduct electricity. It depends on total concentration, charge and mobility of the dissolved ions and on temperature of measurment.<sup>205</sup> Total dissolved solids is the portion of total solids in a water sample that passes through filter with a normal pore size of  $2.0 \mu\text{m}$ .<sup>206</sup> It is a sum of dissolved cations and anions. The following principal cations: Na<sup>+</sup>, Ca<sup>2+</sup>, K<sup>+</sup>, Mg<sup>2+</sup> and anions: Cl<sup>-</sup>, SO<sub>4</sub><sup>2-</sup>, CO<sub>3</sub><sup>2-</sup>, HCO<sub>3</sub><sup>-</sup> and to lesser extent NO<sub>3</sub><sup>-</sup>, B<sup>-</sup>, Fe<sup>3+</sup>, Mn<sup>2+</sup> and F<sup>-</sup> are included in TDS. Water hardness was originaly used as a measure of the capacity of water to precipitate soap.<sup>207</sup> Nowadays total hardness is defined as the sum of dissolved calcium and magnesium, since soap is mainly precipitated with these two ions.

The amount of the trace metals in the water is usually determined by the ICP-MS method. There is no scientific classification of water according to dissolved ions concentration. The commonly used description classification is given in Table 3.8.

Table 3.8. Classification of water according to the concentration of dissolved ions

TDS / mg kg <sup>-1</sup>	Electric conductivity / $\mu\text{S cm}^{-1}$	Hardness as CaCO <sub>3</sub> mg L <sup>-1</sup>	Classification
0 – 70	0 – 140		very soft
70 - 150	140 – 300	0 - 60	soft
150 – 250	300 – 500		slightly hard
250 – 320	500 -640	61 – 120	moderately hard
320 - 420	640 – 840	121 -180	hard
> 420	> 840	> 180	very hard

Deionised water was prepared by Laboratory for binders and ecology by water purification system (Direct Q3 UV, Merck Millipore, Germany).

The concentration of the selected trace elements (As, Cd, Co, Cr, Cu, Hg, Ni, Pb, Sb, V and Zn), calcium (Ca) and magnesium (Mg) in deionised water was measured by ICP-MS (Agilent 7800, Agilent, Santa Clara, CA, USA). The standard procedure according HRN EN ISO 17294-2:2016 without previous digestion was applied.<sup>208</sup> Water sample was stabilized with addition of nitric acid and hydrochloric acid. The same acids were added to method blank, QC solutions and calibration solutions to minimize matrix effect. The method blank and five calibration solutions were used for the preparation of the calibration curve. Distilled deionized water taken through the entire sample preparation was used as method blank. Composition of five calibration solutions and QC solutions are reported in Table 3.9.

Table 3.9. Composition of calibration and QC solutions for trace elements, calcium and magnesium determination in deionised water by ICP-MS

Element	Concentration* / $\mu\text{g mL}^{-1}$					
	Cal.1	Cal.2	Cal.3	Cal.4	Cal.5	QC
As, Cd, Co, Cr, Cu, Hg, Ni, Pb, Sb, V, Zn	0.1	1.0	10	50	100	30
Hg	0.02	0.5	1	1.5	2	1.5
	Concentration* / $\text{mg mL}^{-1}$					
Ca, Mg	0.01	0.1	1	5	10	3

\*Concentration of each specified element

All calibration solutions were prepared by mixing stock solution A, stock solution B, nitric acid, hydrochloric acid and internal standard solution except for mercury for which stock solution C was used. Distilled deionized water was used to fill up to total volume. Steps for calibration solution and QC solutions preparation are reported in Table 3.10 and Table 3.11.

Table 3.10. Volumes of components for trace elements (except Hg), calcium and magnesium determination in deionised water by ICP-MS

Calibration solution	Stock solution A	Stock solution B	HNO <sub>3</sub>	HCl	Inter. Stand. Sol.	Total volume
Cal.1	-	0.5 mL	0.25 mL	0.30 mL	250 $\mu\text{L}$	50 mL
Cal.2	-	5 mL	0.25 mL	0.30 mL	250 $\mu\text{L}$	50 mL
Cal.3	0.5 mL	-	0.25 mL	0.30 mL	250 $\mu\text{L}$	50 mL
Cal.4	2.5 mL	-	0.25 mL	0.30 mL	250 $\mu\text{L}$	50 mL
Cal.5	5 mL	-	0.25 mL	0.30 mL	250 $\mu\text{L}$	50 mL
QC	1.5 mL <sup>1</sup>	-	0.25 mL	0.30 mL	250 $\mu\text{L}$	50 mL

<sup>1</sup>Stock solution A' was used

Table 3.11. Volumes of components for Hg determination in deionised water by ICP-MS

Calibration solution	Stock solution C	HNO <sub>3</sub>	HCl	Inter. Stand. Sol.	Total volume
Cal.1	0.05 mL	0.25 mL	0.30 mL	250 µL	50 mL
Cal.2	1.25 mL	0.25 mL	0.30 mL	250 µL	50 mL
Cal.3	2.50 mL	0.25 mL	0.30 mL	250 µL	50 mL
Cal.4	3.75 mL	0.25 mL	0.30 mL	250 µL	50 mL
Cal.5	5.00 mL	0.25 mL	0.30 mL	250 µL	50 mL
QC	3.75 mL <sup>1</sup>	0.25 mL	0.30 mL	250 µL	50 mL

Stock solution A, stock solution B, stock solution A' and stock solution C were prepared by mixing standard solution, nitric acid and hydrochloric acid. Distilled deionized water was used to fill up to total volume. Steps of stock solutions preparation are reported in Table 3.5.

The equal portions of internal standard solution were added to method blank and sample solution. For each of the analyzed elements the appropriate internal standard was selected (see Table 3.6)

The method blank, the calibration verification standard and QC solutions were used for the quality control during batch analysis. All samples, calibration solutions, method blank, calibration verification standard and QC solution were measured in triplicate and the final result was given as an average.

The sensitivity data, the resolution/axis data and the lens parameters were checked by the tuning before the batch with tune solution. The clear sampler and skimmer cone were used for each batch analysis. The operating conditions of the instrument are reported in table 3.12.

Table 3.12. Operating parameters for Agilent 7800

Parameter	Value
Plasma mode	General purpose
RF forward power / W	1550
Sampling depth / mm	10
Carrier gas flow / L min <sup>-1</sup>	0.99
Spray chamber temperature / °C	2
Extraction lens 1 / V	0
Kinetic energy discriminator / V	5
He cell gas flow / mL min <sup>-1</sup>	4.5

The electric conductivity and pH of deionised water were measured by conductivity and pH meter (MPC 227, Mettler Toledo, Greifensee, Switzerland). Hardness of deionised water expressed as *equivalent CaCO<sub>3</sub> in mgL<sup>-1</sup>* was calculated from determined calcium and magnesium concentration using the formula:

$$\text{Hardness} = 2.497 [\text{Ca}, \text{mg L}^{-1}] + 4.118 [\text{Mg}, \text{mg L}^{-1}]$$

Total dissolved solids were determined by standard procedure given in HRN EN 15216:2008.<sup>209</sup>

### 3.3. Sample preparation

#### 3.3.1. Cement paste preparation

The sample preparation included mixing of cement and water to produce cement paste. The preparation took place in the room with the maintained temperature of  $(20 \pm 2)^\circ\text{C}$  and relative humidity of not less than 50%. Cement pastes were prepared with the water to cement ratio of 0.5 using the standard mortar mixer given in Figure 3.1 (ToniMix, Toni Technik GmbH, Berlin, Germany) and the standard procedure with the modification in cement content: 1000 g of cement was used and amount of water was adjusted to get w/c of 0.5.<sup>210</sup> Deionised water used as leaching agent was used for cement paste preparation. Used cement, water, mixer and moulds were at the temperature  $(20 \pm 2)^\circ\text{C}$ .

Immediately after the mixing procedure, the prepared cement pastes were transferred to prismatic moulds or cylindrical moulds or holders used for *in - situ* XRD measurements.



Figure 3.1 Standard mortar mixer



### 3.3.2. Prismatic samples compaction and curing

The standard moulds were used to prepare samples dimensions  $(40 \times 40 \times 160)$  mm.<sup>210</sup> The prepared cement pastes were transferred to moulds without undue compaction or vibration, and the voids were removed by gently tapping. The excess of paste was removed by gentle sawing motion with a straight-edged ruler. The filled standard mould is shown in Figure 3.2.

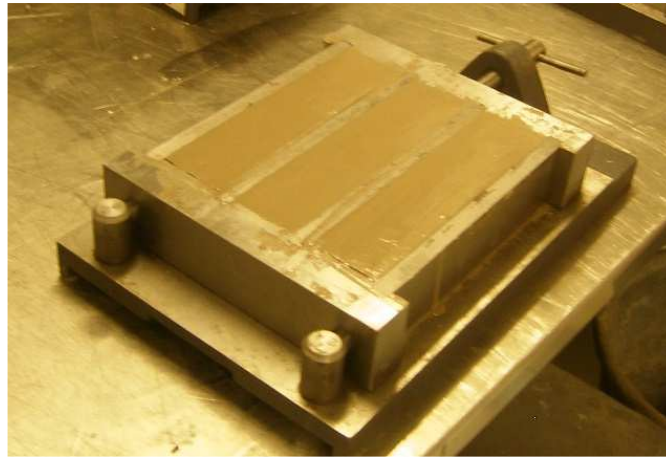


Figure 3.2 Filled standard prismatic moulds

The same moulds type but provided with a hole at the centre of each end face were used to prepare prismatic samples for determination of volume stability. The stainless-steel stub was fitted in the hole and embedded into the sample. This type of moulds is shown in Figure 3.3.

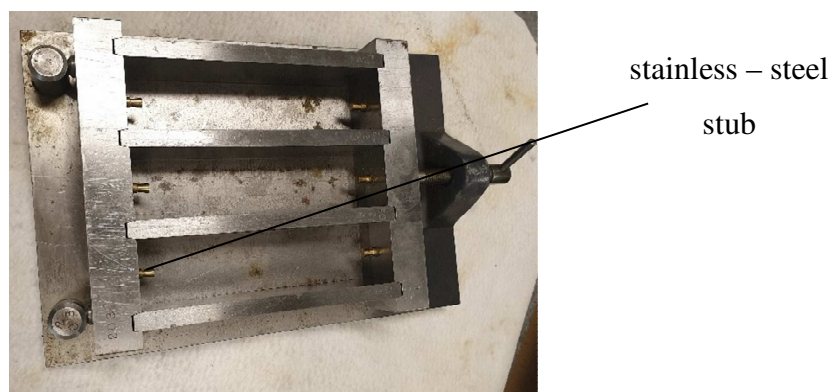


Figure 3.3 Moulds for preparation of samples for determination of volume stability

The filled prismatic moulds were stored in the moist air cabinet (L.T. d.o.o, Šentjernej, Slovenia) at the temperature of  $20.0 \pm 1.0$  °C and the relative humidity not less than 90% for 24 hours. Three prismatic samples dimensions ( $40 \times 40 \times 160$ ) mm were prepared from each mould. The prepared samples were exposed to the tank leaching test.

They were cured in plastic tanks filled with deionised water at a temperature of  $20.0 \pm 2.0$  °C after demoulding. Volume of water was adjusted to provide the ratio of the surface of samples and the volume of water of 1:10. The plastic tanks with stored cement pastes were covered with plastic cover to prevent evaporation. No additional protection against carbon dioxide from air was used. Curing water was changed three times a week (Monday, Wednesday and Friday) to provide the aggressive attack of water media during the hydration period. Cement pastes were cured for 2, 7, 28, 56, 90, 180 and 365 days. The schematic description of tank leaching test is shown in Figure 3.4.

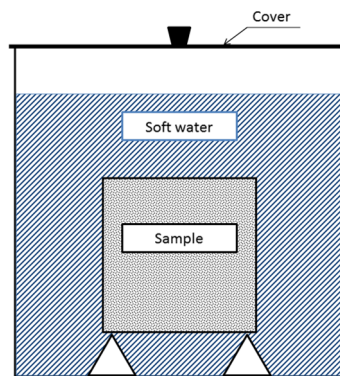


Figure 3.4 Schematic description of tank leaching test

The cured prismatic samples were submitted for the further tests: determination of flexural and compressive strength, secant modulus of elasticity, dimensional stability and mass loss. XRD patterns were collected on the powder collected from prismatic samples. They were also used for the chemical analysis of hydrated cement paste and pore solutions. The tests were carried out at the particular hydration age.

### 3.3.3. Cylindric samples compaction and curing

Cement pastes prepared according to the procedure given in section 3.3.1 and the cylindric mould shown in Figure 3.5 were used to prepare cylindric samples ( $100 \times 200$ ) mm dimensions. The mould was filled by paste without undue compaction or vibration and the voids were removed by gentle tapping. The excess of paste was removed by a gentle sawing motion with a straight-edged ruler.



Figure 3.5 Cylindric mould (100 × 200) mm dimensions

After the compaction, cylindrical samples were cured for 24 hours at temperature  $(20.0 \pm 1.0) ^\circ\text{C}$  and the relative humidity not less than 90%. After demoulding, samples were exposed to the tank leaching test under the same conditions applied to prismatic samples and described in section 3.3.2. Two cylindrical samples were prepared for every cement type. The cured cylindrical samples were submitted for the further tests: determination of water absorption coefficient due to capillary action, determination of permeability to gasses, determination of air voids content and SEM determination. The tests were carried out after 365 days hydration period. The suitable sub-samples were prepared from the cylindrical sample. The preparation of sub-samples is shown in Figure 3.6. The concrete saw was used to cut off sub-samples from the cylindrical sample.

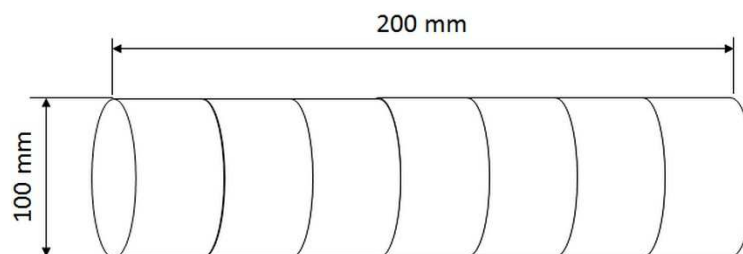


Figure 3.6 Preparation of sub-samples from the cylindrical sample

#### 3.3.4. Obtaining pore solution and prime characterisation

Pore solution was expelled from the prismatic samples using the apparatus shown in Figures 3.7 and 3.8. It consisted of the two steel bodies with the two inner concentric cylinders where the testing sample was placed.

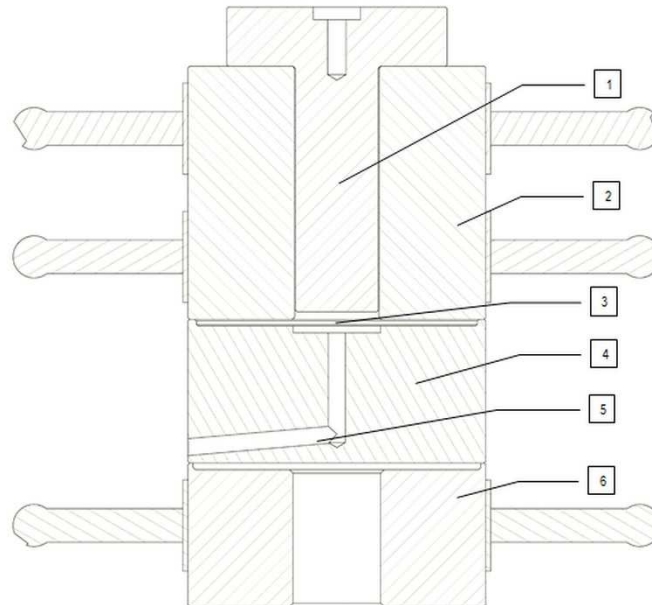


Figure 3.7 Schematic diagram of pore solution expression apparatus

1 – piston; 2,4 – inner concentric cylinder; 3 sample; 5 – drain tube; 6 - base

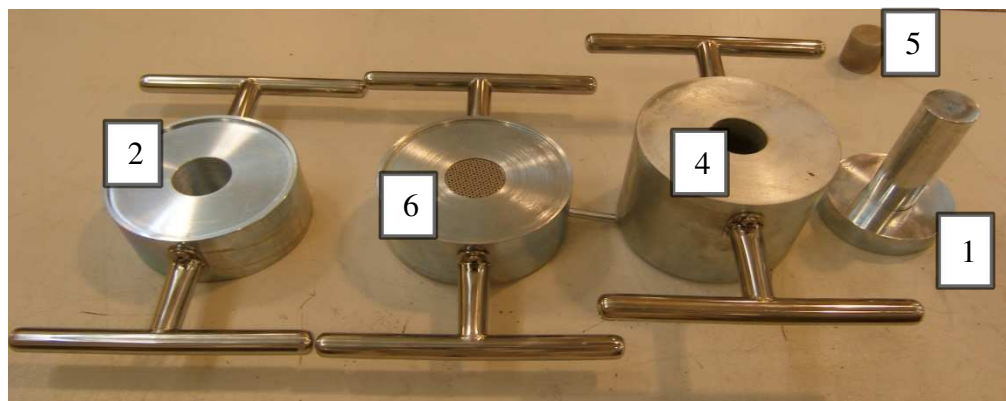


Figure 3.8 Parts of pore solution expression apparatus

1 – piston; 2,4 – inner concentric cylinder; 3 sample; 5 – drain tube; 6 – base

The prismatic sample was removed from the tap water at the particular hydration age and split into two cubes using the standard strength testing machine (Toni NORM, Toni Technik

GmbH, Berlin, Germany).<sup>210</sup> Two cubes were placed inside two inner concentric cylinders of apparatus and were followed by a piston to which pressure of 150 MP and gain power of 0.5 kN mm<sup>-2</sup> was applied. The porous steel lamina was fitted on the bottom of the lower steel body just under the spiral recess connected with the drain tube which drained the fluid into the laboratory dish. No additional grinding or the particle size reduction was applied. The pore solution expression is shown on Figure 3.9.

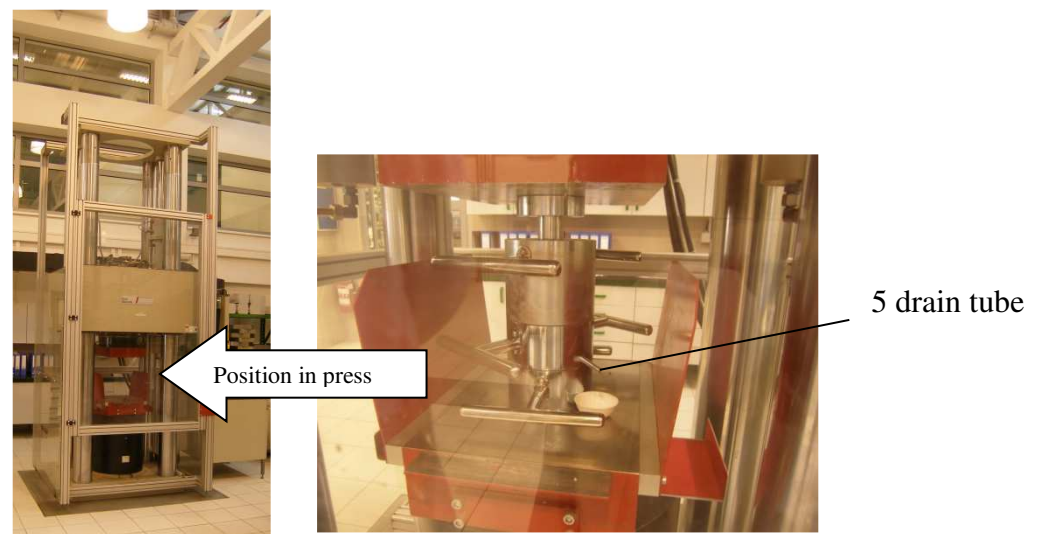


Figure 3.9 Pore solution expression

The pH value of expelled pore solution was measured by a pH meter (MPC 227, Mettler Toledo, Greifensee, Switzerland) immediately after it was expelled from the cement paste. Obtained pore solution was stored in sealed plastic test tube to prevent reaction with atmospheric carbon dioxide and submitted for further determination.

### 3.4. Testing methods

#### 3.4.1. Determination of strength and preparation of samples for chemical analysis

Mechanical strength of cement is the key property for its structural use and is significant from the durability viewpoint. The flexural and compressive strength was determined on prismatic samples according to the procedure given in standard HRN EN 196-1:2016.<sup>210</sup>

The samples were removed from the water not more than 15 minutes before the test was carried out. The standard strength testing machine (Toni NORM, Toni Technik, Berlin, Germany) was used for strength determination (Figure 3.10). The flexural strength was calculated as the arithmetic mean of the three individual results and compressive of the six individual results.

Cubes left after the compressive strength determination were immediately gently ground by hand in agate mortar and homogenised. The samples for XRD measurements and chemical analysis of cement pastes were prepared by the quartering method.



Figure 3.10 The standard strength testing machine

#### 3.4.2. Determination of secant modulus of elasticity

The secant modulus of elasticity in the compression was determined in accordance with the standard HRN EN 12390-13:2013 usually applied for the hardened concrete samples.<sup>211</sup> The test sample was loaded under axial compression, the stresses and strains were recorded and the slope of the secant to the stress-strain curve was determined after three loading cycles. The secant modulus of elasticity in compression corresponds to the secant slope.

The testing machine according to the standard HRN EN 12390-13:2013 used for determination (Toni NORM with deformation measurement device, Toni Technik GmbH, Berlin, Germany) is shown in Figure 3.11. The measured compressive strength was used to

define the stress levels of the test cycle for the determination of secant modulus of elasticity. The secant modulus of elasticity was calculated as the arithmetic mean of the three individual results.

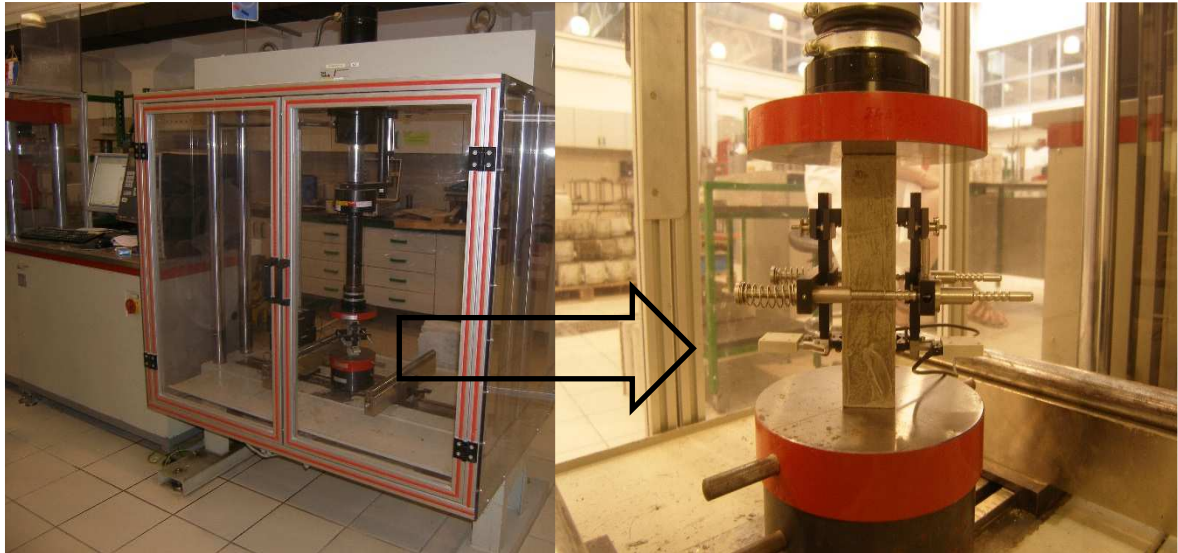


Figure 3.11. Determination of secant modulus of elasticity

#### 3.4.3. Powder X-ray diffraction

The phase composition of hydrated cement paste was determined by powder X-ray diffraction (further: PXRD). Two different measurement principles were applied:

- *in-situ* measurements;
- measurements on powder collected from prismatic samples.

The diffraction patterns were recorded on Panalytical X'pert MPD PRO diffractometer in Bragg-Brentano geometry with  $\text{CuK}\alpha_1$  radiation ( $\lambda = 1.5406 \text{ \AA}$ ) with voltage 45 kV and electric current 40 mA. The diffractograms were collected in the  $2\theta$  range  $9^\circ$  to  $65^\circ$ . The used step was  $0.039^\circ 2\theta$  with integration time of 200 s for each step. Time necessary for collection of one diffractogram was 10.5 minutes.

The *in-situ* diffractograms were collected in period 1 to 48 hours from the start of hydration for selected time periods. They were also performed for 7, 14 and 28 days hydration period. Metal holders with a 27 cm diameter slot and 1.5 mm depth, were used to collect diffraction patterns. The lower part of the holder was filled with the prepared cement paste, gently aligned with edges and covered with Kapton foil and covered with the upper part of the holder. Holder with its parts is shown on Figure 3.12. Kapton foil was removed after the first measurement was finished due to hardening of the cement paste. After 48 hours, holders with

cement paste were stored in plastic vessels with regularly changed deionised water to assure similar curing conditions as applied for the prismatic samples.



Figure 3.12. Metal holder for in-situ XRD measurements

The diffraction patterns were also collected on samples prepared after the compressive strength determination using the same instrument and under the same measuring conditions.

#### 3.4.4. *Determination of chemical composition of cement paste*

The cement paste composition was determined on powder samples prepared from cubic samples left after the compressive strength determination. The analysis was performed immediately after the sample preparation to avoid possible changes in bulk composition due to proceeding hydration and carbonatization. The standard methods described in HRN EN 196-2:2013 were applied to determine the next properties in hydrated cement paste: loss on ignition, content of major oxides (CaO, SiO<sub>2</sub>, Al<sub>2</sub>O<sub>3</sub>, Fe<sub>2</sub>O<sub>3</sub>) and minor oxides (MgO, SO<sub>3</sub>, Na<sub>2</sub>O, K<sub>2</sub>O, CO<sub>2</sub>). Detail list of methods applied for determination of each property is given in Table 3.2.

#### 3.4.5. *Determination of chemical composition of pore solution*

The pH values were measured immediately after the expression and pH meter (Mettler Toledo MPC 227). Expressed pore solutions were stored in sealed plastic test tubes to prevent reaction with atmospheric carbon dioxide before further testing. The following properties were determined in pore solutions: sodium (Na), potassium (K), calcium (Ca) and trace elements (As, Cd, Co, Cr, Cu, Hg, Ni, Pb, Sb, V and Zn) concentration. The concentrations of Na, K, Ca and trace elements were determined by the ICP-MS method using the same instrument as for trace elements analysis in cement and deionised water.



A portion of 1.0 mL of pore solution was diluted to 50 mL volume by ultrapure water and stabilized by addition of nitric acid and hydrochloric acid. The standard procedure denoted in HRN EN ISO 17294-2:2016 and in detail described in article 3.2.2 was applied for further analysis of pore solution composition.<sup>208</sup> Calibration and QC solutions reported in Tables 3.9 to 3.11 were used to create calibration curves and perform analysis. Operating conditions of the instrument are reported in Table 3.12.

#### 3.4.6. Determination of dimensional stability

The method for determination of the dimensional stability in accordance with the standard HRN EN 12617-4:2003, usually applied to grout, mortar or concrete, was applied to determine the shrinkage and the expansion of the cement paste samples.<sup>212</sup> The measurement was carried on the prismatic moulds with the incorporated measurement studs made of stainless steel. The instrument to measure the lengths of samples with accuracy of  $\pm 0.001$  mm and suitable fittings to receive the measurement stud was used. The instrument was calibrated prior to each determination using the wood-lined rod made of invar metal  $160 \pm 1$  mm in length. The instrument for determination of stability with the rod is shown in Figure 3.13.



Figure 3.13. Instrument for dimensional stability determination

Each sample was marked using a waterproof felt tip-pen to ensure always the same position of sample during the measurement. When the calibration rod or sample was rotated about its axis during the measurement, a change less than  $\pm 0.001$  mm was allowed. The sample was dabbed with the moist cloth to remove excess water prior to the determination. The cleanliness and fixity of the measurement studs were checked before each measurement. The final measurement result was calculated as the arithmetic mean of the three individual results.

#### 3.4.7. Determination of the mass loss

The mass loss was determined by weighing the prismatic samples under the water and in air. The prismatic sample was removed from the tank water and immersed into a dish with deionised water connected with the previously tarred balance for weighing under the water shown in Figure 3.14. For the weighing in air the prismatic sample was removed from the tank water and left to dry at room temperature  $20 \pm 2$  °C for 30 minutes. The weighing was carried out for a particular hydration age and the loss of mass was calculated by subtraction of the weights recorded for the two successive hydration ages.



Figure 3.14. The balance for the weighing under the water

#### 3.4.8. Determination of water absorption coefficient due to capillary action

The method of partial immersion in accordance with the standard HRN EN ISO 15148: 2004 was applied to determine the water absorption coefficient of cement pastes.<sup>213</sup> The method is usually applied to different building materials for determination of moisture movement in the hygroscopic capillary system within the material. The coefficient of absorption was determined by measuring the change in mass of the test sample at the bottom surface which was in contact with water. The cylindrical sub-samples prepared according Figure 3.6 were used for determination. The sub-samples were prepared for determination by methods that do not change the original microstructure with no coatings or sealant applied to the sides of the sub-sample. Test was performed at room temperature  $20 \pm 2$  °C and relative humidity not less

than 40%. The samples were weighed with an accuracy of  $\pm 0.1\%$ . The setup for this experiment is shown in Figure 3.15.

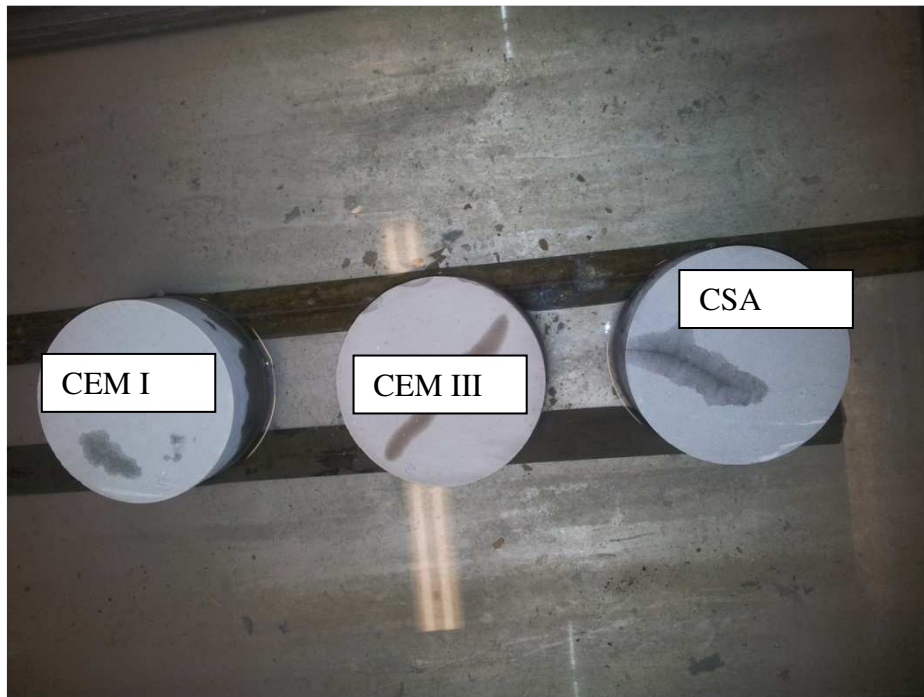


Figure 3.15. Setup for determination of the absorption coefficient due to capillary action

#### 3.4.9. Determination of permeability to gasses

Permeability of material is defined as property by which the material allows a gas to pass through it when it is exposed to differences in pressure. The standard method usually applied to hardened concrete samples described in HRN EN 993-4:2008 was used to determine the permeability of cement pastes with small modifications in sample dimensions and drying temperature.<sup>214</sup> The apparatus shown in Figure 3.16 was used for determination. The cylindrical sub-samples prepared according to Figure 3.6 were used for determination



Figure 3.16. The apparatus for determination of permeability to gasses

A stream of dry gas is passed through the test piece. The pressure drop across the test piece was recorded and the permeability of cement paste was calculated using geometry data (size and shape) of sample. The cylindrical sub-sample prepared according to Figure 3.7 with a  $100 \text{ mm} \pm 0.5 \text{ mm}$  diameter and  $50 \text{ mm} \pm 0.5 \text{ mm}$  height was used for determination. The samples were dried to constant mass in drying oven at  $105 \pm 5^\circ\text{C}$  before measurements. The standard requires  $50 \text{ mm} \pm 0.5 \text{ mm}$  sample diameter and drying temperature of  $110 \pm 5^\circ\text{C}$ . The lower drying temperature was used to avoid changes in microstructure due to decomposition of hydrated phases and formula used for calculation was adjusted to different sample diameters.

#### 3.4.10. SEM determination

The square sub-samples prepared according to Figure 3.6 were used for SEM determination. Samples were polished prior to analysis by applying a procedure for preparation of the sample surface for air voids content described in section 3.4.11. Field emission scanning microscope JSM-7500F was used to obtain secondary electron images (SEI) with magnification between  $100\times$  to  $20\,000\times$ . EDS analysis was performed, too.

#### 3.4.11. Air voids content

The air void structure of cement pastes was determined by the standard linear traverse method usually applied to hardened concrete and described in HRN EN 480–11:2005 with modifications in curing conditions and hydration age.<sup>215</sup> The test surfaces of subsamples prepared according to procedure given in section 3.3.2 were prepared for analysis in full accordance with the standard. The determination was performed with an automated measuring system (Rapid air 457, German Instruments, Inc., Illinois, USA) comprising a computerized

control unit with a monitor, a cross traverse table, a digital camera and a microscope objective. The used system is shown on Figure 3.17.

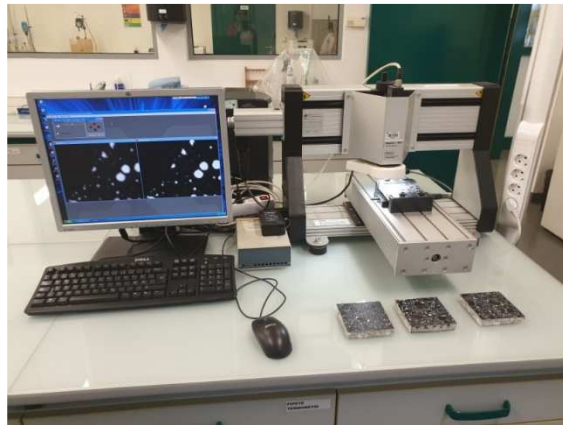


Figure 3.17. System for determination of air voids content with microscope objective

The air void structure was determined by scanning along a series of traverse lines running parallel to the surface. The number of air voids intersected by the traverse lines was recorded. A mathematical analysis of the recorded data gave description of the air void system. The cylindrical sub-samples prepared according to Figure 3.6 were used for determination of air voids system.

## 3.4.12. Used chemicals and reagents

Chemicals and analytic reagents used for chemical analysis according to HRN EN 196-2: 2013, HRI CEN/TR 196-4:2007 and for ICP-MS analysis are listed in Table 3.13 and Table 3.14

Table 3.13. List of the chemicals and analytic reagents used used for chemical analysis according to standards HRN EN 196-2: 2013 and HRI CEN/TR 196-4:2017

Chemical / Analytic reagent	Produced by
Acetic acid, $C_2H_4O_{2(aq)}$ , min. 99,5% p.a. CAS: 64-19-7	Kemika, Croatia
Ammonia solution, $NH_{3(aq)}$ min. 25%, CAS:1336-21-6	Kemika, Croatia
Ammonium acetate, $C_2H_7NO_{2(s)}$ , p.a. CAS: 63-61-8	Kemika, Croatia
Ammonium chloride, $NH_4Cl_{(s)}$ , p.a., CAS: 12125-02-9	Kemika, Croatia
Ammonium heptamolybdate tetrahydrate, $(NH_4)_6Mo_7O_{24} \cdot 4H_2O$ (s), p.a., CAS:12054-85-2	Kemika, Croatia
Ammonium iron(III) – sulfate dodecahydrate, $NH_4Fe(SO_4)_2 \cdot 12H_2O_{(s)}$ , CAS:7783-83-7	Kemika, Croatia
Ammonium thiocyanate, $NH_4SCN$ p.a., CAS:1762-95-4	Kemika, Croatia
Barium chloride dihydrate, $BaCl_2 \cdot 2H_2O_{(s)}$ p.a., CAS: 10326-27-9	Kemika, Croatia
Boric acid, $H_3BO_{3(aq)}$ , p.a., CAS: 10043-35-3	Kemika, Croatia
Calcium carbonate, $CaCO_3$ (s), CAS: 471-34-1	Kemika, Croatia
Citric acid monohydrate, $C_6H_8O_7 \cdot 4H_2O$ (s), CAS:5949-29-1	Kemika, Croatia
Concentrated hydrochloric acid, $HCl_{(aq)}$ , min. 36% ,p.a., CAS: 7647-01-0	Kemika, Croatia
Concentrated nitric acid, $HNO_3$ (aq), min. 65%, p.a., CAS:7697-37-2	Kemika, Croatia
Concentrated phosphoric acid, $H_3PO_4$ (aq), min. 85%, p.a., CAS: 7664-38-2	Kemika, Croatia
Concentrated sulfuric acid, $H_2SO_{4(aq)}$ , min. 96%, p.a., CAS: 7664-93-9	Kemika, Croatia
Copper(II) sulfate pentahydrate, $CuSO_4 \cdot 5H_2O$ (cryst), CAS: 7758-99-8	Merck, Germany
Glycine, $C_2H_5NO_2$ (s) p.a., CAS: 56-40-6	Kemika, Croatia
Hydrofluoric acid, $HF_{(aq)}$ , 48%, CAS: 7664-39-3	Merck, Germany
Magnesium perchlorate, $Mg(ClO_4)_2$ , CAS: 10034-81-8	Alfa Aesar, Germany
Methylthymol blue sodium salt for complexometry, $C_{37}H_{40}N_2Na_4O_{13}S_{(s)}$ CAS:1945-77-3	Kemika, Croatia

Table 3.13. List of the chemicals and analytic reagents used used for chemical analysis according to standards HRN EN 196-2: 2013, and HRI CEN/TR 196-4:2017 – previos page extension

Chemical / Analytic reagent	Produced by
5,5'-Nitrilodibarbituric acid monoammonium salt, Ammonium purpurate, Murexid, $C_8H_8N_6O_6(s)$ CAS: 3051-09-0	Kemika, Croatia
Potassium chloride, $KCl(s)$ , CAS: 7447-40-7	Kemika, Croatia
Potassium hydroxide, $KOH(s)$ , grains 2 to 5 mm, p.a., CAS: 1310-58-3	Kemika, Croatia
Potassium iodate, $KIO_3(s)$ , p.a., CAS:7758-05-6	Kemika, Croatia
Potassium periodate, $KIO_4(s) > 99,5\%$ Pumice stone	BDH Prolabo, UK Kemika, Croatia
Sodium carbonate, $Na_2CO_3(s)$ , anhydrous, CAS: 497-19-8	Kemika, Croatia
Sodium chloride, $NaCl_{(cryst)}$ , p.a., CAS: 7647-14-5	Kemika, Croatia
Sodium hydroxide, $NaOH(s)$ , pellets 2 – 5mm, CAS: 1310-73-2	Kemika, Croatia
Sodium peroxide, $Na_2O_2(s)$ , CAS:1313-60-6	Kemika, Croatia
Sodium thiosulfate pentahydrate, $Na_2S_2O_3 \cdot 5H_2O(s)$ , CAS:7772-98-7	Merck, Germany
Starch, $(C_6H_{10}O_5)_n(s)$ , CAS: 9005-84-9	Merck, Germany
5-sulfosalicylic acid dihydrate, $C_7H_6O_6S \cdot 2H_2O(s)$ , CAS: 5965-83-3	Kemika, Croatia
1-(2-Pyridylazo)-2-naphtol $(s)$ , PAN, CAS:85-85-8	Kemika, Croatia
Tin (II) chloride dyhidrate, $SnCl_2 \cdot 2H_2O(s)$ , CAS: 7772-99-8	BDH PROLABO, UK
Triethanolamine, $C_6H_{15}NO_3(l)$ , CAS: 102-71-6	BDH PROLABO, UK
Titrival concentrate silver nitrate $0.1 \text{ mol L}^{-1}$ , $AgNO_3(l)$ CAS:7761-88-8	Kemika, Croatia
Zinc sulfate heptahydrate, $ZnSO_4 \cdot 7H_2O(s)$ , CAS:7446-20-0	Kemika, Croatia

Table 3.14. List of the chemicals and analytic reagents used used for ICP-MS analysis

Chemical / Analytic reagent	Produced by
Nitric acid, HNO <sub>3</sub> (aq); for trace elements analysis, ≥ 69 %	Honeywell Fluka™
Hydrochloric acid, HCl (aq); for trace elements analysis, 34 % - 37 %	Honeywell Fluka™
Tetrafluoroboric acid, for trace elements analysis	Honeywell Fluka™
Internal standard solution – Internal standard mix 10 µg L <sup>-1</sup> Bi, Ge, In, Li <sup>6</sup> , Sc, Tb, Y matrix 5 % HNO <sub>3</sub>	Agilent Technologies
Standard solution 1 – Stanadard IV – Stock 10 µg mL <sup>-1</sup> Ag, Al, As, Ba, Be, Cd, Co, Cr, Cu, Mn, Mo, Ni, Pb, Sb, Th, Tl, U, V, Zn 1000 µg mL <sup>-1</sup> Ca, Fe, K, Mg, Na Matrix tr. Tartaric acid, 5 % HNO <sub>3</sub>	Inorganic Ventures
Standard solution 2 – Environmental Calibration Standard 10 µg mL <sup>-1</sup> Ag, Al, As, Ba, Be, Cd, Co, Cr, Cu, Mn, Mo, Ni, Pb, Sb, Th, Tl, U, V, Zn 1000 µg mL <sup>-1</sup> Ca, Fe, K, Mg, Na Matrix tr. Tartaric acid, 5 % HNO <sub>3</sub>	Agilent Technologies
Standard solution 3 Tuning solution for ICP-MS 1 ppb Li, Co, Y, Ce, Tl	Agilent Technologies Agilent Technologies



## § 4. RESULTS AND DISCUSSION

### 4.1. Characterization of starting materials

The selection of Portland cement or some other cement type used in construction work is usually based only on strength classification. Sometimes, composition of the selected cement, expressed as amount of Portland cement clinker, is considered during selection. The chemical and phase composition is usually skipped, although these are sources of valuable information for cement implementation.

The chemical composition of CEM I, CEM III and CSA cement expressed as major and minor oxides is reported in Table 4.1.

Table 4.1. Chemical composition (major and minor oxides) of CEM I, CEM III and CSA

Property	w / %		
	CEM I	CEM III	CSA cement
LOI (950 ± 50)°C	2.89	1.40	0.92
Insoluble residue in HCl and Na <sub>2</sub> CO <sub>3</sub>	0.23	0.41	2.54
Insoluble residue in HCl and KOH	0.23	0.30	1.96
CaO	62.90	56.25	40.08
MgO	2.30	3.19	4.66
SiO <sub>2</sub>	19.53	26.29	9.12
Al <sub>2</sub> O <sub>3</sub>	4.58	6.20	32.82
Fe <sub>2</sub> O <sub>3</sub>	2.82	1.93	1.61
SO <sub>3</sub>	3.07	2.40	11.49
S <sup>2-</sup>	0.03	0.23	0.00
Cl	0.013	0.075	0.188
CO <sub>2</sub>	1.99	0.65	0.22
MnO	0.075	0.134	0.157
K <sub>2</sub> O	0.92	0.67	0.71
Na <sub>2</sub> O	0.17	0.15	0.48
Na <sub>2</sub> O <sub>equivalent</sub>	0.78	0.59	1.03

Mass fractions of the major and minor oxides show differences between Portland cements CEM I and CEM III. LOI indicates the amount of material present in Portland cement that was not treated at higher temperatures prior to cement production. It usually accounts for natural gypsum and limestone. The higher mass fraction of LOI for CEM I compared to CEM III indicates higher amounts of natural calcium sulfate (gypsum) or a possible presence of limestone in CEM I. The higher sulfate and CO<sub>2</sub> contents observed in CEM I are also in line with these results. Major clinker phases: alite, belite, aluminite and ferrite in CEM I have been confirmed, while the presence of limestone has not been confirmed by XRPD (Figure 4.1).<sup>216-220</sup>

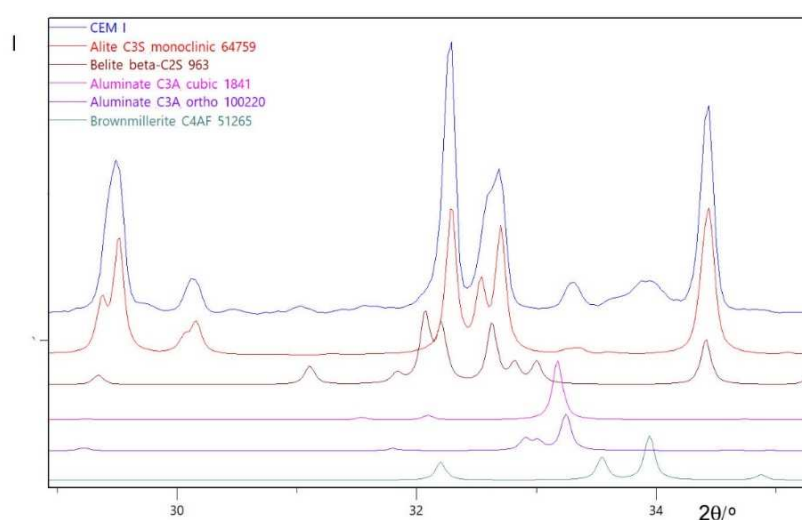


Figure 4.1. XRPD of CEM I in the  $2\theta$  range  $29 - 35^\circ$  with the identified crystalline phases<sup>216-220</sup>

The peak at  $51.7^\circ$  and a shoulder at  $51.9^\circ$ , characteristic for the monoclinic  $M_1$  polymorph, is observed in the CEM I diffractogram (Figure 4.2), as analysed by Taylor<sup>5</sup> (see Fig. 2.4).<sup>216</sup> As the structure of this polymorph is not known, the structure of the very similar  $M_3$  was used for Rietveld refinement.

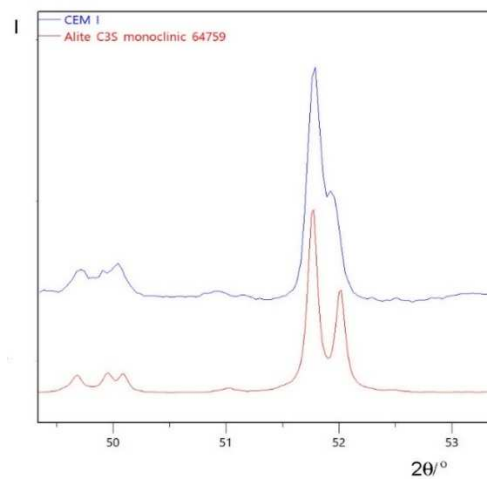


Figure 4.2. Characteristic XRPD pattern of the observed monoclinic  $M_1$  alite polymorph in CEM I (top) and the calculated pattern of the  $M_3$  polymorph (bottom)<sup>216</sup>

The quantitative XRPD analysis shows that alite and belite are the major phases in CEM I (Figure 4.3).<sup>216-226</sup>

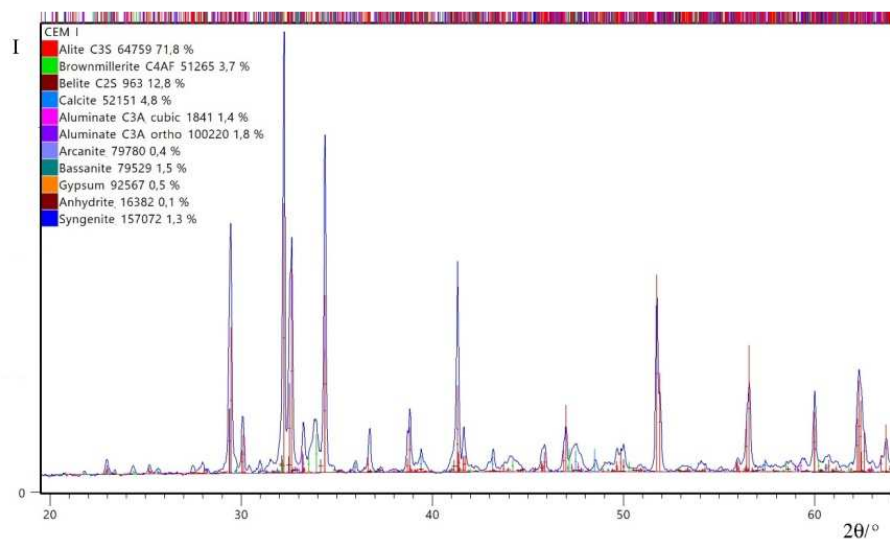


Figure 4.3. QXRPD pattern of CEM I in the  $2\theta$  range 20 – 65°<sup>216-226</sup>

The higher mass fractions of insoluble residues observed for CEM III indicate higher amounts of insoluble silicon, which corresponds to higher silica content in CEM III. These results indicate the possible presence of glassy material in CEM III which has been confirmed by XRPD (Figure 4.4). Currently it is accepted for modern clinkers to contain the glass phase only in rare cases.<sup>227</sup> The glass phase content of 50 – 95 % has been confirmed in the

granulated blast furnace slag depending on the cooling method type.<sup>227</sup> The crystalline phases identified in CEM I are also present in CEM III. The high background indicates a significant amount of the amorphous phase in CEM III as a consequence of added granulated blast furnace slag.<sup>216-218,220,221</sup>

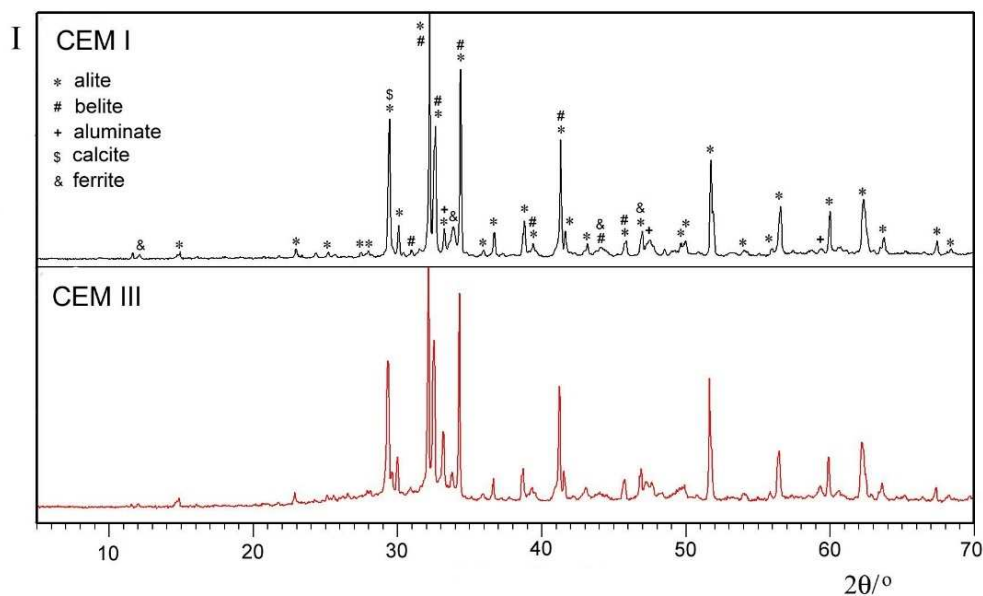


Figure 4.4. XRPD of CEM III in the  $2\theta$  range 9 – 65° with the identified crystalline phases<sup>216-218,220,221</sup>

Chemical composition of the CSA cement is significantly different in comparison to CEM I and CEM III. Lower CaO and SiO<sub>2</sub> and a higher Al<sub>2</sub>O<sub>3</sub> mass fraction indicates that the prime compounds in this cement are calcium sulfoaluminate compounds instead of calcium silicates and calcium aluminate, the prime compounds in CEM I and CEM III. The higher sulfate content and lower LOI also support this conclusion which was confirmed by phase analysis. Ye'elimite is the prime phase in the CSA cement but the presence of belite and other minor phases was also confirmed (Figure 4.5).<sup>216-219,223-225,229-233</sup>

The quantitative phase composition of the analysed cements determined by the Rietveld method is given in Table 4.2. The minor phases (<1.8 %) are not given.

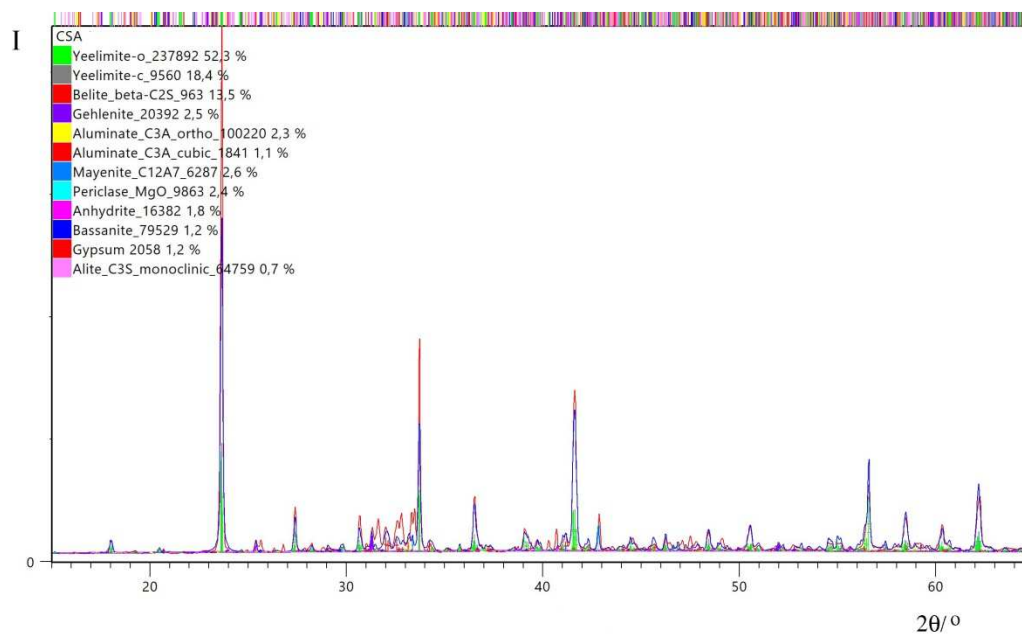


Figure 4.5. XRPD of CSA in the  $2\theta$  range 15 – 65° with the identified crystalline phases.

The numbers that correspond to the known structures of crystalline phases are from Inorganic Crystal Structure Database<sup>216-219,223-225,229-233</sup>

Table 4.2. Phase composition of CEM I, CEM III and CSA cement

Mineral	w / %		
	CEM I	CEM III	CSA cement
C <sub>3</sub> S	71.8	41.0	0
C <sub>2</sub> S	12.8	3.7	13.5
C <sub>3</sub> A	3.2	3.2	3.4
C <sub>4</sub> AF	3.7	8.1	0
C <sub>4</sub> A <sub>3</sub> Ŝ	0	0	70.7
C <sub>2</sub> AS	0	0	2.5
C <sub>12</sub> A <sub>7</sub>	0	0	2.6
anhydrite	0.5	0	1.8
calcite	4.8	2.2	0
periclase	0	0	2.4
glass phase	0	38.0	0

Results of the chemical and phase composition determination indicate that the principal source of differences in the major and minor oxide fractions in CEM I and CEM III is the granulated blast furnace slag. Substitution of 64 % of clinker in CEM III by the granulated blast furnace slag was confirmed by composition determination, given in Table 4.3. Presence of limestone in CEM I was not confirmed.

Table 4.3. Composition of CEM I and CEM III

Cement	Mass fraction in %	
	Clinker	Granulated blastfurance slag
CEM I	100	-
CEM III	36.0	64.0

Table 4.4 shows total concentrations of eleven trace elements in anhydrous CEM I, CEM III and CSA cement. The concentration of all elements, except mercury and lead, are lower in CEM I when compared to CEM III. These data correspond to the findings of other authors for the same cement types.<sup>55</sup> Substitution of clinker by granulated blast furnace slag increases the trace elements concentration in CEM III, except for mercury and lead. Determined trace elements can be divided in two groups: elements with the concentration above 5 mg kg<sup>-1</sup> (Co, Cr, Cu, Ni, Sb, Zn and V) and elements with the concentration below 5 mg kg<sup>-1</sup> (As, Cd, Hg and Pb). Low concentration of some elements is connected to their volatility. Arsenic, cadmium, mercury and lead are considered as highly or moderately volatile elements in the Portland cement kiln system. They are hardly stabilized in Portland cement clinker, while the other elements included in this research are considered as non-volatile, well incorporated within the clinker phases and thus highly abundant in cement.<sup>55</sup>

Table 4.4. Content of the trace elements in CEM I, CEM III and CSA cement

w(trace element) / mg kg <sup>-1</sup>											
Cement	Sb	As	Cd	Cr	Co	Cu	Hg	Ni	Pb	V	Zn
CEM I	10.3	4.30	0.50	67.8	5.3	63.8	0.03	17.4	1.19	39.5	312
CEM III	36.4	4.40	0.60	547	15.6	2368	0.02	374	<0.080*	205	1056
CSA cement	3.7	12.1	0.40	119.5	16.6	127.4	0.01	110	184	231.5	125.3

\* In µg kg<sup>-1</sup>

Volatile arsenic and especially lead, show higher abundance in the CSA cement than in CEM I and CEM III. The lower required formation temperature for the calcium sulfoaluminate clinker and higher amounts of industrial waste materials potentially used as raw materials in its production enable higher levels of lead and arsenic incorporation. Lower levels of antimony, cadmium and mercury in the CSA cement are presumably the result of lower input values through raw materials and fuels. The abundances of other trace elements are in the range of values observed for CEM I and CEM III. Investigation of the trace elements content in CSA cements is less often encountered in the literature.

The pure cement constituents, clinker, gypsum and slag as well as raw materials for clinker preparation were not available for this research. Thus, a deep study of input pathways of the trace elements in cement within this research was not possible.

Electrical conductivity, pH value, hardness and total dissolved solids content of deionized water used for preparation and curing of the cement paste samples, reported in Table 4.5, satisfied the requirements for very soft water (classification is given in Table 3.8).

Table 4.5. Electric conductivity, pH value, TDS content and hardness of deionised water

Property	Value	Unit
El. conductivity	0.44	µS cm <sup>-1</sup>
TDS	0.22	mg L <sup>-1</sup>
pH	6.35	-
Hardness	0.04	equivalent CaCO <sub>3</sub> mg L <sup>-1</sup>

Leaching potential of deionized water was confirmed by the total concentration of the selected eleven trace elements, calcium and magnesium, Table 4.6.

Table 4.6. Trace elements, calcium and magnesium in deionised water

Element	Concentration/ $\mu\text{g mL}^{-1}$
	Soft water
As	< 0.030*
Cd	< 0.006*
Co	< 0.008*
Cr	< 0.056*
Cu	< 0.203*
Hg	< 0.009*
Ni	< 0.042*
Pb	< 0.080*
Sb	< 0.005*
V	< 0.020*
Zn	< 1.06*
Ca	0.013 mg L <sup>-1</sup>
Mg	0.003 mg L <sup>-1</sup>

\* Limit of determination for each specified element



## 4.2. Hydration of cement pastes

Despite limitations in implementation of XRPD on hydrated cement pastes, diffractograms are valuable sources of information on hydration process. Powder patterns of the CEM I paste show that alite from anhydrous cement is consumed during the 365 days hydration period. There is still some alite present after 365 days (Figure 4.6).<sup>216,221,234-235</sup> Crystalline phases during hydration and leaching observed by XRPD can give us valuable information. The crystalline hydrated phase, portlandite was observed after the 1.5 day hydration period and there is an increase up to 7 days during which the amount of ettringite also increases. In 28 days of the hydration period no further significant increase in portlandite or ettringite was observed. This indicates that leaching does not affect the CEM I paste significantly and is in line with the observed strength behaviour. Reduction of ettringite is observed from 56 to 365 days of hydration. This is in agreement with the strength decrease observed for the 365 days hydration period. A very small peak at  $9.9^\circ 2\theta$  corresponds to monosulphate. For the 365 days hydration period an increase of calcite due to carbonatization of the samples was observed.

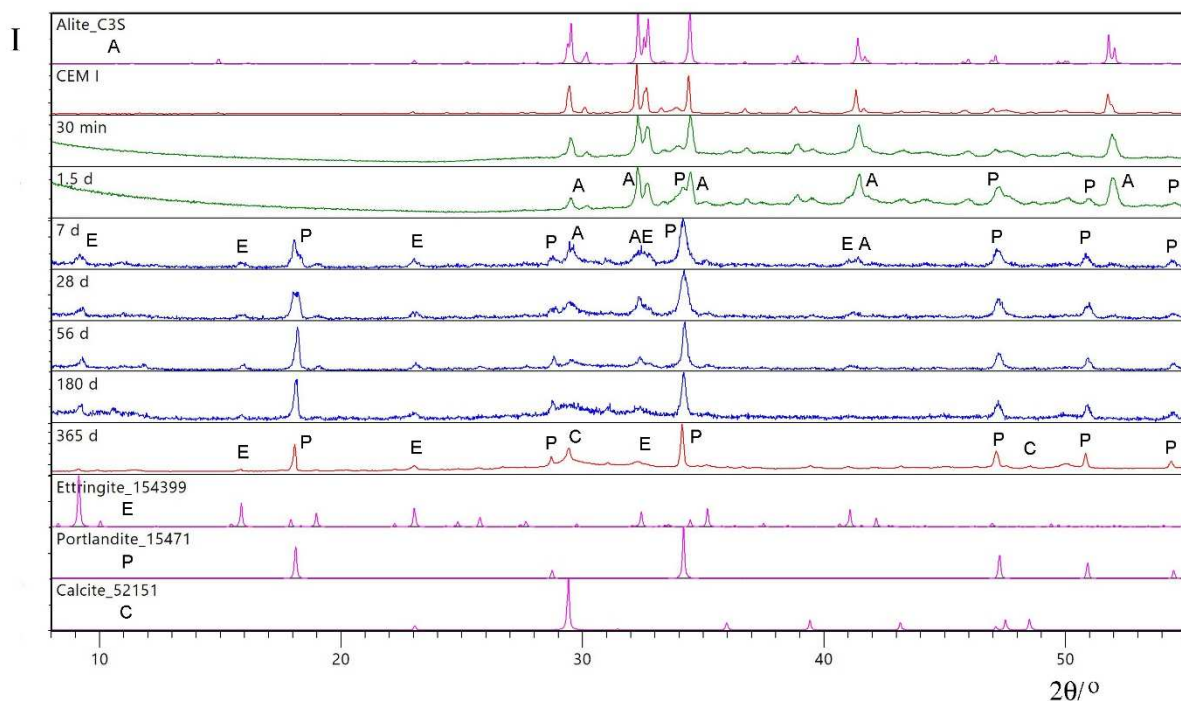


Figure 4.6. XRPD of CEM I cement paste in the  $2\theta$  range  $8 - 55^\circ$ . Observed powder patterns for CEM III and the CEM III paste after 365 days of hydration and leaching are shown red

color. *In-situ* patterns are shown in green color. Patterns of hydrated and leached CEM III paste are shown in blue color. Calculated powder patterns of known crystal structures are shown in pink color<sup>216,221,232-235</sup>

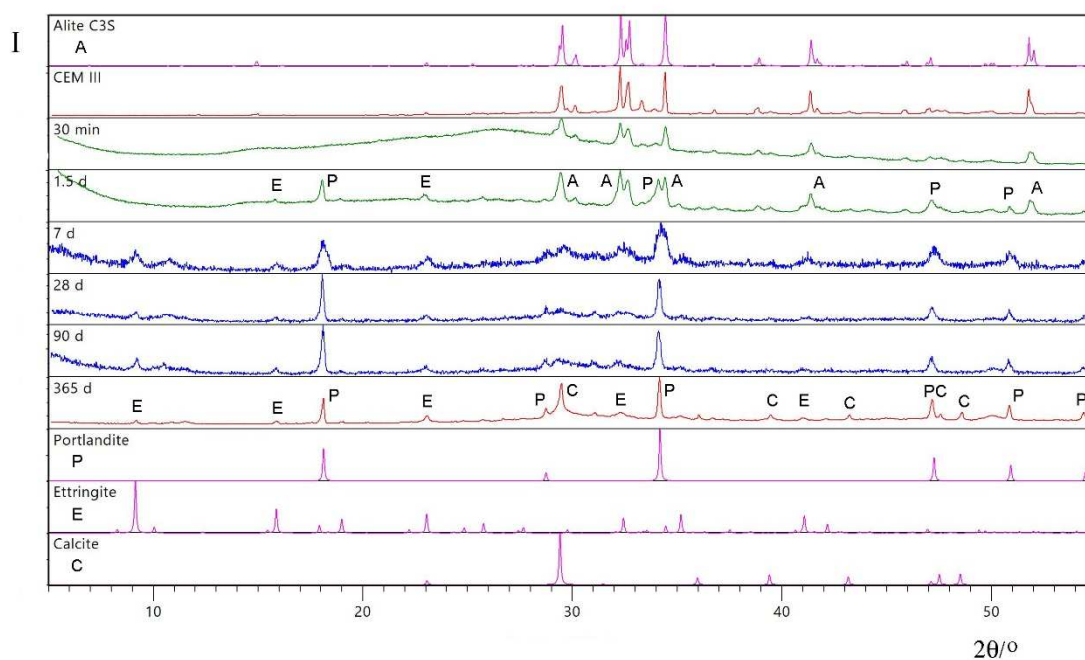


Figure 4.7. XRPD of CEM III cement paste in the  $2\theta$  range  $8 - 55^\circ$

with the identified crystalline phases. Observed powder patterns for CEM III and the CEM III paste after 365 days of hydration and leaching are shown red color. *In-situ* patterns are shown in green color. Patterns of hydrated and leached CEM III paste are shown in blue color. Calculated powder patterns of known crystal structures are shown in pink color<sup>216,221,232-235</sup>

At the beginning of CEM III hydration there is high background corresponding to the amorphous phase which is consequence of granulated blastfurnace addition (Figure 4.7) Crystalline portlandite is formed after 1.5 days hydration period and also some ettringite. The decrease of ettringite observed for CEM I is also observed for CEM III in the same hydration period, corresponding to the strength behaviour. The formation of calcite increases with hydration. Alite is fully consumed after 365 days.

The sample of CSA cement reacts with water faster since ettringite is already formed after 12 hours and the major phase Ye'elimitite is almost completely consumed within 7 days of the

hydration period (Figure 4.8).<sup>216,221,235-236</sup> Ettringite and stratlingite are the major crystalline phases formed by CSA hydration. Formation of calcite increases with hydration.

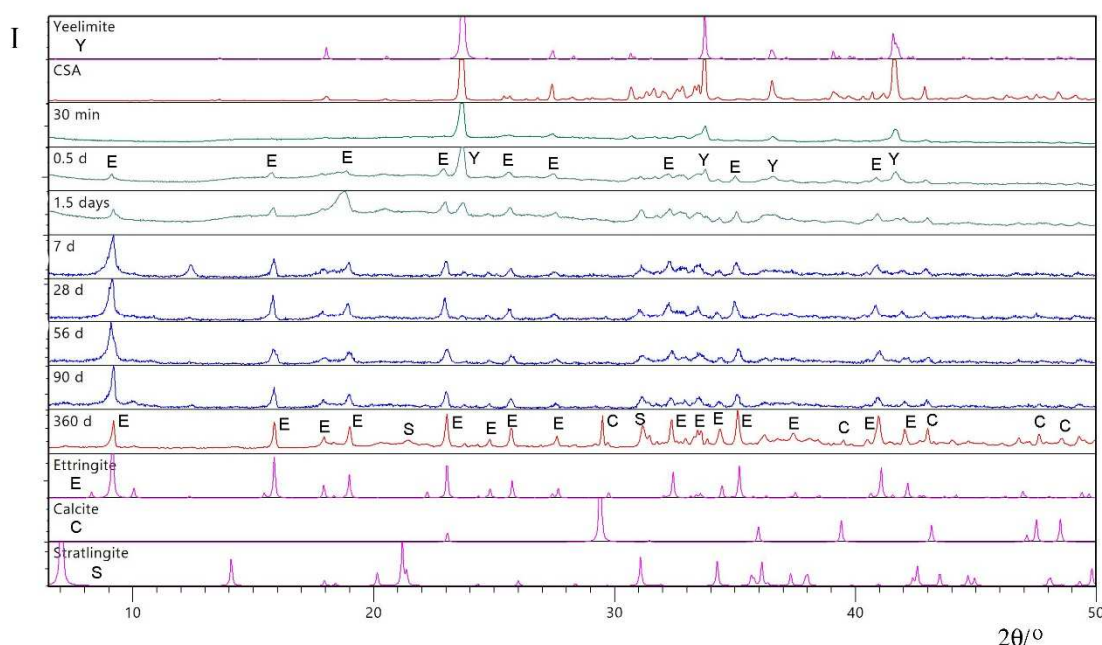


Figure 4.8. XRPD of CSA cement paste in the  $2\theta$  range  $8 - 55^\circ$  with the identified crystalline phases.<sup>216,221,235-236</sup> Calculated powder patterns of known crystal structures are shown in pink color. Observed powder patterns for CSA cement and the CSA cement paste after 365 days of hydration and leaching are shown red color. *In-situ* patterns are shown in green color. Patterns of hydrated and leached CSA cement paste are shown in blue color. known crystal structures

The diffraction patterns for XRPD *in-situ* measurements show that carbonatization is dominant process on the surface in all cement paste samples. Figure 4.9. shows that for 7 days hydration period the pattern corresponding to calcite dominates in diffraction patterns of all cement pastes.<sup>221</sup> This indicates that XRPD *in-situ* measurements are not suitable for leaching studies due to formation of calcite on the surface of the samples.

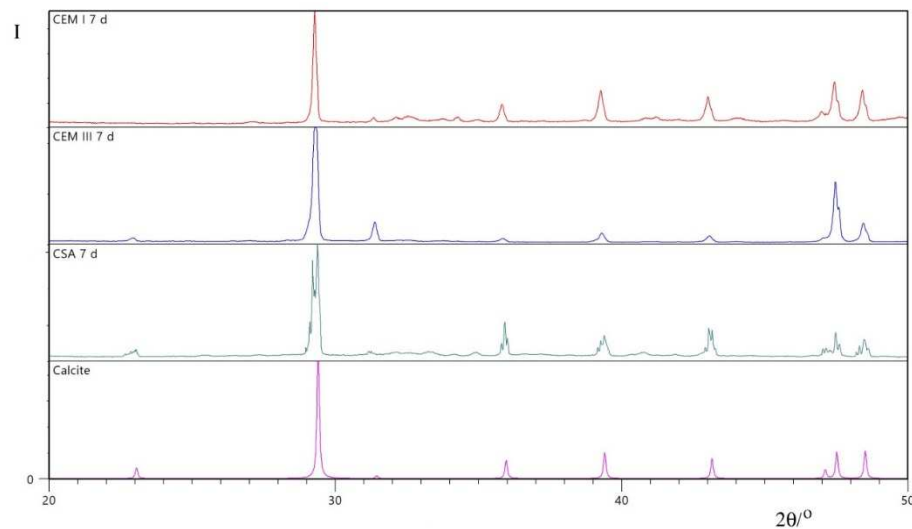


Figure 4.9 *In-situ* XRPD of CEM I, CEM III and CSAC cement pastes in the  $2\theta$  range  $8 - 55^\circ$  <sup>221</sup>

### 4.3. Mechanical and physical properties of hydrated cement pastes

Strength, secant modulus of elasticity, dimensional and mass stability are the key mechanical and physical properties of the Portland cement paste important for its application and are included in almost every research in this field.

The final flexural and compressive strength for CEM I, CEM III and CSA cement pastes shows decrease upon leaching, Table 4.7. Within the 28 days hydration period no strength reduction is observed. This indicates that hydration of all three cement types in this period is not affected by leaching. The first reduction is observed for the CSA cement paste after the 56 days hydration period for both flexural and compressive strength. Strength shows a decreasing trend up to the 365 days hydration period with the final 70 % reduction for flexural and 13 % for compressive strength.

Table 4.7. Flexural and compressive strength for CEM I, CEM III and CSA cement pastes after leaching

Hydration period / days	Strength / MPa					
	Flexural			Compressive		
	CEM I	CEM III	CSA cement	CEM I	CEM III	CSA cement
2	3.5	3.9	5.0	19.3	20.0	32.7
7	5.1	5.6	6.0	31.3	31.9	37.7
28	7.2	7.8	4.1	49.4	51.8	36.3
56	8.2	8.6	3.5	57.0	60.7	35.3
90	8.7	9.1	2.0	61.3	65.7	34.2
180	9.2	4.3	1.9	65.0	69.1	32.7
365	4.9	4.2	1.8	56.0	42.3	32.5

For the CEM III paste reduction of flexural strength of 53 % is observed after 180 days. The decline of compressive strength of 13 % and 61 % for CEM I and CEM III, respectively, is observed after the 365 days leaching period. The CEM I paste loses flexural strength for 53%. The decrease of flexural and compressive strength is the result of the long-term leaching process. It also indicates that susceptibility towards leaching increases in the order CEM I < CEM III < CSA cement.

The loss of strength as a consequence of leaching or some other degradation process is usually accompanied by a decline of the secant modulus of elasticity. No decline in secant modulus of elasticity for CEM I, CEM III and CSA cement pastes are observed during the leaching period of 365 days. On the contrary, increase is observed for all three cement types (see Table 4.8). The secant modulus of elasticity is strongly correlated with porosity of the cement paste. It increases with decrease of porosity. This indicates that long-term leaching process did not increase porosity of CEM I, CEM III and CSA cement pastes and that the observed loss of strength is a consequence of changes in the chemical composition of the hydration products.

Table 4.8. Modulus of elasticity for CEM I, CEM III and CSA cement pastes after leaching

Hydration period / days	Modulus of elasticity / GPa		
	CEM I	CEM III	CSA cement
2	7.45	7.26	9.80
7	10.83	10.99	11.02
28	14.26	14.50	11.19
56	15.05	15.32	11.34
90	15.91	15.80	11.00
180	16.51	19.40	13.41
365	21.33	22.35	15.78

Figure 4.10 shows that no significant dimensional instability is observed during the hydration period. Shrinkage behaviour of both Portland cements as well as of the CSA cement is common. Figure 4.11 shows that no significant change of mass is observed during the hydration period. The observed volume and mass stability indicate that no expansive product, such as expansive ettringite is formed during the long-term leaching process.

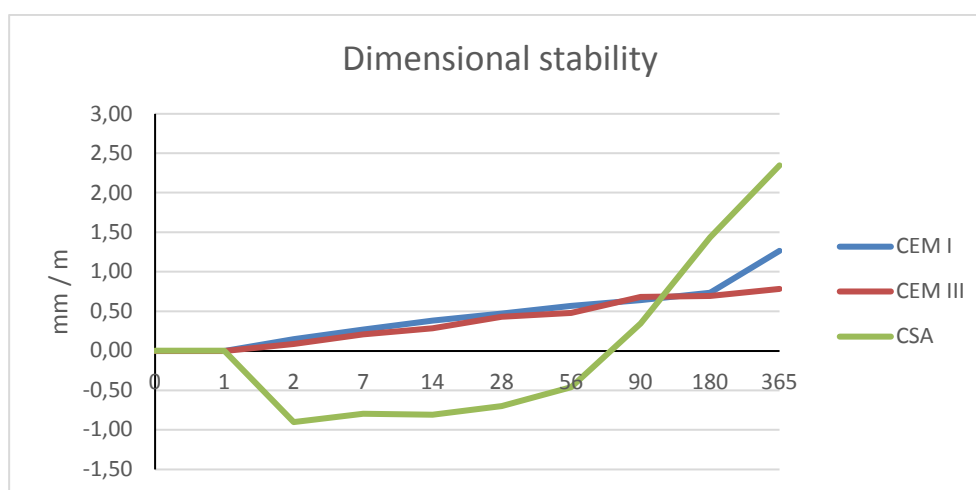


Figure 4.10. Dimensional stability for CEM I, CEM III and CSA cement pastes after 365 days hydration

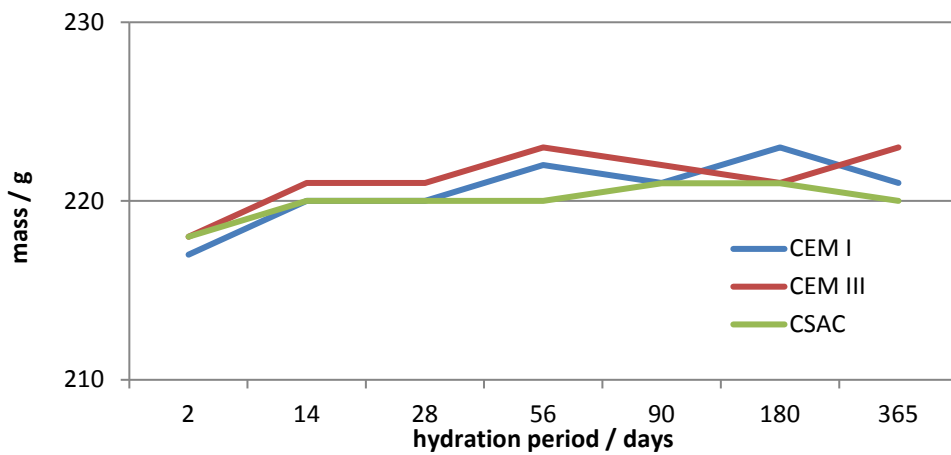


Figure 4.11. Mass changes for CEM I, CEM III and CSA cement pastes after leaching

#### 4.4. Microstructural properties

Figure 4.12 shows microstructure of CEM I, CEM III and CSA cement paste after the 365 days leaching period, observed by scanning electron microscopy. In the CEM I paste (Figure 4.5 A) large areas of plate-like portlandite and areas of tightly packed spherical grains of the C-S-H gel together with needle-like ettringite are visible. In the CEM III paste (Figure 4.12 B), portlandite is closely intermixed with the C-S-H gel and needle-like ettringite. The highest amount of ettringite is observed in the CSA cement paste (Figure 4.12 C and 4.12 D). The microstructure and morphology of hydration products does not indicate any deterioration due to leaching. The compositions of hydration phases confirmed by EDS spectra are shown in Figures 4.13, 4.14 and 4.15. The microstructure corresponds to an increase of the modulus of elasticity for all cement pastes.

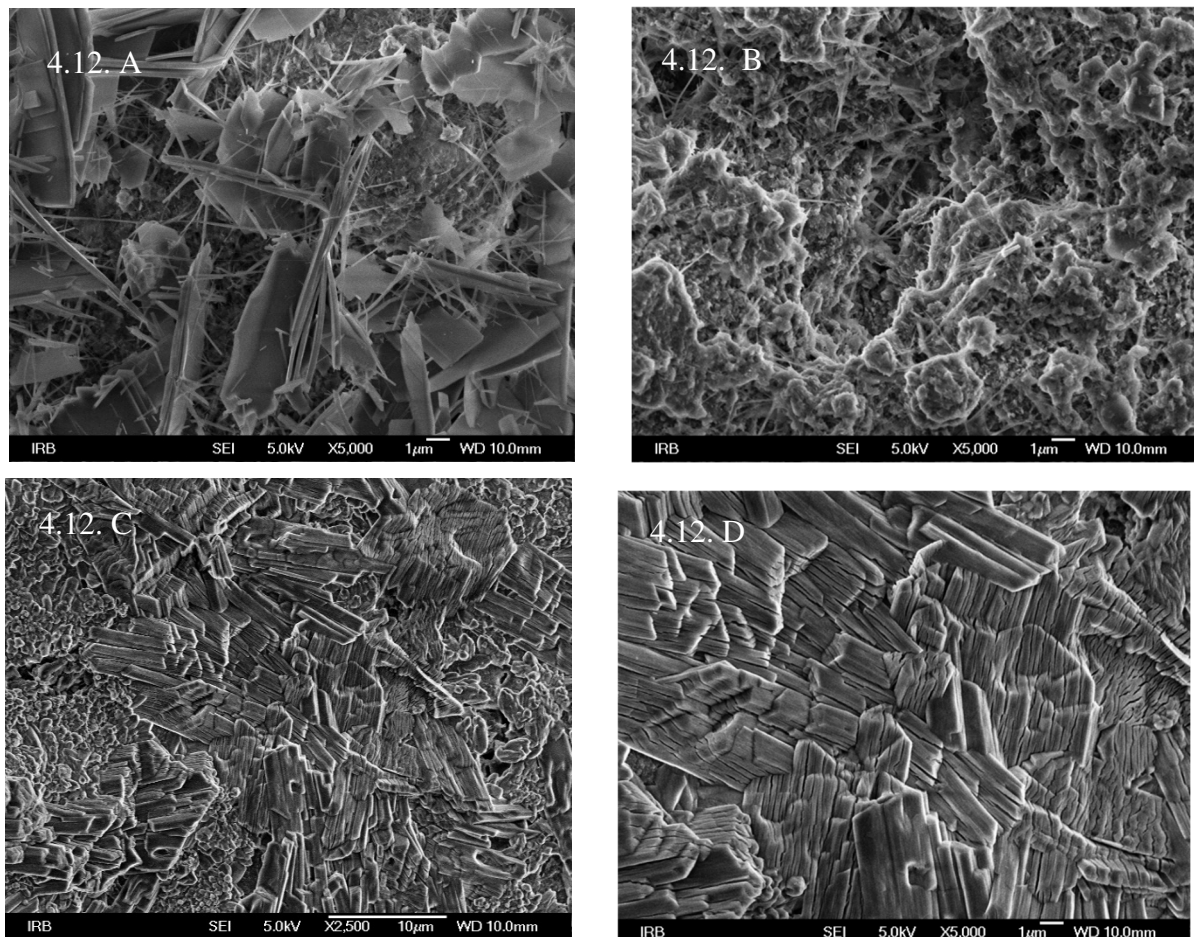


Figure 4.12. Microstructure of A) CEM I, B) CEM III; C) and D) CSA cement paste after leaching



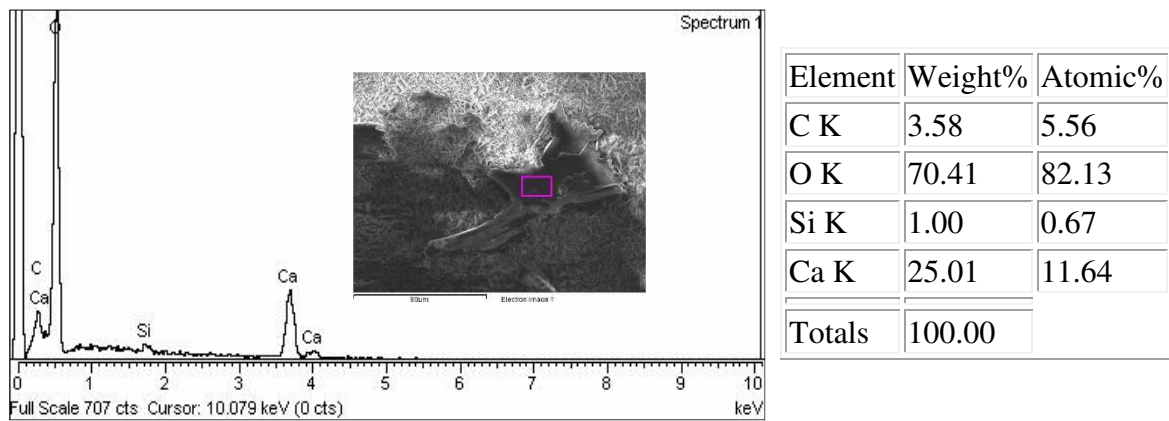


Figure 4.13. EDS spectra of portlandite from the CEM I paste after leaching

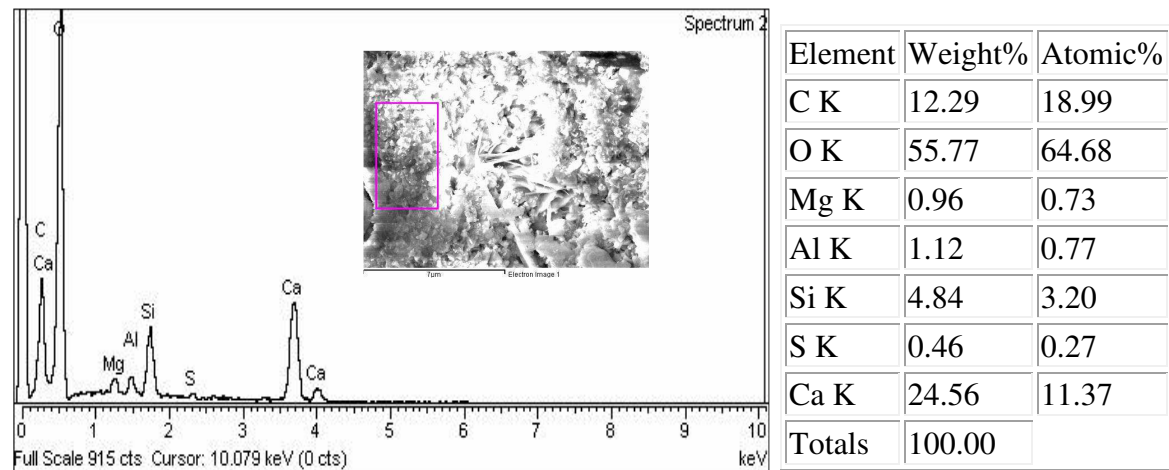


Figure 4.14. EDS spectra of the C-S-H gel from the CEM III paste after leaching

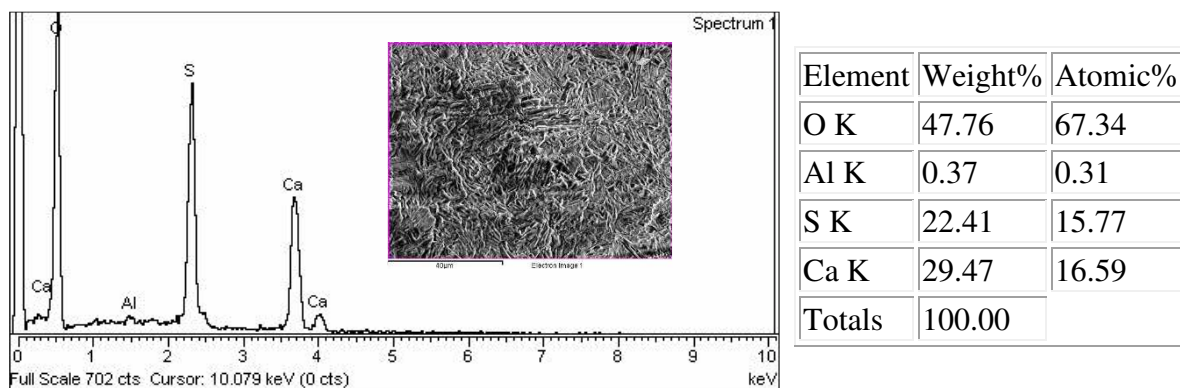


Figure 4.15. EDS spectra of ettringite from the CSA cement paste after leaching

The content of air voids for CEM I, CEM III and CSA cement pastes shows increase in the 365 days leaching period (Table 4.9). The lowest increase (around 7 %) is observed for CEM I and the highest (around 60 %) for CEM III. The increase of around 33 % is observed for CSA. This is fully in line with the observed decrease of compressive strength. Microscopic determination of air voids content includes determination of closed microscopic pores filled with air with a diameter between 0 and 4000  $\mu\text{m}$ .

Table 4.9. Air void content in CEM I, CEM III and CSA cement paste after leaching

Leaching period / days	Air voids content / %		
	CEM I	CEM III	CSA
28 days	0.29	0.12	0.12
365 days	0.31	0.19	0.16

Porosity of cementitious materials can be well estimated by measuring water absorption due to capillary action. Materials with higher water absorption values are more porous. Susceptibility towards leaching of Portland cement pastes increases with increased porosity. Capillary action was measured on samples after a 365 days hydration period. Figure 4.16 shows that CSA cement paste is more porous than CEM I and CEM III. CEM III paste has the lowest porosity. This indicates that susceptibility towards leaching decreases in the order CSA > CEM I > CEM III.

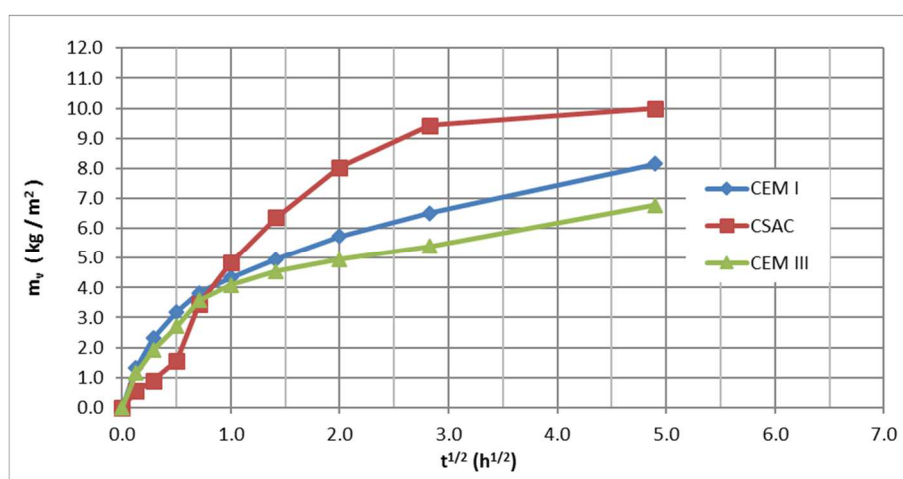


Figure 4.16. Water absorption due to capillary action after 365 hydration period

It was not possible to determine permeability to gasses of CEM I, CEM III and CSA cement pastes due to decomposition of samples during determination. The presumable cause of sample decomposition is the necessary drying procedure before measurement, although modified (lower temperature) drying procedure was applied. Drying may causes degradation of hydration products and decomposition of cement samples.

#### 4.5. Cement paste and pore solution composition

The composition of CEM I, CEM III and CSA cement pastes after leaching, given in Tables 4.10, 4.11 and 4.12, show decrease of calcium, sodium and potassium in all cement types in the course of time. The results indicate leaching and correspond to the previous research results. The highest loss (around 6 %) of calcium is observed for CSA and the lowest (around 1 %) for CEM III. The loss around 2 % is observed for CEM I.

Sodium and potassium are also leached from the cement paste. The abundances of potassium in cement pastes and pore solutions are not correlated with its content in anhydrous cements. The highest potassium levels are observed for anhydrous CEM I and CEM III cement paste after 2 days hydration period. This indicates that potassium in CEM III is mainly incorporated within the clinker phases, however in CEM I as well as in CSA it is predominantly present in the form of the ready soluble sulfate salt. In CEM I and CEM III sodium is mainly incorporated within the clinker phases but present in the form of ready soluble sulfate salts in the CSA cement. The highest decline observed for sodium and potassium is observed for the CSA cement, and then for CEM III and CEM I indicating that susceptibility towards leaching decreases in this order. Aluminium and iron have a constant concentration in the course of time, while silicon and magnesium show a slight increase. This indicates that phases containing aluminium and iron are not affected by leaching.

Alkalinity of the CSA cement pore solution is lower than that of CEM I and CEM III (see Table 4.13). Decline of the pH value in the course of time is observed for all pore solutions and corresponds to the decline in the concentration of alkalis (Figure 4.17). The increase in calcium concentration has been observed for 28 days hydration period for all cement types (Figure 4.18). Exception is the CEM III pore solution after a 7 days hydration period. The observed decrease of calcium corresponds with consumption of CH necessary for activation of slag. The increase of calcium pore solution concentration in all three cement types in the 28 days hydration period indicates that pastes are not affected by leaching. The decline in calcium pore solution concentration is observed between 28 days and 180 days. This

indicates the loss of calcium caused by leaching. The finally observed increase in calcium pore solution concentration corresponds to the decrease of calcium content in all three cement pastes and indicates dissolution of calcium containing hydration products. Calcium pore solution behaviour is fully in line with the observed strength behaviour. The results for cement pastes and pore solutions indicate that the resistance towards leaching is significantly better in CEM I and CEM III pastes under the given experimental conditions in comparison to the CSA cement.

Table 4.10. Composition of the CEM I paste after leaching

Hydration period / days	w / %							
	CaO	MgO	Al <sub>2</sub> O <sub>3</sub>	Fe <sub>2</sub> O <sub>3</sub>	SiO <sub>2</sub>	SO <sub>3</sub>	K <sub>2</sub> O	Na <sub>2</sub> O
2	58.05	3.62	6.22	2.04	26.71	2.56	0.49	0.31
7	57.72	3.86	6.28	2.07	26.94	2.43	0.43	0.26
28	57.40	3.99	6.39	2.06	27.01	2.57	0.40	0.18
56	57.09	4.03	6.49	2.09	27.23	2.48	0.41	0.19
90	57.03	4.06	6.43	2.09	27.27	2.54	0.36	0.21
180	57.22	4.06	6.59	2.08	27.11	2.54	0.35	0.05
365	56.91	4.01	6.65	2.08	27.38	2.64	0.31	0.03

Table 4.11. Composition of the CEM III paste after leaching

Hydration period / days	w / %							
	CaO	MgO	Al <sub>2</sub> O <sub>3</sub>	Fe <sub>2</sub> O <sub>3</sub>	SiO <sub>2</sub>	SO <sub>3</sub>	K <sub>2</sub> O	Na <sub>2</sub> O
2	57.55	3.80	6.32	2.14	26.95	2.40	0.59	0.26
7	57.25	4.03	6.24	2.10	27.19	2.51	0.50	0.18
28	57.46	3.87	6.43	2.10	27.13	2.52	0.37	0.12
56	57.48	3.97	6.39	2.05	27.11	2.52	0.37	0.12
90	57.46	4.01	6.47	2.10	27.03	2.48	0.37	0.08
180	57.67	3.74	6.42	2.01	27.23	2.63	0.30	0.00
365	56.92	3.83	6.63	2.13	27.59	2.62	0.28	0.00

Table 4.12. Composition of the CSA cement paste after leaching

Hydration period / days	w / %							
	CaO	MgO	Al <sub>2</sub> O <sub>3</sub>	Fe <sub>2</sub> O <sub>3</sub>	SiO <sub>2</sub>	SO <sub>3</sub>	K <sub>2</sub> O	Na <sub>2</sub> O
2	37.53	2.48	4.12	1.40	17.57	1.56	0.38	0.17
7	37.05	2.61	4.04	1.36	17.59	1.62	0.32	0.12
28	36.87	2.48	4.13	1.35	17.41	1.62	0.24	0.08
56	36.66	2.54	4.07	1.31	17.29	1.60	0.24	0.08
90	36.64	2.56	4.13	1.34	17.24	1.58	0.24	0.05
180	36.35	2.36	4.05	1.26	17.16	1.66	0.19	0.00
365	35.16	2.36	4.09	1.32	17.04	1.62	0.17	0.00

Table 4.13. pH value of pore solutions after leaching

Leaching period/days	pH value		
	CEM I	CEM III	CSA cement
2	13.45	13.85	13.19
7	13.44	13.77	13.08
28	13.41	13.51	12.89
56	13.37	13.34	12.64
90	13.27	13.10	11.90
180	12.95	12.66	11.98
365	12.90	13.39	11.03

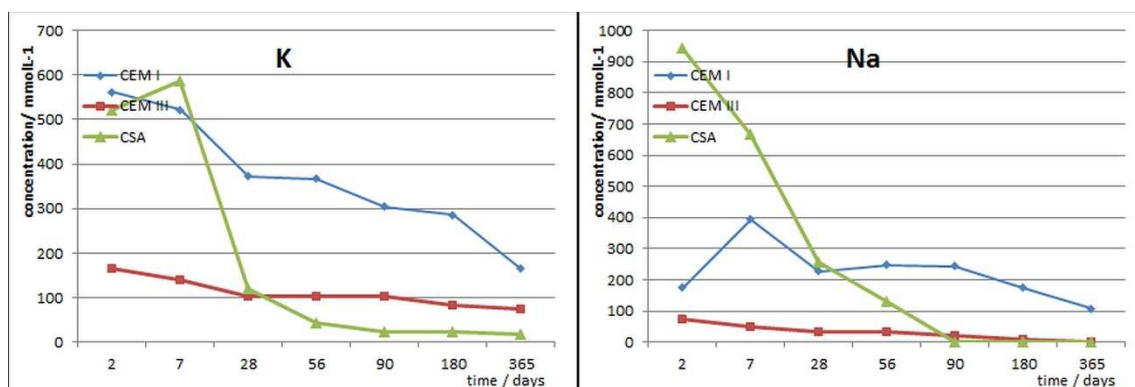


Figure 4.17. Development of the pore solution concentration of K and Na in the course of time for leached cement pastes

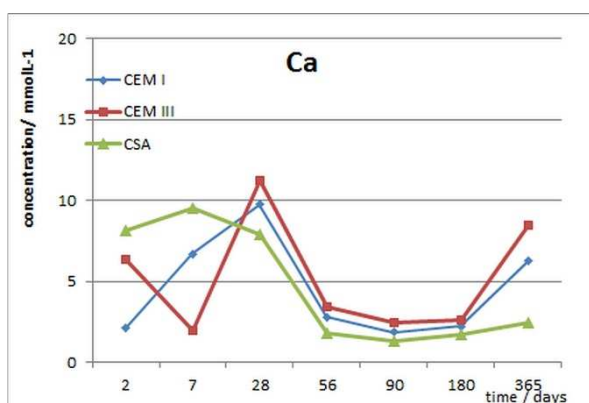


Figure 4.18. Development of the pore solution concentration of Ca in the course of time for leached cement pastes

Concentration of the soluble trace elements in the pore solution, shown in Figures 4.19, 4.20 and 4.21 support their low solubility and good immobilization in the high alkaline cement paste. The highest concentrations are observed for copper, chromium and vanadium in CSA cement paste and they correspond with high concentrations of these elements in anhydrous CSA cement. The extremely low pore solution concentration of arsenic, cadmium, mercury and lead corresponds to their low abundance in anhydrous CEM I and CEM III. The low abundance of cadmium in CSA cement also results in constantly low concentration of this element in pore solution. The extremely lower concentration of lead in CSA cement pore solution does not correspond with its high abundance in CSA cement. This result indicates very good immobilization of lead within CSA cement pastes. The behaviour of all other trace elements (Co, Cr, Cu, Hg, Ni, Sb and V) except Zn is the same for CSA cement paste. The

very high concentrations (especially for Cr and V) are significantly reduced in the course of time. Only Zn shows slight increasing tendency. The mobility of selected trace elements in CSA cement pastes is not correlated with decline in pore solution pH value. This indicates that leaching does not affect immobilization of CSA cement which makes it very suitable for the waste immobilization. The high abundance of AFm and AFt phases is presumably responsible for the good trace elements immobilization in CSA cement pastes.

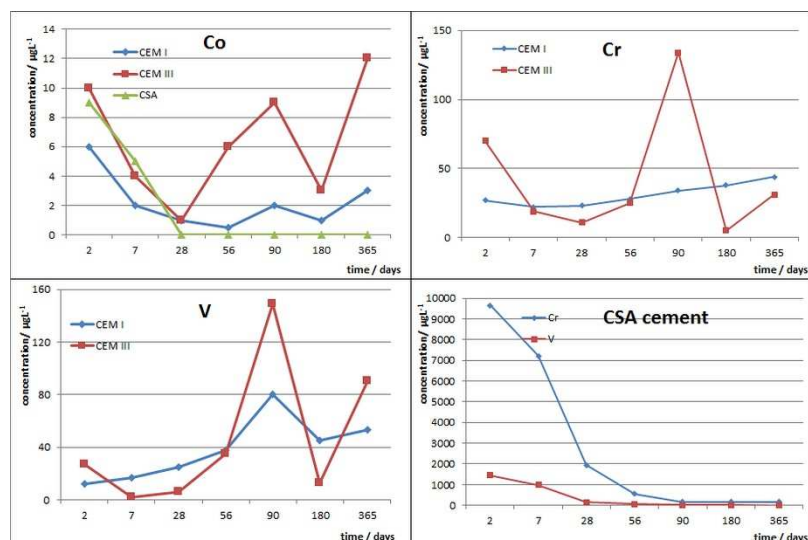


Figure 4.19. Development of the pore solution concentration of Co, Cr and V in the course of time for leached cement pastes

Mercury in CEM I and CEM III pastes behaves similarly to cadmium and lead but shows the highest solubility among the trace elements included in this research. This indicates that the higher content of mercury incorporated in the Portland cement clinker phases could potentially present an environmental risk for Portland cement type. A slight increase of the arsenic pore solution concentration indicates decrease in the calcium hydroxide content caused by leaching, therefore the higher content of arsenic in the cement paste could possibly present an environmental risk. The lower concentration of antimony at the beginning of hydration increases in the course of time in CEM I as well as in CEM III pore solutions. The immobilization of antimony depends on the pH value and the calcium concentration. The increased solubility of antimony supports decalcification of hydrated CEM I and CEM III cement phases caused by leaching. Antimony incorporated in the clinker phases could potentially present an environmental risk.

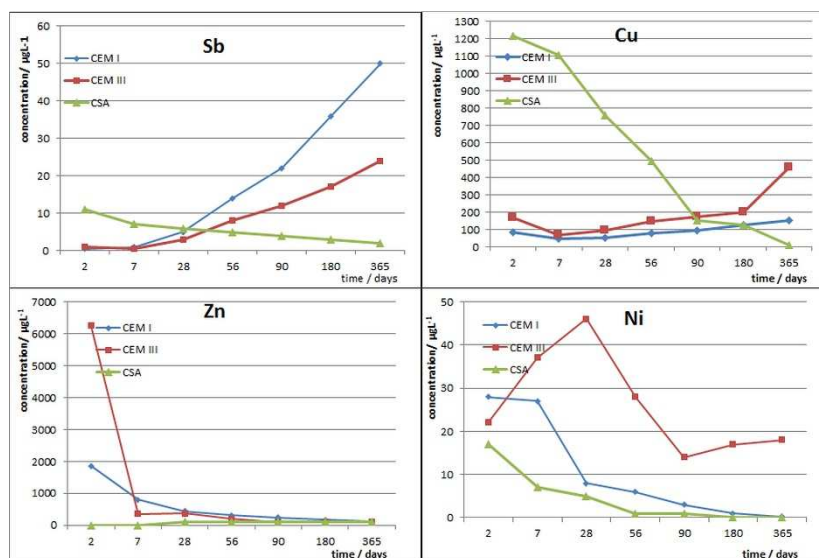


Figure 4.20. Development of the pore solution concentration of Sb, Cu, Zn and Ni in the course of time for leached cement pastes

Increase of the copper concentration in CEM I and CEM III pore solution is observed after 7 days. Since the only indicated mechanism of copper immobilization in the cement paste is the ion exchange with calcium from the C-S-H gel, this indicates degradation of C-S-H and a potential environmental risk. A quite high concentration of zinc in CEM III and CEM I decrease in the course of time. Despite the decrease of pH values of the pore solutions, they are still alkaline. Mobility of zinc increases below pH 7. Behaviour of zinc in CEM I and CEM III pore solution does not indicate any deleterious reaction. The decrease of nickel concentration in the pore solution corresponds to the decrease in pH. Nickel behaviour in the pore solution indicates a deleterious reaction in CEM I and CEM III cement paste. Chromium and vanadium show an increasing but a less clear trend. Cobalt pore solution concentration is scattered. A difference in behaviour of these elements in CEM I and CEM III pastes is observed. This indicates possible different incorporation of chromium, vanadium and cobalt within hydrated and non-hydrated CEM I and CEM III. It was not possible to correlate our results for these elements with degradation of the cement paste caused by leaching. The behaviour of these elements should be carefully considered in the environmental risk assessment due to ups and downs observed for these elements.



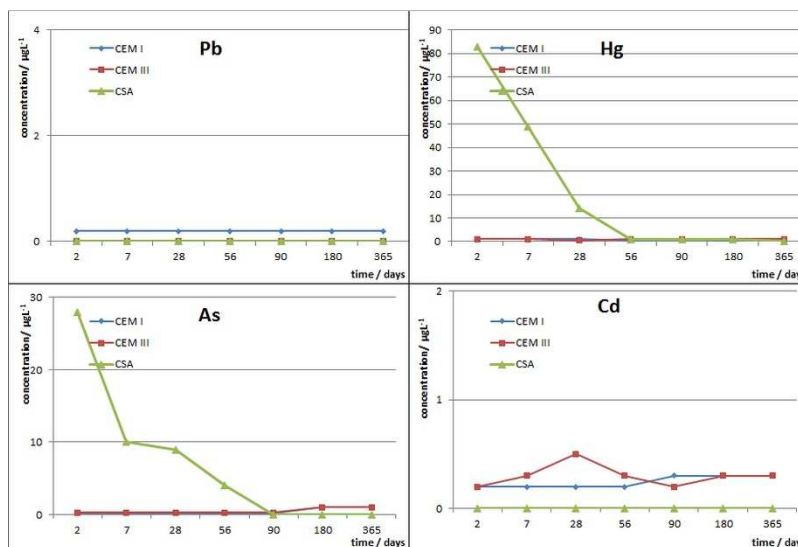


Figure 4.21. Development of the pore solution concentration of Pb, Hg, As and Cd in the course of time for leached cement pastes

## § 5. CONCLUSION

The formation of crystalline hydrated phases, portlandite and ettringite and their abundance after the 28 days hydration period indicates that Portland cement pastes are not affected by leaching in this period. The reduction of ettringite observed from 56 days to 365 days of hydration for Portland cement pastes corresponds to strength reduction observed in this period. The composition of hydrated Portland cement pastes does not support dissolution of aluminium containing hydration products (e.g. ettringite). This indicates that the simple transformation of ettringite to monosulfate could be a possible source of ettringite reduction. The abundance of the major crystalline phases formed by calcium sulfoaluminate cement hydration, does not indicate any leaching after the 365 days hydration period. Leaching of calcium and alkalis in all cement pastes and pore solutions, accompanied by alkalinity decrease, indicates changes in chemical composition of C-S-H or quantity of CH. Portlandite is not observed in the CSA cement paste. Carbonatization of the samples is observed in all cement pastes in the course of time. It is only significant for XRPD *in-situ* measurements, which are measured on the surface of the samples, and does not cause formation of ettringite in the late period of hydration.

The microstructure and morphology of hydration products after the 365 hydration period does not indicate any deterioration due to the leaching. The increase in closed pore volume observed from 56 days to 365 days hydration period indicates changes in the pore system which is in line with observed strength decrease. The lower capillary porosity of Portland cement pastes compared to calcium sulfoaluminate cement paste after 365 days hydration period reduces the susceptibility of Portland cement pastes towards leaching. Increase of the modulus of elasticity in the hydration period indicates no substantial decrease in overall porosity in the course of time. Powder patterns of cement pastes show that expansive compounds are not formed by leaching, which corresponds with volume and mass stability.

Strength, the most important property of cement paste is affected by leaching. The long term-leaching decreases the flexural and compressive strength of the cement pastes after 56 days or more under the given experimental conditions. According to strength, cement based on calcium sulfoaluminate compounds is more susceptible towards leaching than Portland cement based on calcium silicate and calcium aluminate compounds. The leaching rate

depends decisively on the type of cement used. Cement paste with a higher C-S-H content is less susceptible towards leaching.

Result of research indicates that leaching causes changes in chemical composition and structure of the C-S-H gel which results in strength loss. These changes should be confirmed by further investigations.

The immobilization of the trace elements in calcium sulfoaluminate cement paste is not affected by leaching, thus the concentration of the trace elements in pore solution cannot be used in leaching studies for this cement type. The increasing concentrations of arsenic, mercury, antimony and copper and the decreasing trend of nickel in Portland cement pore solutions support chemical degradation by leaching. Behaviour of chromium, vanadium and cobalt cannot be related to degradation by leaching due to observed up and downs.

The long-term leaching tests, at least 365 days or longer, are necessary to unambiguously determine the leaching effect on the cement pastes. The immature cement paste may be used in leaching tests and can thus shorten the period of testing. XRPD *in-situ* and permeability to gasses are not suitable techniques to be applied in leaching studies.

Cement based on calcium sulfoaluminate compounds are not recommended to be used in structures exposed to leaching but are very suitable for trace metals immobilization. A new sustainable cement solution could be based on the mixture of calcium silicate, calcium aluminate and calcium sulfoaluminate compounds. The suitable proportions should be determined by further research.

## § 6. LIST OF ABBREVIATIONS

Cement chemistry notation is used including abbreviations of oxides, phases in non-hydrated cement (clinker) and hydrated cement. The abbreviations of analytical techniques and used materials are also given.

A	aluminium oxide ( $\text{Al}_2\text{O}_3$ )
AFm	aluminate ferrate monosulfate
AFt	aluminate ferrate trisulfate
AH <sub>3</sub>	aluminium hydroxide
BSEI	backscattered electron image
C	calcium oxide ( $\text{CaO}$ )
CA	calcium aluminate
C <sub>4</sub> A $\bar{3}$	tetracalcium      trialuminate sulfate, Ye'elimite
CSA	calcium sulfoaluminate
C-S-H	calcium silicate hydrate
C <sub>3</sub> A	tricalcium            aluminate, aluminate
C <sub>4</sub> AF	tetracalcium alumino ferrite, ferrite
CH <sub>2</sub>	calcium sulfate (gypsum)
C <sub>2</sub> S	dicalcium silicate , belite
C <sub>3</sub> S	tricalcium silicate, alite
EDS	energy    dispersive    X-ray spectrometry
F	iron (III) oxide ( $\text{Fe}_2\text{O}_3$ )
H	water ( $\text{H}_2\text{O}$ )
ICP-MS	inductively coupled plasma mass spectrometry
K	potassium oxide ( $\text{K}_2\text{O}$ )

---

LOI	loss on ignition
M	magnesium oxide (MgO)
M <sub>1,2</sub>	monoclinic
N	sodium oxide (Na <sub>2</sub> O)
QC	quality control
QXRPD	quantitative X-ray powder diffraction
R	rhombohedral
S	silicon dioxide (SiO <sub>2</sub> )
$\bar{S}$	sulfate (SO <sub>3</sub> )
SCM	supplementary cementitious materials
SEI	scanning electron imaging
SEM	scanning electron microscopy
T	triclinic
TG	thermogravimetry
TDS	total dissolved solids
w/c	water to cement ratio
XRPD	X-ray powder diffraction

## § 7. BIBLIOGRAPHY

1. K. L. Scrivener and R. J. Kirkpatrick, *Cem. Concr. Res.* **38** (2008) 128 – 136.
2. C. D. Lawrence, The production of Low – Energy cements, in: P. C. Hewlett (Ed.) *Lea's Chemistry of Cement and Concrete Fourth Edition*, Oxford, Elsevier, 2005, pp. 421 - 470.
3. C. Shi, A. F. Jiménez and A. Palomo, *Cem. Concr. Res.* **41** (2011) 750 - 763.
4. F. P. Glasser, Future directions in the cement industry, in: R.K. Dir, M.D. Newlands, L. J. Csetenyi (Eds.) *Role of Cement Science in Sustainable Development*, London, Thomas Telford, 2003, pp. 1 - 16.
5. H. F. W. Taylor, *Cement Chemistry 2nd Edition*, London, Thomas Telford, 1997, pp. 1 - 28.
6. J. Radić and J. Bleiziffer, Durability of Concrete Structures, in: J. Radić (Ed.) *Concrete Structures 4: Sanations*, Hrvatska sveučilišna naklada, Građevinski fakultet Sveučilišta u Zagrebu, Secon HDGK, 2008, pp. 83 – 164 (in Croatian).
7. F. Adenot and M. Buil, *Cem. Concr. Res.* **22** (1992) 489 - 496.
8. M. Mainguy, C. Tognazzi, J. M. Torrenti and F. Adenot, *Cem. Concr. Res.* **30** (2000) 83 - 90.
9. F. P. Glasser, J. Marchand and E. Samson, *Cem. Concr. Res.* **38** (2008) 226 - 246.
10. C. Carde, R. François and J. M. Torrenti, *Cem. Concr. Res.* **26** (1996) 1257 - 1268.
11. F. H. Heukamp, F. J. Ulm and J. T. Germaine, *Cem. Concr. Res.* **31** (2001) 767 - 774.
12. G. J. Verbeck and R. H. Helmuth, Structures and physical properties of cement paste, Proceedings of the 5th International Symposium on the Chemistry of Cement, Volume 1, Tokyo, Japan, 1968, pp. 1 - 32.
13. P. K. Mehta and P. J. M. Monteiro, *Concrete: Microstructure, Properties and Materials*, New York, McGraw-Hill, 2006, pp. 203 - 251.
14. Q. Y. Chen, M. Tyrer, C. D. Hills, X. M. Yang and P. Carey, *Waste Manag.* **29** (2009) 390 - 403.
15. P. Faucon, P. Le Bescop, F. Adenot, P. Bonville, J.F. Jacquinot, P. Pineau and B. Felix, *Cem. Concr. Res.* **26** (1996) 1707 - 1715.
16. K. Haga, S. Sotou, M. Hironaga, S. Tanaka and S. Nagasaki, *Cem. Concr. Res.* **35** (2005) 1764 - 1775.
17. Y. Maltais, E. Samson and J. Marchand, *Cem. Concr. Res.* **34** (2004) 1579 - 1589.
18. A. Hildago, S. Petit, C. Domingo, C. Alonso and C. Andrade, *Cem. Concr. Res.* **37** (2007) 63 - 70.
19. K. Yokozeiki, K. Watanabe, N. Sakata and N. Otsuki, *Appl. Clay. Sci.* **26** (2004) 293 - 308.
20. A. Đureković, Cement and cementitious composites and concrete additives, Školska knjiga, Zagreb, 1996, pp. 1-20 (in Croatian).

21. V. Ukrainczyk, *Concrete*, Alcor, Zagreb, 1994, pp. 11 - 39 (in Croatian).
22. R. G. Blezard, The History of Calcareous Cements, in: P. C. Hewlett (Ed.) *Lea's Chemistry of Cement and Concrete Fourth Edition*, Oxford, Elsevier, 2005, pp. 1-23.
23. <https://cembureau.eu/media/1716/activity-report-2017.pdf> (accessed 28. February 2019.)
24. C. D. Lawrence, The Constitution and Specification of Portland cements, in: P. C. Hewlett (Ed.) *Lea's Chemistry of Cement and Concrete Fourth Edition*, Oxford, Elsevier, 2005, pp. 131 - 193
25. I. Maki and S. Chromý, *Cem. Concr. Res.* **8** (1978) 407 - 414.
26. I. Maki and S. Chromý, *Cemento* **75** (1978) 247 - 252.
27. I. Maki, *Cemento* **76** (1979) 167 - 176.
28. I. Maki and K. Kato, *Cem. Concr. Res.* **12** (1982) 93 - 100.
29. I. Maki, Relationship of processing parameters to clinker properties; influence of minor components, Proceedings of the 8th International Congress on the Chemistry of Cement, Volume 1, Rio de Janeiro, Brasil 1986, pp. 34 - 47.
30. V. V. Timashev, Cinétique de la clinkérisation structure et composition du clinker et ses phases, Proceedings of the 7th International Congress on the Chemistry of Cement, Volume 1, Paris, 1980, pp.I-3/1- I-3/19 (english translation).
31. I. Maki and K. Goto, *Cem. Concr. Res.* **12** (1982) 301 - 308.
32. I. Maki, *Cemento* **81** (1984) 165 - 174.
33. I. Maki, Processing Conditions of Portland Cement Clinker viewed from the Fine Textures of the Constituent Minerals, in: E. M. Gartner and H. Uchikawa (Eds.), *Cement Technology*, American Ceramic Society, Westerville, 1994, pp. 3-17.
34. P. Barnes, C. H. Fentiman and J. W. Jeffery, *Acta Cryst.* **A36** (1977) 353 - 356.
35. K. Niesel and P. Thormann, *Tonind. Zeit.* **91** (1967) 362 - 369.
36. M. Regourd and A. Guinier, The crystal chemistry of the constituents of portland cement clinker, Proceedings of the 6th International Congress on Chemistry of Cement, Volume 1, Moscow, Soviet Union, 1974, pp. 1 - 82.
37. P. Monda and J. W. Jeffery, *Acta Cryst.* **B31** (1975) 689 - 697.
38. I. Maki, *Cem. Concr. Res.* **3** (1973) 295 - 313.
39. I. Maki, *Cem. Concr. Res.* **4** (1974) 87 - 97.
40. D. K. Smith, *Acta Cryst.* **15** (1962) 1146 - 1152.
41. I. G. Richardson, C. Hall and G.W. Groves, *Adv. Cem. Res.* **5** (1993) 15 - 21.
42. R. H. Bogue, *Ind. Eng. Chem.* **1** (1929) 192 - 197.
43. H. F. W. Taylor, *Adv. Cem. Res.* **2** (1989) 73 - 77.
44. G.L. Saoût, V. Kocaba and K. Scrivener *Cem. Concr. Res.* **41** (2011) 133 - 148.
45. P. Stutzman, A. Heckert, A. Tebbe and S. Leigh, *Cem. Concr. Res.* **61-62** (2014) 40 - 48.

46. A. M. Harrison, H. F.W. Taylor and N.B. Winter, *Cem. Concr. Res.* **15** (1985) 775 - 780
47. H. F. W. Taylor, *Adv. Cem. Res.* **2** (1989) 73 - 77.
48. A. K. Chatterjee, X – Ray Diffraction, in: V. S. Ramachandran and J.J. Beaudoin (Eds.), *Handbook of Analytical Tehniques in Concrete Science and Technology*, Noyes Publications/Wiliam Andrew Publishing, LLC New York, 2001, pp. 275 - 327.
49. A. I. Boikova, Chemical compositon of raw materials as the main factor responsible for the composition, structure and properties of clinker phases, Proceedings of the 8th International Symposium on the Chemistry of Cement, Volume 1, Rio de Janeiro, Brasil, 1986, pp. 19 - 33.
50. M. A. G. Aranda , A. G. De la Torre and L. León – Reina, *Rew. Mineral. Geochem.* **74** (2012) 169 - 209.
51. P. E. Stutzman, P. Feng and J.W. Bullard *Journal of Resarch of the National Institute of Standards and Technology* **121** (2016) 47 - 107.
52. H. M. Rietveld, *Appl. Cryst.* **2** (1969) 65 - 71.
53. L. León – Reina, A. G. de la Torre, J. M. Porra – Vásquez, M. Cruz, L. M. Ordonez, X. Alcobé, F. Gispert – Guirado, A. Larrañaga – Varaga, M. Paul, T. Fuellman, R. Schmidt and A. M .G. Aranda *J. Appl. Cryst.* **42** (2000) 1 - 11.
54. I.G. Richardson, *Cem. Concr. Res.* **38** (2008) 137 - 158.
55. M. Achternbosch, K. R. Bräutigam, N. Hartliebe; C. Kupsch, U. Richers, P. Stemmermann and M. Gleis., Heavy metals in cement and concrete resulting from co-incereton of wastes in cement kilns with regard to the legitimacy of waste utilization, FZK, Karlsruhe, **2003**, pp. 15 – 105.
56. S. Bodaghpour, N. B. Joo and S. Ahamdi, *Int. J. Geol.* **6** (2012) 62 - 67.
57. C. J. Engelsen, *Effects of mineralizes in cement production*, Concrete Innovation Centre, Trondheim, 2007, pp. 4 - 15.
58. D. Herfort, G. K. Moir, V. Johansen, F. Sorrentino and H. Bollio - Arceo, *Adv. Cem. Res.* **22** (2010) 187 - 194.
59. J. M. Díez, J. Madrid and A. Macías, *Cem. Concr. Res.* **2** (1999) 479 - 485.
60. F. P. Glasser, The Burning of Portland Cement , in: P. C. Hewlett (Ed.) *Lea's Chemistry of Cement and Concrete Fourth Edition*, Oxford, Elsevier, 2005, pp. 195 - 240.
61. S. Sinyoung, P. Songsiriritthigul, S. Asavapisit and P. Kajitvichyanukul, *J. Hazard. Mater.* **191** (2011) 296 - 305.
62. J. I. Bhatta, *Effect of Minor Elements on Clinker and Cement Performance*, Portland Cement Association, Shokie, Illinious, 2006, pp. 35.
63. H. Hornain, *Rev. Mater. Constr.* **671-672** (1971) 203 - 218.
64. K. Kolovos, T. Tsvivilis and G. Kakali, *Cem. Concr. Compos.* **27** (2005) 163 - 170.
65. X. W. Ma, H. X. Chen and P. M. Wang, *Cem. Concr. Res.* **40** (2010) 1681 - 1687.



66. S. Sinyoung, E. Taweekitwanit and P. Kajitvitchyanukul, *Adv. Mater. Res. (Durnten – Zurich, Switz.)* 1103 (2015) 121 - 127.
67. H. Bolio - Arceo and F. P. Glasser, *Adv. Cem. Res.* **12** (2000) 173 - 179.
68. D. Knöefel, *ZKG Int.* **31** (1978) 157 - 161.
69. L. Wang, R. D. Li, Y. L. Li and L. H. Wei, *Adv. Mat. Res.* **347-353** (2010) 2160 - 2164.
70. Y. Yang and J. Xue, Q. Huang, *Sci. World. J.* **2103** (2013), 1 - 6
71. L. Wang, Y. Jin, R. D. Li and Y. Nie, *J. Chem. Ind. Eng.* **62** (2011) 816 - 822.
72. G. Cornelis, C. A. Johnson, T. V. Gerven and C. Vandecasteele, *Appl. Geochem.* **23** (2008) 955 - 976.
73. H.F.W. Taylor, *Cement Chemistry 2nd Edition*, London, Thomas Telford, 1997, pp.113 - 156.
74. A. Đureković, Cement and cementitious composites and concrete additives, Institut građevinarstva Hrvatske i Školska knjiga, Zagreb 1996, pp 21 - 251.
75. H. F. W. Taylor, Chemistry of cement hydration, Proceedings of the 8th International Symposium on the Chemistry of Cement, Volume 1, Rio de Janeiro, 1986, pp. 82 - 110.
76. J. J. Chen, J. J. Thomas, H. F. W. Taylor and H. M. Jennings, *Cem. Concr. Res.* **34** (2004) 1499 - 1519.
77. A. B. Carpenter, R. A. Chalmers, J. A. Gard, K. Speakman and H. F. W. Taylor, *Am. Mineral.* **51** (1966) 56 - 74.
78. N. Hara and N. Inoue, *Cem. Concr. Res.* **10** (1980) 677 - 682.
79. J. E. Rossen, Composition and morphology of C-A-S-H in pastes of alite and cement blended with supplementary cementitious materials, PhD Thesis, École Polytechnique Fédérale de Lausanne, Switzerland, 2004, pp. 9 - 12.
80. S. Merlino, E. Bonaccorsi and A. R. Kampf, 14Å: crystal structure and OD character, in: D. Rammlmair, J. Mederer, T. Oberthür, R. B. Heimann and H. Pentinghaus (Eds.), *Applied Mineralogy*, Balkema, Rotterdam, 2000, pp 859-861.
81. E. Bonaccorsi, S. Merlino, and H. F.W. Taylor, *Cem. Concr. Res.* **34** (2004) 1481 - 1488.
82. K. Garbev, M. Bornefeld, G. Beuchle and P. Stemmermann, *J. Am. Ceram. Soc.* **91** (2008) 3015 - 3023.
83. E. Bonaccorsi, S. Merlino and A. R. Kampf, *J. Am. Ceram. Soc.* **88** (2005) 505 – 512.
84. I. G. Richardson, *Cem. Concr. Res.* **34** (2004) 1733 – 1777.
85. L. S. Dent Glasser, E. E. Lachowski, K. Mohan and H. F.W. Taylor, *Cem. Concr. Res.* **8** (1978) 733 - 740.
86. P. J. Le Sueur, D. D. Double and G. W. Groves, Chemical and porphological studies of the hydration of tricalcium silicate, *Proc. Br. Ceram. Soc.* **35** (1984) pp. 249 - 266.
87. M. W. Grutzeck and D. M. Roy, *Nautre* **223** (1969) 492 – 494.

88. D. J. Rayment and A. J. Majumdar, *Cem. Concr. Res.* **12** (1982) 133 - 140.
89. H. F. W. Taylor and D. E. Newbuury, *Cem. Concr. Res.* **14** (1984) 565-573.
90. I. G. Richardson and G. W. Groves, *J. Mater. Sci.* **28** (1993) 265 - 277.
91. G. W. Groves, P. J. Le Sueur and W. Sinclair, *J. Am. Ceram. Soc.* **69** (1986) 353 - 356.
92. I. G. Richardson, *Cem. Concr. Res.* **29** (1999) 1131 - 1147.
93. H. F. W. Taylor, *J. Am. Ceram. Soc.* **69** (1986) 464 - 467.
94. S. Chatterji and J. W. Jeffery, *Nature* **209** (1966) 1233 - 1234.
95. S. Diamond, Cement paste microstructure—an overview at several levels, in: Hydraulic cement pastes: Their structure and properties; Proceedings of a conference held at the University of Sheffield; 8–9th April 1976. Slough: Cement and Concrete Association; 1976. pp. 2 – 30.
96. S. Goto, M. Daimon, G. Hosaka and R. Kondo, *J. Am. Ceram. Soc.* **59** (1976) 281 - 284.
97. R. B. Williamson, *Prog. Mater. Sci.* **15** (1972) 189 - 286.
98. H. M. Jennings, B. J. Dalgleish and P. L. Pratt, *J. Am. Ceram. Soc.* **64** (1981) 567 - 572.
99. K. Fujii and W. Kondo, Hydration of Tricalcium Silicate in a Very Early Stage, Proceedings of 5th International Symposium on the Chemistry of Cement, Volume II, Tokyo, Japan, 1968, pp. 362 - 371.
100. G. W. Groves, *Mater. Res. Soc. Symp. Proc.* **85** (1985) 3 - 12.
101. J. D. Bernal and H. D. Megaw, *Proc. Roy. Soc.* **A151** (1935) 384 - 420.
102. H. E. Petch, *Acta. Cryst.* **14** (1961) 950 - 957
103. R. J. Bartlett and G. D. Purvis, *Int. J. Quantum Chem.* **14** (1978) 561 – 581.
104. J. Skalny and J.F. Young, Mechanisms of portland cement hydration, Proceedings of the 8th International Symposium on the Chemistry of Cement, Volume 2, Paris, France 1980, pp. II - 1/3 - 1/45.
105. J. J. Beaudoin, *Matér. Constr.* **20** (1987) 27 - 31.
106. H. F. W. Taylor and A. B. Turner, *Cem. Concr. Res.* **17** (1987) 613 - 623.
107. H. F. W. Taylor, *Cement Chemistry 2nd Edition*, London, Thomas Telford, 1997, pp. 187 - 225.
108. G. Renaudin, A. Mesbah, B. Z. Dilnesa, M. Fracois and B. Lottenbach, *Curr. Inorg. Chem.* **5** (2015) 1 - 10.
109. G. W. Groves, *Cem. Concr. Res.* **11** (1981) 713 - 718.
110. D. Viehland, J. - F. Li, L. - J. Yuan and Z. Xu, *J. Am. Ceram. Soc.* **79** (1996) 1731 - 1744.
111. G. Strohmauch and H.-J. Kuzel, *ZKG Int.* **41** (1988) 358 - 360.
112. J. W. Bullard, H. M. Jennings, R. A. Livingston, A. Nonat, G. W. Scherer, J. S. Sweitzer, K. L. Scrivener and J. J. Thomas, *Cem. Concr. Res.* **41** (2011) 1208 - 1223.

113. H. F. W. Taylor, *Cement Chemistry 2nd Edition*, London, Thomas Telford, 1997, pp. 227 - 259.
114. T. C. Powers, Physical Properties of Cement Paste, Proceedings of the 4th International Conference on the Chemistry of Cement, Volume 2, Washington, USA, 1960, pp. 577 - 613.
115. IUPAC Manual of symbols and terminology Appendix 2, Part 1 „Colloid and surface chemistry, *Pure Appl.Chem*, **31** (1972) 578 - 638.
116. S. Diamond, *Cem. Concr. Comp.* **26** (2004) 919 – 933.
117. K. L. Scrivener, *Cem. Concr. Comp.* **26** (2004) 935 – 945.
118. D. L. Coke and M. Y. A. Mollah, *J. Hazard. Mater.* **24** (1990) 231 - 253.
119. D. Bonen and S. L. Sarkar, The Present State – of – the – art of Immobilization of Hazardous Heavy Metals in Cement – based Materials, in: M. W. Grutzeck and S. L. Sarkar (Eds.) *Advances in Cement and Concrete Research*, Engineering Foundation Conference held at New England Center, the University of Hampshire, Durham, NH, American Society of Civil Engineers, New York, 1994, pp. 481 - 498.
120. F. P. Glasser, Chemistry of Cement – Solidified Forms, in: R. D. Spence (Ed.) *Chemistry and Microstructure of Solidified Waste Forms*, Boca Raton, Lewis Publishers, 1993, pp. 1 - 39.
121. A. Poletitini, R. Pomi and P. Sirini, *Environ. Sci. Technol.* **36** (2002) 1584 - 1591.
122. I. Moulin, J. Rosea, W. Stone, J. - Y. Bottereo, F. Mosnier and C. Haelmel, Lead, zinc and chromium (III) and (VI) speciation in hydrated cement phases, in: G. R. Woolley, J. J. J. Goumans, P. J. Wainwright (Eds.), *Waste Materials in Construction*, Elsevier, Amsterdam, 2000, pp. 269-280.
123. F. Ziegler, R. E. M. Scheidegger, C. A. Johnosn, R. Dahren and E. Wieland, *Environ. Sci. Technol.* **35** (2001) 1550 - 1555.
124. P. Kumarathanan, G. J. McCarthy, D. J. Hassett and D. F. Pflughoeft - Hassett, Oxyanion substituted ettringites: synthesis and characterization, and their potential role in immobilization of As, B, Cr, Se and V, Proceedings of the Material Research Society Symposium, Volume 178, Cambridge University Press, 1989, pp. 83 - 104.
125. O. P. Shrivastava and F.P. Glasser, *React. Solids* **2** (1986) 261 - 268.
126. K. Noshita, T. Nishi, T. Yoshida, H. Fujihara, N. Saito and S. Tanaka, Categorization of cement hydrates by radionuclide sorption mechanism, Proceedings of the Material Research Society Symposium, Volume 663, Cambridge University Press, 2001, pp. 115 - 121.
127. T. Phenrat, T. F. Marhaba and M. Rachakornkij, *J. Hazard. Mat.* **118** (2005) 185 - 195.
128. M. Atkins, F. P. Glasser, L. P. Moroni and J. J. Jack, *Thermodynamic modeling of blended cements at elevated temperatures (50-90°C)*, Aberdeen University, United Kingdom, 811 DoE1HMIP1RR/94.011, 1994.

129. F. K. Cartledge, L. G. Butler, D. Chalasani, H. Eaton, F. P. Frey, E. Herrera, M. T. Tittlebaum and S. Yang, *Environ. Sci. Technol.* **24** (1990) 867 - 873.
130. C. H. Mattus, A. J. Mattus, Literature review of the interaction of select inorganic species the set and properties of cement and methods of abatement through pretreatment in: T.M. Gilliam, C.C. Wiles (Eds.), *Stabilization and Solidification of Hazardous, Radioactive and Mixed Wastes: 3rd Volume*, ASTM, Philadelphia, 1996, pp. 609 - 633.
131. A. M. Scheidegger, E. Wieland, A. C. Scheinost, R. Dähn and P. Spieler, *Environ. Sci. Technol.* **34** (2000) 4545 - 4548.
132. M. Vespa, D. Raehn, E. Wieland, D. Grolimund and A. M. Scheidegger, *Czech. J. Phys.* **56D** (2006) D599 - D607
133. F. Ziegler, R. Giere and C. A. Johnson, *Environ. Sci. Technol.* **35** (2001) 4556 - 4561.
134. V. Dutré and C. Vandecasteele, *Waste Manag.* **1** (1995) 55 - 68.
135. J. E. Aubert, B. Husson and N. Sarramone, *J. Hazard. Mater.* **147** (2007) 12 - 19.
136. G. Cornelis, B. Etschmann, T. V. Gerven and C. Vandecasteele, *Cem. Concr. Res.* **42** (2012) 1307 - 1316.
137. G. Cornelis, T. V. Gerven, R. Snellings, J. Elsen and C. Vandecasteele, *Appl. Geochem.* **26** (2011) 809 - 817.
138. D. C. Johnson, N. J. Coleman, J. Lane, C. D. Hills and A. B. Pole, A preliminary investigation of the removal of heavy metal species from aqueous media using crushed concrete fines, in: G. R. Woolley, J. J. J. Goumans, P. J. Wainwright (Eds.), *Waste Materials in Construction*, Elsevier, Amsterdam, 2000, pp. 1044 - 1049.
139. A. Vollpracht, B. Lothenbach, R. Snellings and J. Haufe, *Mater. Struct.* **49** (2016) 3341 - 3367.
140. R. D. Hooton, M. D. A. Thomas and T. Ramlochan, *Adv. Cem. Res.* **22** (2010) 203 - 210.
141. A. Goldschmit *Cem. Concr. Res.* **12** (1982) 743 - 746.
142. M. Michaux, P. Fletcher and B. Vidick, *Cem. Concr. Res.* **19** (1989) 443 - 456
143. J. Duchesne and M. A. Bérubé, *Cem. Concr. Res.* **24** (1994) 221 - 230.
144. J. Tritthart, *Cem. Concr. Res.* **19** (1989) 586 - 594.
145. B. Lottenbach and F. Winnefeld, *Cem. Concr. Res.* **36** (2006) 209 - 226.
146. S - Y. Hong and F. P. Glasser, *Cem. Concr. Res.* **29** (1999) 1893 - 1903.
147. J. Kempel, O. Çorpuroğlu, The interaction of pH, pore solution composition and solid phase composition of carbonated blast furnace slag cement activated with aqueous Na-MFP, Proceedings of the 15th Euroseminar on Microscopy Applied to Building materials, Delft University of Technology, Delft, 2015, pp. 287 - 296.

148. Institute for Prospective Technological Studies, Sustainable Production and Consumption Unit, European IPPC Bureau, Best Available Techniques (BAT) Reference Document for the Production of Cement, Lime and Magnesium Oxide, 2013.
149. [https://cembureau.eu/media/1500/cembureau\\_2050roadmap\\_lowcarboneconomy\\_2013-09-01.pdf](https://cembureau.eu/media/1500/cembureau_2050roadmap_lowcarboneconomy_2013-09-01.pdf) (accessed 28 February 2019).
150. L. Bacarello, J. Kline, G. Walenta and E. Gartner, *Mater. Struct.* **47** (2014) 1055 – 1065.
151. Croatian Standards Institute, HRN EN 197-1:2012 Cement – Part 1: Composition, specification and conformity criteria for common cements (EN 197-1:2011).
152. E. Gartner, *Scientific and Societal Issues involved in developing sustainable cements*, in: R.K. Dir, M.D. Newlands, L. J. Csetenyi (Eds.) *Role of Cement Science in Sustainable Development*, London, Thomas Telford, 2003, pp. 445 - 458.
153. L. Zhang, M. Su and Y. Wang, *Adv. Cem. Res.* **11** (1999) 15 - 21.
154. T. Sui and Y. Yao, Recent progress in special cements in China, Proceedings of the 11th International Congress on the Chemistry of Cement, Volume 4, Durban, South Africa, 2003, pp. 2028 - 2032.
155. J. Péra and J. Ambroise, *Cem. Concr. Res.* **34** (2004) 671 - 676.
156. D. Gastaldi, F. Canonico and E. Boccaleri, *J. Mater. Sci.* **44** (2009) 5788 - 5794.
157. W. Lan and F.P. Glasser, *Adv. Cem. Res.* **8** (1996) 127 - 134.
158. H. Saalfeld and W. Depmeier, *Krist. Tech.* **7** (1972) 229 - 233.
159. P. E. Halstead and A. E. Moore, *J. Appl. Chem.* **12** (1962) 413 - 417.
160. Z. Peixing, C. Yimin, S. Piping, Z. Guanying and H. Wenmel, The crystal structure of C4A3 $\bar{5}$ , Proceedings of the 9th International Congress on the Chemistry of Cement, New Delhi, India 1992, pp. 201 - 208.
161. W. J. Calos, C. H. Kennard, A. K. Whittaker and R. L. Davis, *J. Solid State. Chem.* **119** (1995) 1 - 7.
162. I. Pajares, A. G. Dela Torre, S. Martinez - Ramirez, S. Puertas, M. T. Blanco - Varela and M. A. G. Aranda. *Powder Diffr* **17** (2002) 281 - 286.
163. C. W. Hargis, J. Moon, B. Lothenbach, F. Winnefeld, H. R. Wenk and P. J. M. Monteiro, *J. Am. Ceram. Soc.* **97** (2014) 892 - 898.
164. A. Cuesta, A.G. Dela Torre, E. R. Losilla, K.V. Petterson, P. Rejmak, A. Ayuela, C. Frontera and M.A.G. Aranda, *Chem. Mater.* **25** (2013) 1680-1687.
165. F. Bullerjahn, D. Schmitt and M. Ben Haha, *Cem. Concr. Res.* **59** (2014) 87-95
166. M. A. G. Aranda and A .G. Dela Torre, Sulfoaluminate cements, in F. Pacheco – Torgal, S. Jalali and J. Labrinda (Eds.) *Eco – efficient concrete*, Cambridge, Woodhead Publishing Limited, 2013, pp. 488 - 522.

167. F. Winnefeld and S. Barlag, *J. Therm. Anal. Calorim.* **101** (2010) 949 - 957.
168. G. Álvaerz - Pinazo, A. Cuesta, M. García - Maté, I. Santacruz, E. R. Losilla, A. G. De la Torre, L. León - Reina and M. A. G. Aranda, *Cem. Concr. Res.* **42** (2012) 960 - 971.
169. I. Janotka, U. Krajci and S. C. Mojumdar, *Cerm. Silik.* **51** (2007) 74 - 81.
170. M. C. Martín - Sedeño , A. J. M. Cuberos, A. G. De la Torre, G. Álvaerz - Pinazo, L. M. Ordóñez, M. Gateshki and M. A. G. Aranda, *Cem. Concr. Res.* **40** (2010) 359 - 369.
171. Q. Zhou, N. B. Milestone and M. Hayes, *J. Hazard. Mater.* **136** (2006) 120 - 129.
172. J. Li, H. Ma and H. Zhao, *Key Eng. Mater.* **334-335** (2007) 421 - 424.
173. J. Beretka, B. De Vito, L. Santoro, N. Sherman and G. L. Valenti, *Cem. Concr. Res.* **23** (1993) 1205 - 1214.
174. S. Sahu and J. Majling, *Cem. Concr. Res.* **24** (1994) 1065 - 1072.
175. J. Majling and J. Strigac, *Adv. Cem. Res.* **11** (1999) 27 - 34.
176. P. Arjunan, M. Silsbee and D. M. Roy, *Cem. Concr. Res.* **29** (1999) 1305 - 1311.
177. P. K. Mehta and P. J. M. Monteiro, *Concrete: Microstructure, Properties and Materials*, McGraw-Hill, New York, 2006, pp. 177 - 203.
178. F. Adenot and M. Buil, *Cem. Concr. Res.* **22** (1992) 489 - 496.
179. M. Mainguy, C. Tognazzi, J. M. Torrenti and F. Adenot, *Cem. Concr. Res.* **30** (2000) 83 - 90.
180. T. H. Wee, J. Zhua, H. T. Chua and S. F. Wong, *ACI. Mater. J.* **98** (2001) 184 - 193.
181. S. Kamali, B. Gerrard and M. Moranville, *Cem. Concr. Compos.* **25** (2003) 451 - 458.
182. J. Jain and N. Neithalath, *Cem. Concr. Comps.* **31** (2009) 176 - 185.
183. F. P. Glasser, J. Marchand and E. Samson, *Cem. Concr. Res.* **38** (2008) 226 - 246.
184. R. D. Hooton, M. D. A. Thomas and T. Ramlochan, *Adv. Cem. Res.* **22** (2010) 203 - 210.
185. P. K. Mehta and P. J. M. Monteiro, *Concrete: Microstructure, Properties and Materials*, McGraw-Hill, New York, **2006**, pp. 203 - 251.
186. P. Faucon, F. Adenot, M. Jorda and R. Cabrillac, *Mater. Struct.* **30** (1997) pp. 480 - 485.
187. P. Faucon, F. Adenot, J. F. Jacquinet, J. C. Petit, R. Cabrillac and M. Jorda, *Cem. Concr. Res.* **28** (1998) 847 - 857.
188. C. Carde, R. Francois and J. M. Torrenti, *Cem. Concr. Res.* **26** (1996) 1257 - 1268.
189. F. H. Heukamp, F. J. Ulm and J. T. Germaine, *Cem. Concr. Res.* **31** (2001) 767 - 774.
190. G. J. Verbeck and R. H. Helmuth, Structure and physical properties of hardened cement, Proceedings of the 5th International Symposium on the Chemistry of Cement, Volume 3, Tokyo, Japan, 1968, pp. 1-32.
191. Q. Y. Chen, M. Tyrer, C. D. Hills, X.M. Yang and P. Carey, *Waste Manag.* **29** (2009) 390 - 403.

192. A. Hidalgo, S. Petit, C. Domingo, C. Alonso and C. Andrade, *Cem. Concr. Res.* **37** (2007) 63 - 70.
193. K. Yozeki, K. Watanabe, N. Sakata and N. Otsuki, *Appl Clay Sci.* **26** (2004) 293 - 308.
194. C. Carde, R. François and J. M. Torrenti, *Cem. Concr. Res.* **26** (1996) 1257 - 1268
195. T. Matschei, B. Lotenbach and F. P Glasser, *Cem. Concr. Res.* **37** (2007) 118 - 130
196. A. Berton, J. Duchesne and G. Escadeillas, *Cem. Concr. Res.* **35** (2005) 155 - 166
197. H. Saito and A. Deguchi, *Cem. Concr. Res.* **30** (2000) 1815 - 1825.
198. Croatian Standards Institute, HRN EN 196-2: 2013 Methods of testing cement – Part 2: Chemical analysis of cement (EN 196-2:2013).
199. American Society for Testing and Materials, ASTM C 114 – 07 Standard test methods for analysis of hydraulic cement.
200. G. Morrision, H. Cheng and M. Grasserbauer, *Pure Appl. Chem.* **51** (1979) 2243 - 2250.
201. A. Santro, A. Held, T.P.J. Linsinger, A. Perez and M. Ricci, *Trends Analyt. Chem.* **89** (2017) 34 - 40.
202. Croatian Standards Institute, HRI CEN/TR 196-4:2017 Methods of testing cement – Part 4: Quantitative determination of constituents (CEN/TR 196-4:2007).
203. K. Scrivener and A. Nonat, *Cem. Concr. Res.* **41** (2011) 651 - 665.
204. T. Degen, M. Sadki, E. Bron, M. König, G. Nèner, *Powder. Diffr.* **29 (S2)** (2014) S13 – S18
205. American Public Health Association, American Water Works Association, Water Environmental Federation, R. B. Barid A. D. Eaton, E.W. Rice, *Standard methods 23rd editon* Washington DC, 2017, pp. 2 - 56.
206. American Public Health Association, American Water Works Association, Water Environmental Federation, R. B. Barid A. D. Eaton, E.W. Rice, *Standard methods 23rd editon* Washington DC, 2017, pp. 2 - 66.
207. American Public Health Association, American Water Works Association, Water Environmental Federation, R. B. Barid A. D. Eaton, E.W. Rice, *Standard methods 23rd editon* Washington DC, 2017, pp. 2 - 48.
208. Croatian Standards Institute, HRN EN 17294-2:2016 Water quality – Application of inductively coupled plasma mass spectrometry (ICP-MS) – Part 2: Determination of selected elements including uranium isotopes (ISO 17294-2:2016; EN ISO 17294-2:2016).
209. Croatian Standards Institute, HRN EN 15216:2008 Characterization of waste - Determination of total dissolved solids (TDS) in water and eluates (EN 15216:2007).
210. Croatian Standard Institute, HRN EN 196-1: 2016 Methods of testing cement – Part 1: Determination of strength (EN 196-1:2016).

211. Croatian Standards Institute, HRN EN 12390-13:2003 Testing hardened concrete - Part 13: Determination of secant modulus of elasticity in compression (EN 12390-13:2013).
212. Croatian Standards Institute, HRN EN 12617-4:2003 Products and systems for the protection and repair of concrete structures – Test methods – Part 4: Determination of shrinkage and expansion (EN 12617-4:2002).
213. Croatian Standards Institute, HRN EN ISO 15148:2004 Hygrothermal performance of building materials and products - Determination of water absorption coefficient by partial immersion (ISO 15148:2002; EN ISO 15148:2002).
214. Croatian Standards Institute, HRN EN 993-4:2008 Methods of test for dense shaped refractory products - Part 4: Determination of permeability to gases (EN 993-4:1995).
215. Croatian Standards Institute, HRN EN 480-11: 2005 Admixtures for concrete, mortar and grout - Test methods - Part 11: Determination of air void characteristics in hardened concrete (EN 480-11:2005)
216. F. Nishi, Y. Takeuchi, Y. Maki, *Z. Kristallogr. Cryst. Mater.* **172** (1985) 297 – 314
217. K. H. Jost, B. Ziemer, R. Seydel, *Acta Crystallogr. B* **33** (1977) 1696 – 1700
218. P. Mondal, J. W. Jeffery, *Acta Crystallogr. B* **31** (1975) 689 – 697
219. Y. Takeuchi, Maki I., *Z. Kristallogr. Cryst. Mater.* **152** (1980) 259 – 307
220. A. C. Jupe, J. K. Cockoroft, P. Barnes, S. L. Colston, G. Sankar, C. Hall, *J. Appl. Cryst.* **34** (2001) 55 – 61
221. T. Pialti, F. Demartin, C.M. Gramaccioli, *Acta Crystallogr. B* **54** (1998) 515 – 523
222. K. Ojima, Y. Nishihata, A. Sawada, *Acta Crystallogr. B* **51** (1995) 287 – 293
223. C. Bezon, A. Nonant, A. N. Christensen, M. S. Lehmann, *J. Solid State Chem.* **117** (1995) 165 – 176
224. P. F. Schofield, C. C. Wilson, I. C. Stretton, *Z. Kristallogr. Cryst. Mater.* **215** (2000) 707 - 710
225. A. Kirfel, G. Will, *Acta Crystallogr. B* **36** (1980) 2881 – 2890
226. P. Ballirano, G. Belardi, A. Maras, *Neu. Jb. Mineral. Abh.* **182** (2005) 15 – 21
227. H. F. W. Taylor, *Cement Chemistry 2nd Edition*, London, Thomas Telford, 1997, pp. 55 - 87.
228. H. F. W. Taylor, *Cement Chemistry 2nd Edition*, London, Thomas Telford, 1997, pp. 261 - 295.
229. A. Guesta, A. G. De la Torre, E. R. Losilla, V. K. Peterson, P. Rejmak, A. Ayuela, C. Frontera, M. A. G. Aranda, *Chem. Mater.* **25** (2013) 1680 - 1687
230. A. Saalfeld, W. Depmeier, *Krist. Tech.* **7** (1972) 229 – 233
231. V. I. Mokeera, E. S. Makarov, *Geokhimiya* **1979** (1979) 1541 – 1544
232. H. Bartl, T. Scheller, *Z. Kristallogr. Cryst. Mater.* **95** (1936) 175 – 175
233. S. Sasaki, K. Fujino, Y. Takeuchi, *Proceedings of the Japan Academy* **55** (1979) 43 – 48



- 
234. H. E. Petch, *Acta Crystallogr.* **14** (1961) 950 – 957
235. M. R. Hartman, R. Berliner, *Cem. Concr. Res.* **36** (2006) 364 – 370
236. I. Santacruz, G. Alvarez-Pinazo, A. Cabeza, A. Cuseta, J. Sanz, M.A.G. Aranda, *Adv. Cem. Res.* **28** (2016) 13 - 22